TESTING AND ANALYSIS OF A FREE PISTON LINEAR MACHINE WITH GAS SPRINGS

EIRIK LIND HÅNES

NORWEGIAN UNIVERSITY OF LIFE SCIENCES
DEPARTMENT OF MATHEMATICAL SCIENCES AND TECHNOLOGY
MASTER THESIS 30 CREDITS 2012

Pre face

The testing and analysis performed in this thesis has been in collaboration with Resonator AS. The staff at Resonator has been available for discussions and assisted with the practical tests. For this I am grateful. Particularly I want to thank Anders Bostad and Andrè Dahl Jacobsen your contributions have been invaluable.

Working on this project has been a challenging and interesting task, and I think it has made me a better engineer.

I want to thank my advisor Tor Anders Nygaard, your critical insight has been very useful. My external assessor John Sidders has been a valuable resource, thank you.

I also want to thank Bjørn Brenna at the University Work Shop for evaluating my technical drawings and designs. I want to thank Geir Terjesen for discussions regarding some of the structural components.

Servi AS has let me use their test facilities for the initial liquid and gas pressure tests, this was critical for getting the project on track, thank you. There are many suppliers that have helped me answer technical questions; Lindber & Lund, Huhnseal, Otto Olsen and Trelleborg, I am grateful for your help.

I want to thank Anders Myhr for helping me with the setup of the thesis. Your contribution is appreciated.

Finally I want to thank my fellow students, family and friends. You're everyday input is what maters the most.

Ås, 31.1.2012

_____

Eirik Lind Hånes

Abstract

This thesis is written in collaboration with Resonator AS, a company developing free piston linear machines for down-the-hole drilling applications. The free piston linear machine is designed to create heavy vibrations, which are used to break the rock. A successful product relies on the ability to deliver a sufficient hammering energy per blow to break the rock, at a high frequency, yielding a high rate of penetration (ROP). To reach the goal of making a faster drilling machine, Resonator has targeted electrical power density and stiff springs in the free piston linear machine, as critical factors. They have found mechanical springs inadequate for their application and are therefore researching the use of gas springs in a free piston linear machine. This thesis is focusing on the use of gas spring in a free piston linear machine.

The use of gas springs in a free piston linear machine is analyzed and tested, important parameters for the performance of such a machine are investigated with emphasis on the gas springs. Critical design factors found are structural design, thermal design, surface specifications, seal configuration, lubrication and tolerances. These areas are investigated in detail for the tested prototype. Advantages and disadvantages for the use of gas springs in such a machine are discussed; the main advantage found is that high frequencies' seem to be obtainable, the main disadvantage is the friction in the gas springs causing heat generation and decreased efficiency.

A linear spring equivalent for gas spring stiffness is derived to ease analysis of systems using high velocity gas springs. This linear spring equivalent has been used to predict the resonate frequency of the machine. Test results show good coherence between the predicted frequency and the measured. The gas spring stiffness equivalent has also been used to optimize the gas spring chamber size.

Based on the tests and analysis performed, improvements have been made to the prototype machine tested, and future improvements are suggested. The changes done to the original design yielded a substantial performance gain. Based on the analysis, it seems to be possible to further improve the machine performance by implementing the suggested improvements. Improvements are suggested in structural design, thermal design, surface texture, seal configuration, lubrication and tolerances.

To confirm the results from the tests and analysis found in this thesis further testing needs to be performed.

Table of contents

List of figures

List of tables

Nomenclature

Fold-out

Symbol	Explanation	Unit
A	Area	m^2
A_p	Amplitude of piston	m
a_p	Piston acceleration	m/s^2
A_s	Amplitude of stator	m
a_s	Stator acceleration	m/s^2
c	Damping coefficient	
c_r	Damping coefficient rod supports	
c_s	Damping coefficient stator tube	
$\dot{E}_{fp_n}$	Heat generation due to friction at piston n	W
$\dot{E}_{g-EL}$	Heat generation in stator due to electrical losses	W
$\dot{E}_{g-fric}$	Heat generation due to friction	W
$\dot{E}_{gr}$	Heat generation due to friction and damping at rod supports	W
$\dot{E}_{gs}$	Heat generation due to friction and damping in stator tube	W
E_i	Energy per blow	J
f	Frequency	Hz
F_{fp_n}	Friction force gas spring piston n	N
F_{fr_n}	Friction force rod n	N
F_{gs_n}	Gas spring force (in gas spring n)	N
F_d	Damping force	N
F_{el}	Electrical force	N
F_f	Frictional force	N
F_{fs}	Friction force stator tube	N
F_L	Force from applied load	N
F_T	Total force in bolt	N
h	Convection heat transfer coefficient	$w/m^2\ K$
$k_{GS_{net}}$	Net gas spring stiffness equivalent	N/m
k_{Ts}	Top spring stiffness	N/m
m_m	Total Mass of machine	kg
m_p	Mass of piston	kg
m_s	Mass of stator	kg
n	Number of moles	
p	Pressure	N/m^2
p_0	Gas spring initial pressure	bar
q_{g-p}	Heat transfer between gas and gas spring piston	W
q_{g-s}	Heat transfer between gas and stator	W
q_{p-p}	Heat transfer to gas spring piston due to frictional heat generation	W
q_{p-s}	Heat transfer between piston and stator	W
q_{p-s}	Heat transfer to stator due to frictional heat generation at gas spring piston	W
q_{r-p}	Heat transfer to rod due to frictional heat generation	W
q_{r-s}	Heat transfer to stator due to frictional heat generation at piston rod	W
q_{s-p}	Heat transfer to piston due to frictional heat generation in statortube	W
q_{s-s}	Heat transfer to stator due to frictional heat transfer in stator tube	W
q_{conv}	Convectional heat transfer to surroundings	W
q_{rad}	Radiation heat transfer to surroundings	W
R	Electrical resistance	ohm
R_a	Arithmetic average distance	μm
R_{max}	Maximum valley to peak	μm
R_k	Kernel surface roughness	μm
R_{pkx}	Full peak height	μm
R_{pk}	Reduced peak height	μm
R_{vk}	Reduced valley depth	μm
R_{vkx}	Full valley depth	μm
R_{mr}	Material contact area	$fraction$
R_u	Universal gas constant	$J/(mol\ K)$
ROP	Rate of penetration	$m/hour$
P_{h_m}	Maximum available hammering power	W
$P_{El_{in}}$	Electrical power in to the machine	W
t	time	s
T_∞	Temperature of medium surrounding the machine	w
T_r	Energy transfer rate	
V	Volume	m^3
v_p	Piston speed	m/s
v_s	Stator speed	m/s
W_{el}	Electrical work	J
W_{fric}	Frictional work	J
x	Position along the vertical axis of the machine	m
x_p	Piston x position relative to global, x_p =0 at zero amplitude	m

x_s	Stator x position relative to global, x_s =0 at zero amplitude	m
x_{rel}	Relative displacement; stator – piston. $x_{rel} = 0$ at zero amplitude	m
x_{max}	Maximum relative displacement between stator and piston	m
γ	Polytrophic coefficient	
μ_k	Kinetic friction coefficient	
σ_A	Deformation due to pre-tightening in the elements that experience a decreasing load when the load F_L is applied	mm
σ_b	Boltzman constant	
σ_{bolt}	Tensile stress bolt	N/mm^2
σ_T	deformation due to pre-tightening in the elements that experience an increasing force when the load $F_L$is applied	mm
ω	Angular velocity	rad/s

Abbreviation	**Explanation**	**Unit**
2B	The resonator prototype version 2B.	
DCF	Dynamic chip formation	
SE	Specific energy	N/m^2
CS2	Coordinate system 2, $x_p = x_p + x_s = x$, $x_s = 0$	
Resonator	The company Resonator AS	
The Resonator	The resonator machine	
FEA	Finite Element Analysis	

Accent	**Explanation**
$\dot{x}$	Derivative (of x)
$\ddot{x}$	Double derivative (of x)
$\bar{x}$	Average (of x)
$\vec{x}$	The vector x

1. Introduction

The master thesis is written in cooperation with Resonator AS, which is a company that is developing a resonating free-piston tubular permanent magnet linear machine. They are researching the use of such a machine for down-the-hole (DTH) percussion drilling.

In the future Resonator hopes that their technology can help reduce the cost of drilling. Drilling costs are one of the main costs when utilizing geothermal energy (Bostad 2011). Resonator hopes that by reducing the price of drilling they can make geothermal energy more attractive, and that this in time will help cut the global emissions of CO_2, since geothermal energy is a sustainable and renewable energy source (Tester 2005).

Resonator is also investigating the use of their machine for drilling in other markets such as oil and gas. For the oil and gas industry drilling contributes to a large portion of the total cost, therefore reducing drill time and thereby cost is essential (Bostad 2011). Resonator thinks that in time their concept can outperform conventional drilling methods in the oil and gas industry.

Resonator have built several prototypes, the latest prototype is called prototype 2B. It was produced during the summer 2011 and the parts was delivered to Resonator late summer early fall 2011. A layout of prototype 2B is shown in Figure 1.

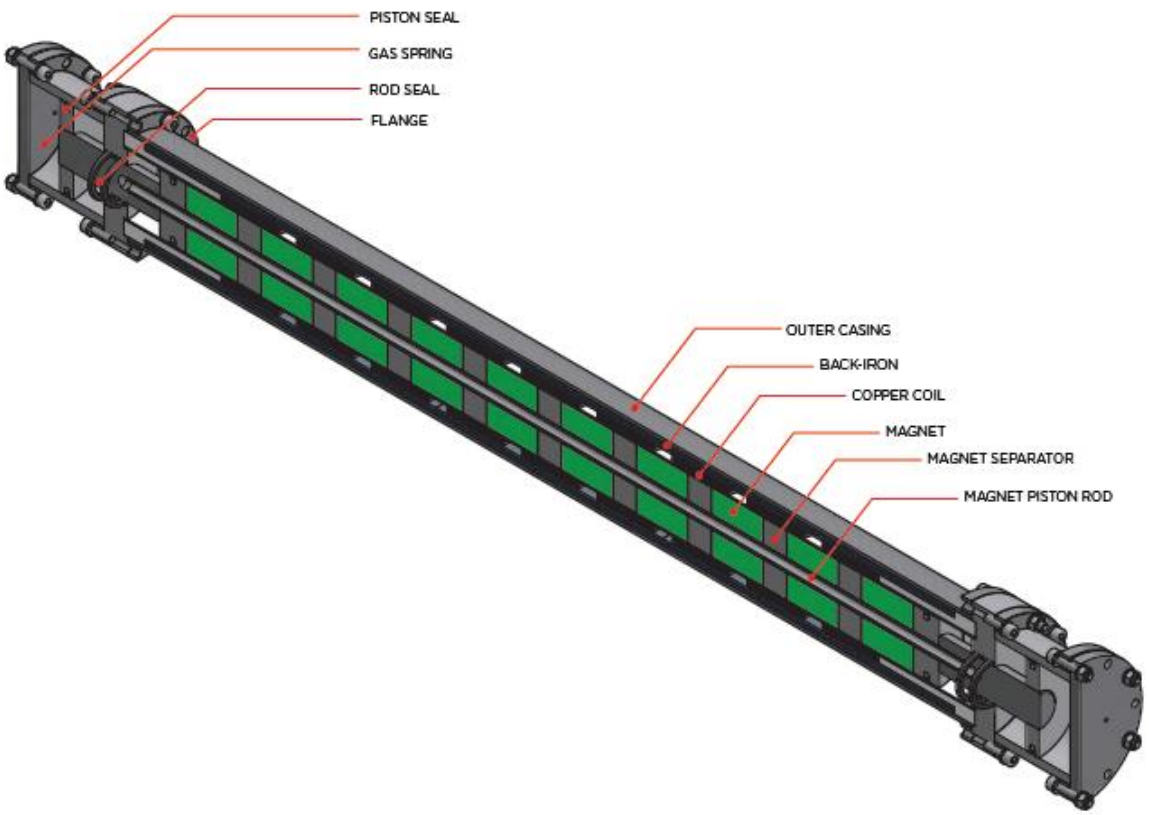

Figure 1, Layout of prototype 2B, (Resonator AS 2011)

Figure 1 show that the machine consists of a large magnet piston moving inside a copper coil (stator), with a spring attached between the magnet piston and stator in each end. When an electrical current is exited in the copper coil, this creates a magnetic field generating a force between the magnet and the stator. The direction of the force depends on the direction of the current. By changing the direction of the current the piston and stator moves back and forth (in opposite direction). The springs in each end works as short-term energy storage, and by tuning the electrical frequency to the natural frequency of the mass-spring system a high frequency and amplitude with a relatively low electrical input can be obtained. The natural frequency of the system depends on the mass of the piston and stator and the total spring stiffness.

Resonator wants to use the machine to hit on a drill bit, so that the kinetic energy of the stator is transferred to the rock. For the rock to break the energy transferred must be large enough to break the rock. The energy transferred depends on the mass of the stator/outer casing and its velocity. It is desired to obtain a high frequency as this can increase the rate of penetration of a future DTH drilling machine, therefore the machine relies on stiff springs (Bostad 2011).

The previous prototypes made by Resonator have proven several important properties of the resonator concept (Bostad 2011):

- Electromagnetic energy transfer between coils and permanent magnet piston helps to maintain and reinforce the resonant behavior
- The ability to use the concept for percussive drilling.

Resonator wants to investigate the use of gas springs in their free piston linear machine instead of mechanical springs. This is because they found the mechanical springs on the market unsatisfactory with respect to stiffness and fatigue life(Resonator AS 2011).

Gas springs are filled with nitrogen (usually) and the stiffness of a gas spring depends on the piston area and the internal pressure. The internal pressure will change during the stroke depending on the gas spring volume, giving an increased force when compressed. The pressure in the gas springs can become very high and gas springs therefore relies on good seals. (*Kaller gas spring selection guide* 2009).

When investigating commercially available gas springs no satisfactory products where found, the rated maximum relative velocity and frequency were too low. Investigating products on the seal market showed that much higher velocities and frequencies were obtainable using the latest technology in reciprocating seals (Resonator AS 2011). Based on this research Resonator decided to develop the prototype 2B (Figure 1) which is a free piston linear machine with gas springs. The main purpose of this prototype is to analyze and test the gas spring performance.

There are other companies that make percussive drill hammers (i.e Wassara). To outperform today's available drill hammers Resonator has targeted 100 Hz as the necessary hammering frequency. It is also required to transfer sufficient energy at each blow to break the rock at this frequency (Bostad 2011).

1.1. 2B Prototype nominal values

Based on the design calculations Resonator estimated the following nominal values for the 2B prototype, Table 1.

Table 1, Nominal values / design requirements for the 2B prototype, Resonator AS

Description	Unit	Values
Maximum piston velocity	m/s	10
Piston frequency	Hz	100
Piston amplitude	m	0.016
Initial pressure	Bar	60
Maximum working pressure	Bar	330
Maximum pressure difference piston seal	Bar	300
Maximum pressure difference rod seal	Bar	330
Life time	Cycles	$2 * 10^6$
Operating temperature	C	Maximum internal, 200 C
Working medium		Nitrogen
Surrounding pressure	Bar	1 atm.
Surrounding temperature	^oC	25
Surrounding medium		Stagnant air, 25 C
Material		Super duplex steel
Seal material		Trelleborg M12 (PTFE blend)

2. Scope

The use of gas springs in a free piston linear machine is unexplored, to find the limitations for the use of gas springs one must first obtain a good understanding of the system and gas springs in general. With this knowledge the Prototype 2B can be analyzed and the analysis performed can be checked with practical tests. Based on the understanding obtained during tests and analysis, design improvements might be suggested. The main areas of focus are

- Analyze the use of gas springs in a free piston linear machine
    - Get an overview of the mechanical relationships in a free piston resonating machine and investigate how some key parameters affect the performance of such a machine.
    - Get an overview of the major heat generation in the machine and how heat transfer trough the machine and to the surroundings.
- Analyze important factors affecting the gas springs performance
- Analyze the prototype 2B designed and constructed by Resonator AS, with emphasis on the gas springs.
- Test the prototype 2B and suggest improvements based on tests and analysis, focusing on the gas springs.

The prototype 2B is already designed and manufactured; the focus is therefore on similar solutions to those selected in the 2B prototype. Significantly different concepts are not to be investigated in detail.

3. Background

One of Resonators main goals is to reduce the cost of drilling. The rate of penetration (ROP) is one of the most important parameters in drilling, because reducing drill time will greatly reduce the drill cost (Bostad 2011). Hustrulid and Fairhust (Hustruli.Wa & Fairhurs.C 1972) formulated the following expression for ROP:

(1)

$$\mathrm{ROP} = \frac{\mathrm{E_i\ f\ T_r}}{\mathrm{A\ SE}}$$

Where $\mathrm{E_i}$ is the energy per blow (*J*), f is the hammering frequency, $\mathrm{T_r}$ is the energy transfer rate between the machine and the rock, A is the drill hole area (m^2) and SE is the rock's specific energy ($(Nm/m^3$) which is the energy per area necessary to break the rock. Equation (1) shows that the rate of penetration is proportional to both energy per blow and the hammering frequency. Further the ROP is inversely proportional to the drill hole area and the specific energy.

This expression for ROP is considered as a reliable equation for estimating the penetration rate(Kahraman et al. 2003). There are however some limitations, the drill bit must transfer sufficient energy to fracture the rock; dynamic chip formation (DCF). It seems that increasing the impact energy past this point is less effective, so that increasing the hammering frequency is better use of energy (Green 2005). Resonator wants to utilize this idea to be able to increase ROP compared to competing hammers.

Based on existing hammers (Bostad 2011) calculated the impact energy per area to be approximately 0.04 J/mm^2 for hammers with hole diameters between 50 and 100 mm. From this we can write an approximate design equation:

(2)

$$\mathrm{E_i T_r} = 0.04[J/mm^2]\ \mathrm{A}$$

The necessary impact energy to break the rock may be less than this depending mainly on the rock type. But if resonator is going to develop a hammer with a higher ROP than competing hammers they should aim for approximately this impact energy and a higher frequency than its competitors.

3.1. Forces, velocities, accelerations and mechanical energy

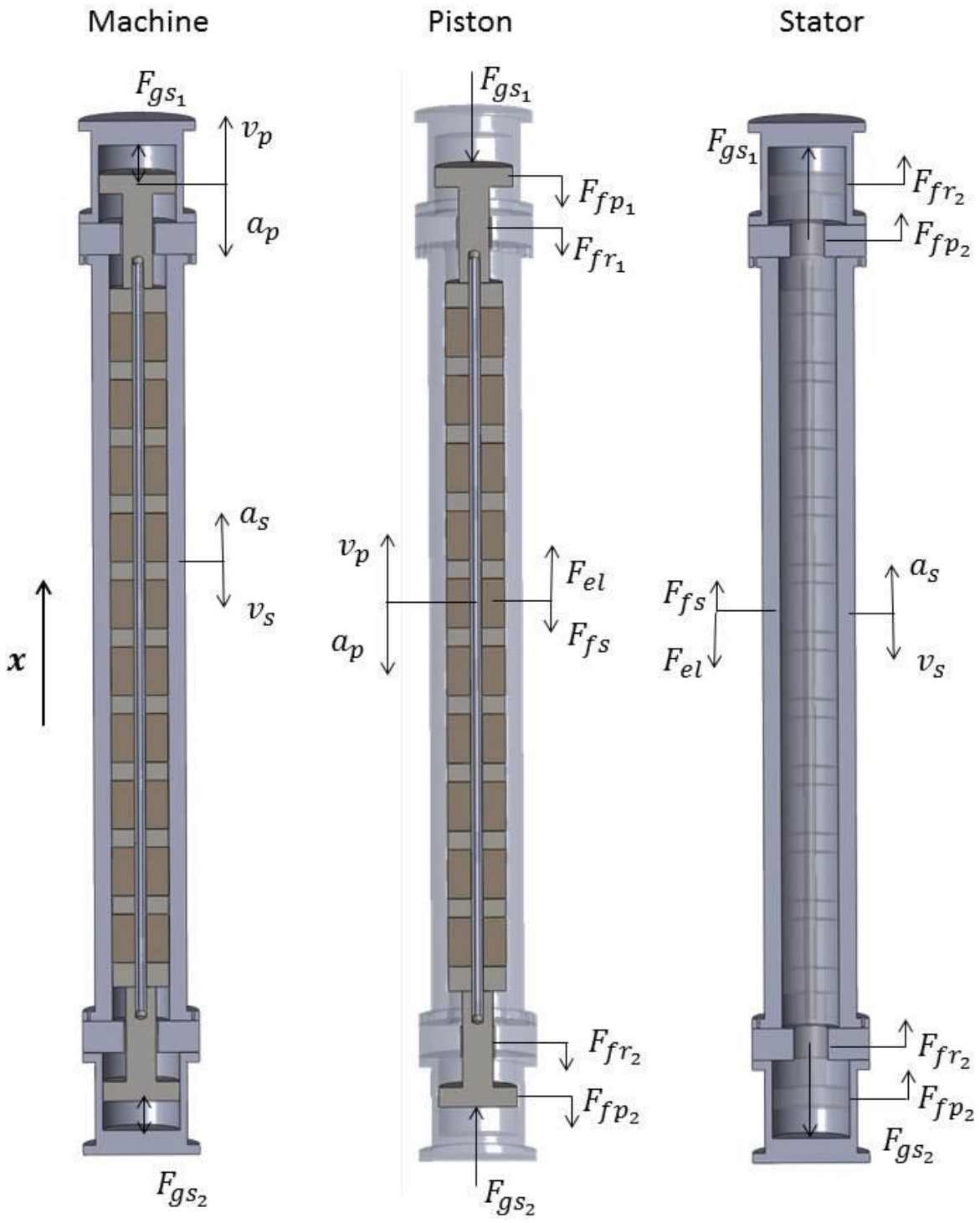

Figure 2, Showing the major forces, velocities and accelerations in the 2B prototype at one instant (single acting gas springs)

Figure 2 shows the major forces, velocities and accelerations in the 2B prototype with single acting gas springs, working at one point during the working cycle. Gravity is neglected as it plays a minor role. If we summarize the forces acting on the stator casing and the magnet piston we get:

$$\sum \mathrm{F_{piston}} = \mathrm{F_{el}} + \mathrm{F_{gs_2}} - \mathrm{F_{gs_1}} - \mathrm{F_{fr_1}} - \mathrm{F_{fr_2}} - \mathrm{F_{fp_1}} - \mathrm{F_{fp_2}} - \mathrm{F_{fs}}$$

$$\sum \mathrm{F_{stator}} = \mathrm{F_{gs_1}} + +\mathrm{F_{fr_2}} + \mathrm{F_{fp_1}} + \mathrm{F_{fp_2}} + \mathrm{F_{fs}} - \mathrm{F_{el}} - \mathrm{F_{gs_2}}$$

Table 2, Explanation of symbols Figure 2

Symbol	Explanation	Unit
$\boldsymbol{a_p}$	Piston acceleration	m/s^2
$\boldsymbol{a_s}$	Stator acceleration	m/s^2
$\boldsymbol{F_{gs_n}}$	Gas spring force (in gas spring n)	N
$\boldsymbol{F_{fp_n}}$	Friction force gas spring piston n	N
$\boldsymbol{F_{fr_n}}$	Friction force rod n	N
$\boldsymbol{F_{fs}}$	Friction force stator tube	N
$\boldsymbol{F_{el}}$	Electrical force	N
$\boldsymbol{v_p}$	Piston speed	m/s
$\boldsymbol{v_s}$	Stator speed	m/s

3.1.1 Gas spring forces

The gas springs use nitrogen gas and the machine operates at high frequencies, this means that we can estimate the gas spring forces using the ideal gas law (Jewett & Serway 2010) and the pressure volume relationship for a adiabatic process (Jewett & Serway 2010).

(3)

$$\mathrm{pV} = \mathrm{nR_u T}$$

(4)

$$\mathrm{pV^{\gamma}} = \mathrm{constant}$$

Where p is pressure, V is volume, n is the number of moles, $\mathrm{R_u}$ is the universal gas constant and γ is the polytrophic gas coefficient.

This yields the following expression for a single acting gas spring force $\mathrm{F_{gs_n}(x)}$ as a function of piston position.

(5)

$$\mathrm{F_{gs_n}(x_{rel})} = \mathrm{A_{gs} p_0} \left[\frac{\mathrm{x_{gsc}}}{\mathrm{x_{gsc}} - \mathrm{x_{rel}}}\right]^{\gamma}$$

Where $\mathrm{x_{rel}}$ is the relative displacement between the stator and the piston, $\mathrm{A_{gs}}$ is the gas spring area, $\mathrm{P_0}$ is the initial pressure at $\mathrm{x_{rel}} = 0$ and $\mathrm{x_{gsc}}$ is the initial gas spring length. For simplicity we can

change the coordinate system so that the stator is stationary and $x_p = x_{rel} = x$ (CS2). For a machine with two single acting gas springs this gives:

(6)

$$F_{gs_1}(x) = A_{gs} p_0 \left[\frac{x_{gsc}}{x_{gsc} - x}\right]^{\gamma}$$

(7)

$$F_{gs_2}(x) = A_{gs} p_0 \left[\frac{x_{gsc}}{x_{gsc} + x}\right]^{\gamma}$$

3.1.2 Frictional forces

Frictional forces are difficult to estimate without test data. The friction depends on many factors, and the most important factors are; what type of lubrication regime that are present (Boundary, thin film, thick film or Solid lubrication)(Szeri 2011), the load and the sliding speed. For the stator tube and rod friction (F_s and F_{fr}) no manufacturer data or test data are available. But generally the friction force F_f is:

(8)

$$F_f = \mu_k * F_{normal}$$

Where μ_k is the kinetic friction coefficient and F_{normal} is the normal force. For the rod supports and the stator tube the normal force should be small if everything is perfectly aligned. However, if there are any misalignment the normal forces can increase considerably.

If there is lubrication present we expect some viscous damping:

(9)

$$F_d = cv$$

Where F_d is the damping force, c is the damping coefficient and v is the relative velocity.

For the piston seal the following expression for friction force F_{fp_n} was developed based on manufacturer data (Wangen 2011). This can also be derived from Figure 6 knowing the Poisson's ratio for the o-ring material and the dimensions.

(10)

$$F_{fp_n} = 0.491 p_{gs_n} + 103.2$$

Where p_{gs_n} is the internal pressure (bar) in gas spring n. If there is a double acting gas spring it is the highest of the two pressures that dictates the friction.

From equation (3) and (4) we get the gas spring pressure p_{gs_n}, still using CS2:

(11)

$$p_{gs_{1(x)}} = p_0 \left[\frac{x_{gsc}}{x_{gsc} - x}\right]^{\gamma}$$

(12)

$$p_{gs_1}(x) = p_0 \left[\frac{x_{gsc}}{x_{gsc} + x}\right]^{\gamma}$$

This gives

(13)

$$F_{fp_1} = 0.491 p_0 \left[\frac{x_{gsc}}{x_{gsc} - x}\right]^{\gamma} + 103.1$$

(14)

$$F_{fp_2} = 0.491 p_0 \left[\frac{x_{gsc}}{x_{gsc} + x}\right]^{\gamma} + 103.1$$

3.1.3 Electrical force

The average electrical force acting on the magnet piston and stator $\overline{F_{el}}$ must be large enough to overcome friction and recharge the machine after impact before the next impact. For one cycle we can write the following equation:

(15)

$$\int W_{el} = \int W_{fric} + E_i$$

Which expands to the following equation for one cycle

(16)

$$\bar{F}_{el}\, 4\, x_{max} = \int_0^{4\, x_{max}} W_{fric}(x)dx + E_i$$

Where W_{el} is the electrical work, $W_{fric}(x)$ is the work done by friction, x_{max} is the amplitude and E_i is the energy per blow. Rearranging:

(17)

$$\bar{F}_{el} = \frac{1}{4\, x_{max}} \int_0^{4\, x_{max}} W_{fric}(x)dx + \frac{E_i}{4\, x_{max}}$$

Since the stator tube and rod friction (F_s and F_{fr}) is not determined the required electrical force cannot be calculated accurately. To get an estimate one can assume some constants in equation (8) and (9) to obtain the sliding friction at the rod supports and in the stator tube, and the damping force.

3.1.4 Mechanical energy

The 2B prototype use the kinetic energy of the stator housing to break the rock, so that when the stator of the machine hit the drill bit, the energy transfer to the rock is:

(18)

$$\left[\frac{1}{2} m_s v_s^2\right] = E_i T_r$$

Where m_s is the mass of the stator housing, v_s is the speed of the stator housing, E_i is the impact energy and T_r is the energy transfer rate between the stator housing and the rock.

To be able to break the rock at impact, we need to have a specific kinetic energy stored in the stator before impact. Using equation (2) we can write the following equation at impact:

(19)

$$\left[\frac{1}{2} m_s v_s^2\right] = 0.04[J/mm^2]\, A_{hole}$$

When gas springs are used like in the 2B prototype the maximum relative velocity are limited by the seals. For the Resonator machine the maximum relative velocity is set to 10 m/s (Trelleborg 2011a), limited by the seals.

3.2. Thermal analysis

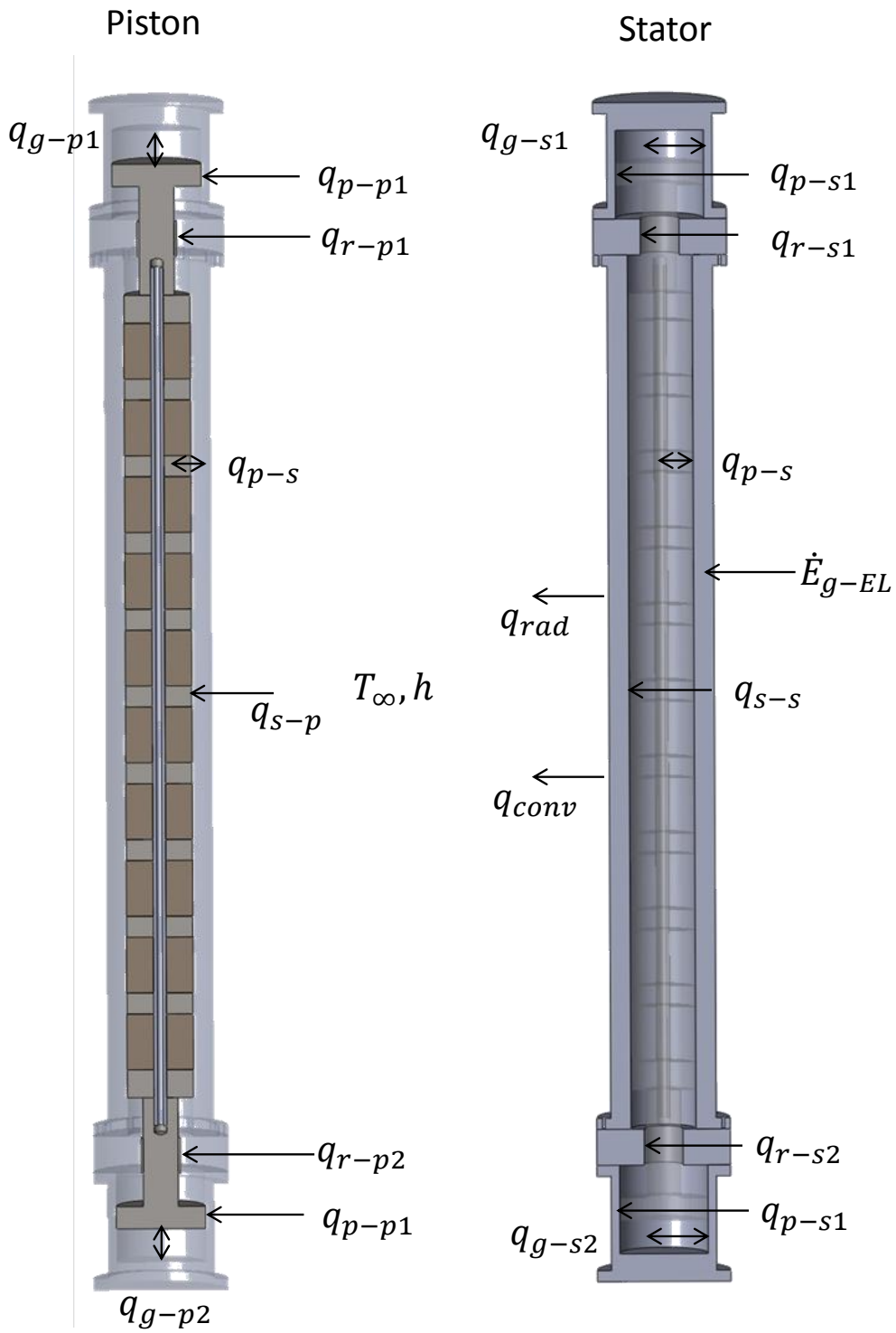

Figure 3, Major heat transfers piston and stator.

Figure 3 Shows the major heat transfer in and from the 2B prototype. The whole machine has to be studied, as heat can flow between the gas springs and the rest of the machine. This means that the gas springs performance is influenced by how the heat generation and cooling is in the rest of the machine. Table 3 explains the symbols used in Figure 3.

Table 3, Explanation of symbols Figure 3

Symbol	Explanation	Unit
$\dot{E}_{g-EL}$	Heat generation in stator due to electrical losses	w
$\dot{E}_{g-fric}$	Heat generation due to friction	w
h	Convection heat transfer coefficient	w/m^2K
T_∞	Temperature of medium surrounding the machine	$^\circ C$
q_{g-p}	Heat transfer between gas and gas spring piston	w
q_{p-p}	Heat transfer to gas spring piston due to frictional heat generation	w
q_{r-p}	Heat transfer to rod due to frictional heat generation	w
q_{p-s}	Heat transfer between piston and stator	w
q_{s-p}	Heat transfer to piston due to frictional heat generation in statortube	w
q_{g-s}	Heat transfer between gas and stator	w
q_{p-s}	Heat transfer to stator due to frictional heat generation at gas spring piston	w
q_{r-s}	Heat transfer to stator due to frictional heat generation at piston rod	w

3.3. Electrical heat generation

To compute the electrical heat generation we need to know the electrical current going through the machine. To compute the necessary current to drive the machine we need to know the electrical force $\mathrm{F_{el}}$ necessary to drive the machine. Based on Faradays Law of induction we can then compute the necessary current(Wildi 2006). For the 2B prototype the following relationship between the current $\mathrm{I_{s,\ rms}}$ (rms value) and the average electrical force $\overline{\mathrm{F}}_{\mathrm{el}}$ was derived by Resonator.

(20)

$$\mathrm{I_{s,\ rms}} = \frac{\overline{\mathrm{F_{el}}}}{30\ \mathrm{N/A}}$$

One can expect a linear increase in electrical force $\mathrm{F_{el}}$ by increasing the length of the electrical machine, holding other parameters constant(Wildi 2006).

Electrical heat generation can be divided into three parts; copper losses, eddy current losses and iron losses in the back iron.

The heat generation from copper losses $\mathrm{P_{cu}}$ can be computed from the following equation(Wildi 2006):

(21)

$$\mathrm{P_{cu}} = \mathrm{RI_s^2}$$

Where R is the electrical resistance in the copper wire and I_s is the current in the stator.

Eddy current losses are more difficult to estimate. It depends on the piston velocity, machine design temperature and the magnetic field strength(Wildi 2006). Since the Eddy current losses are difficult to compute analytically (in this type of machine), they are usually computed using finite element analysis (FEA). Resonator has estimated the eddy current losses for the 2B prototype to be about 200W at $P_{el} = 3500W$.

To estimate the iron losses P_{fe} we can assume that all the Iron losses are in the back iron. Then we can compute the back iron losses based on the manufacturer data. (Assume similar design as the 2B prototype).

(22)

$P_{fe} = 20{,}4 \frac{W}{kg}$ @ 1.5 T magnetizing @ 100 Hz (*Somaloy SMC-Rings data sheet Resonator batch 1* 2011)

The total electrical heat generation $\dot{E}_{g-EL}$ is the sum of the copper-losses, eddy-current losses and back-iron losses. The total electrical heat generation at nominal values is estimated to 400 W giving an electrical efficiency of 89% (Resonator AS 2011).

3.4. Mechanical heat generation

When the frictional forces are determined, we can determine the frictional heat generation.

Generally the equation frictional heat generation $\dot{E}_{g-fric}$ is:

(23)

$$\dot{E}_{g-fric} = F_f \dot{x}$$

Where F_f are the frictional force(s) and $\dot{x}$ is the velocity.

The heat generation from viscous damping can be estimated in a similar way(Jewett & Serway 2010):

(24)

$$\dot{E}_{g-damp} = F_d(x)\dot{x} = c\dot{x}\dot{x} = c\dot{x}^2$$

Where $F_d(x)$ are the damping force(s), c is the damping coefficient and $\dot{x}$ is the velocity.

Equation (7), (8), (12), (13), (36) and (37) gives us the following equations for heat generation that leads to heat transfer into the machine.

Heat generation at piston one, assuming the viscous damping at the pistons to be neglect able:

(25)

$$\dot{E}_{fp_1} = 0.491 p_0 \left[\frac{x_{gsc}}{x_{gsc} - x}\right]^{\gamma} \dot{x} + 103.1\,\dot{x}$$

Heat generation at piston two:

(26)

$$\dot{E}_{fp_2} = 0.491 p_0 \left[\frac{x_{gsc}}{x_{gsc} - x}\right]^{\gamma} \dot{x} + 103.1\,\dot{x}$$

Heat generation at the two rod supports combined, assuming similar frictional and damping forces at the two rod supports:

(27)

$$\dot{E}_{gr} = F_{fr}\,\dot{x} + c_r \dot{x}^2$$

(28)

$$\dot{E}_{gs} = F_{fs}\dot{x} + c_s \dot{x}^2$$

3.5. Heat transfer due to heat generation

The first law of thermodynamics states that "*The increase in the amount of energy stored in a control volume must equal the amount of energy that enters the control volume, minus the amount of energy that leaves the control volume"(Incropera et al. 2010: 19).* From this we can write that the change in stored energy $\dot{E}_{st}$ in a control volume is:

(29)

$$\dot{E}_{st} = \dot{E}_{in} - \dot{E}_{out} + \dot{E}_g$$

Where E_{in} and E_{out} is the energy transport across the control surfaces and E_g is the thermal energy generation.

In a simplified system we can define four control volumes for the 2B prototype; each of the gas spring chambers, the piston and the stator. It is clear that all of these control volumes will have a non-uniform temperature distribution especially the piston and stator due to a large thermal mass and uneven heat generation in the machine. However since the piston and stator is separated by low thermal conductivity materials and we have gas in the gas spring chambers this is a natural way to divide the machine. To be able to perform a more accurate thermal analysis we will have to conduct a finite element analysis. Defining control volumes and heat flows are none the less a useful tool on the way to a full transient thermal finite element model.

Generally heat can transfer between the control volumes in three ways; by conduction, convection and radiation. Generally we have (Incropera et al. 2010):

Heat transfer by conduction in its simplest form, 1D

(30)

$$q_{con} = -kA\frac{dT}{dx}$$

The net radiative heat transfer to a surface may be expressed in terms of the emissive power E_{bi} and the absorbed irradiation J_i

(31)

$$q_i = \frac{E_{bi} - J_i}{(1 - \epsilon_i)/\epsilon_i A_i}$$

Where ϵ_i is the emissivity and A_i is the surface area, and E_{bi} can be expressed as $\sigma_b T_i^4$, where σ_b is the Stefan-Boltzmann constant and T is the surface temperature.

Due to the small value of the Stefan-Boltzmann constant ($5.67 * 10^{-8}$) radiation is usually not a significant source of heat transfer in low to moderate temperatures with small temperature differences.

Heat transfer by convection

(32)

$$q_{conv} = hA(T_s - T_\infty)$$

Where h is the convection coefficient, A is the surface area, T_s is the surface temperature and T_∞ is the fluid temperature.

The section above has shown the governing principles for heat transfer in and from the machine. To model the machine a finite element analysis is the recommended method.

3.6. Work done on and by gas

The work done compressing gas is defined (Moran & Shapiro 2010) as:

(33)

$$W_{gas} = \int_{v_i}^{v_f} p \, dv$$

If we assume that we have an adiabatic compression and expansion in the machine we can write (eq. (3)+(30))

(34)

$$W_{m-gas} = \int_{v_i}^{v_f} \frac{c}{v^\gamma} dv$$

Similarly the work done by the gas on the machine is

(35)

$$W_{gas-m} = \int_{v_f}^{v_i} \frac{c}{v^\gamma} dv$$

So that W_{m-gas} - $W_{gas-m} = 0$, this is however not entirely true since there will be some heat transfer between the gas and the machine during the cycle. This heat transfer depends on the temperature difference between the gas and the gas spring housing, and the convection coefficient between the gas and the housing.

3.7. Lubrication

To generate the necessary impact energy, the free piston linear machine needs to obtain a high relative velocity between the magnet piston and the stator. With increasing velocity and frequency lubrication become increasingly important.

Lubrication affects the wear, friction and cooling of the machine. Proper lubrication design greatly reduces friction wear and heat generation. Lubrication is often split up in four different types; thick film lubrication, mixed lubrication, boundary lubrication and solid lubrication (Szeri 2011). Figure 4 shows the different lubrication regimes in a journal bearing, friction coefficient μ, viscosity η, sliding speed U and load W. We can expect a similar behavior for a reciprocating piston(Flitney & Brown 2007).

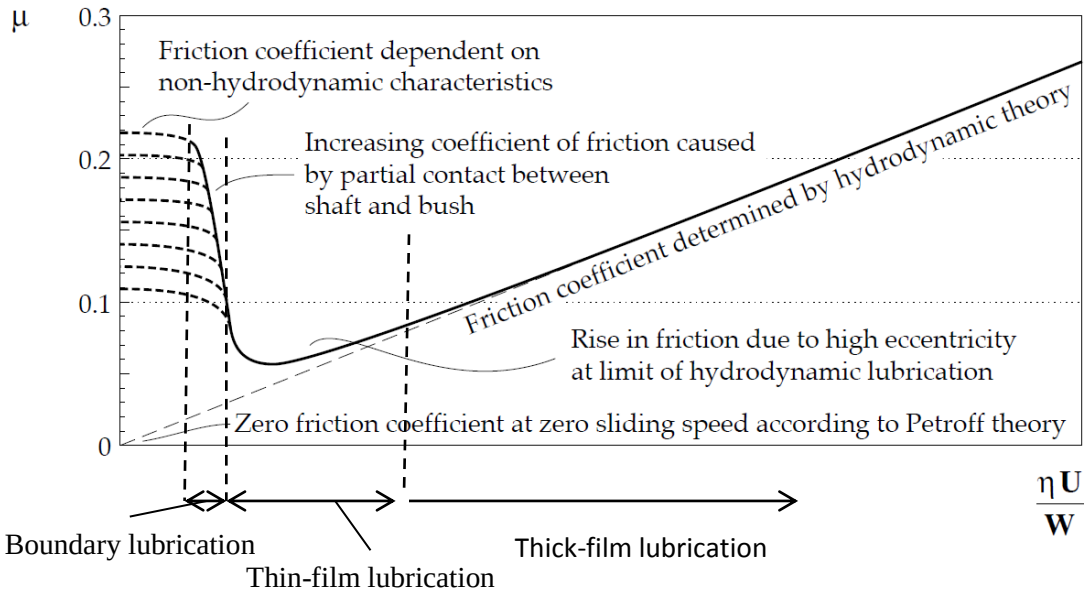

Figure 4, Illustation of the different types of lubrication, (Stachowiak & Batchelor 2005)

Thick-film lubrication is the most desired form of lubrication, it offers the lowest wear and friction, and the best cooling. Thick film lubrication occurs when the film thickness exceeds about 2.5 µm. The friction *f* in thick-film lubrication depends on the specific load, speed and the lubricant bulk viscosity.

Mixed lubrication occurs when we have a varying degree of thin-film lubrication. In this lubrication regime the coefficient of friction depends on the surface roughness, and the material properties of the lubricant and solid materials. For increasing smoothness the curve in Figure 4 shifts to the left.

In boundary lubrication the film is so thin that the fluid properties are no longer the same as those of the bulk. Sometimes the fluid film becomes thinner than the surface asperities then the other properties than the fluid viscosity become important (Stachowiak & Batchelor 2005).

Solid lubrication is based on some materials strong mechanical anisotropy. It relies on some materials ability to be strong in compression and weak in shear along certain directions (sliding direction). Solid lubrication is generally only used where liquid lubrication is not possible(Stachowiak & Batchelor 2005).

3.8. Seals

The gas springs need both static and dynamic seals. When designing the prototype 2B Resonator was in contact with many seal suppliers to find suitable sealing solutions. Especially their demands to the reciprocating seals proved to be challenging.

Gas spring cross section	Number	Description
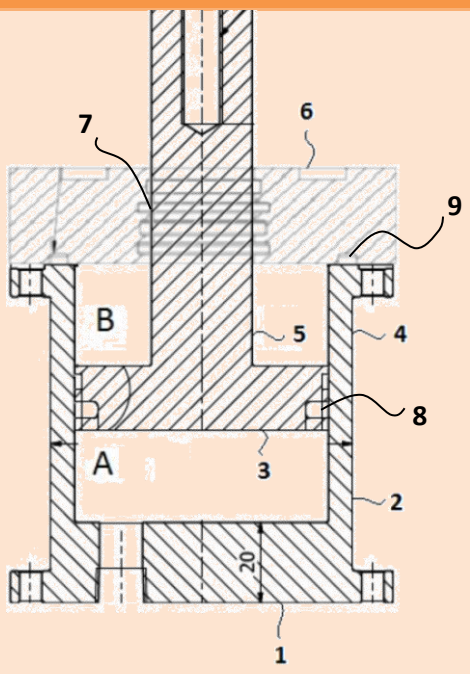	1	End of gas spring / machine
	2, 4	Gas spring cylinder
	3	Gas spring piston
	5	Gas spring rod, connects to magnet piston
	6	Gas spring flange / end flange, supports gas spring rod.
	7	Rod seal
	8	Piston seal
	9	Static flange seal
	A	Outer gas spring chamber
	B	Inner gas spring chamber

Figure 5, Gas spring cross section, (Pedersen 2011)

Figure 5shows the gas spring cross section and a description of the major parts in the gassprings. From Figure 5 we se that there is one seal arangement at the piston and one in the flange. The seal arangment in the flange (sealing around the rod) is only necessary if using double acting springs.

There is also a static seal between the flange and the gas spring cylinder. This seal is also only necessary in double acting mode.

3.8.1 Reciprocating seals

The prototype 2B gas spring has two different reciprocating seals, two at the rod and one at the piston, the seal groves are shown in Figure 5. Figure 6- Figure 8 shows the piston and rod seal in detail, and their working principle.

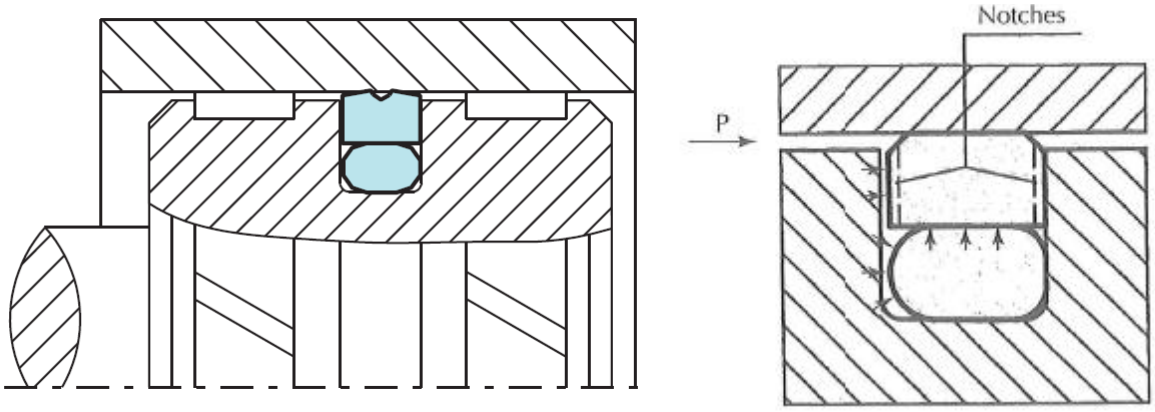

Figure 6, LHS, Piston Seal with back o-ring energizer, Turcon® Glyd Ring® Hz, (Trelleborg 2011a)

Figure 7, RHS, Piston seal seal working Principe, (Flitney & Brown 2007)

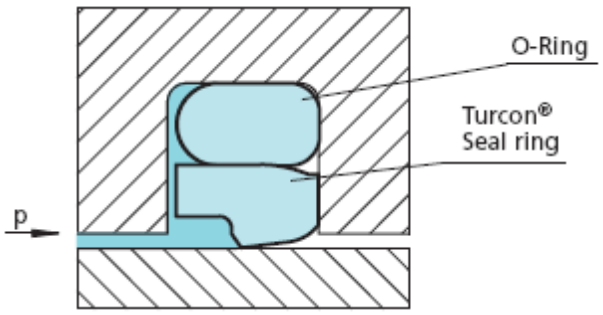

Figure 8, Rod seal with back o-ring energizer, turcon stepseal 2k, (Trelleborg 2011a)

When choosing a reciprocating seal there is many parameters to consider; Table 4 summarizes the most important and shows the required values for the 2B prototype and how they relate to typical values.

Table 4, Seal selection parameters (Flitney & Brown 2007), (Trelleborg 2011a), (Bostad 2011)

Seal selection	
Parameter	**2B requirement**
Fluid	Inert gas
Pressure	High, 30 MPa
Speed	Extreme, 10 m/s
Frequency	Extreme, 100 Hz
Leakage	Dynamic, 1%/hr Static, .1%/hr<
Life expectancy	Extreme, minimum $2*10^6$ cycles -> 5.5 hours @ 100 Hz
Production quantity	Small, prototype production
Operating temperature	Preferred to be up to 200 C, minimum 100 C.
Operating environment	Can be hermetically sealed, challenging to control lubrication

The seals used are self-energizing and pressure energized, the seals relies on initial compression of the back o-ring to provide an initial sealing force, Figure 7. This gives a consistent interference force and a design with wider tolerances, which makes manufacturing easier (Flitney & Brown 2007). The seals used are made of Trelleborgs proprietary Polytetrafluoroethylene (PTFE) blend called M12.

According to research done on other elastomeric sealing solutions[1], the seals selected to the prototype 2B are some of the best on the market for this application. Good seals however are only a part of the total solution.

During operation reciprocating seals are subjected pressure cycles and frictional forces from relative motion. The dynamic pressure and force components are unlikely to be precisely concentric around the circumference which can lead to a considerable distortion force on the seal. This again can lead to deformation and failure of the seal (Flitney & Brown 2007). Because of these forces the seal and grove design are important, especially in high speed high frequency applications like the 2B prototype. And using a seal with good support is therefore essential.

The film thickness between the seal and the mating surface is an important factor in a sealing solutions (Wangen 2011), a too thick film will lead to unnecessary leakage, while a too thin film can lead to pour lubrication and increased wear. The film thickness can vary with factors such as pressure, sliding speed and direction (to or from pressure side). However the most significant factor governing the film under the seal is the entry geometry. The sharpness of the edge cause a certain contact stress which controls the fluid film thickness, this behavior is not easy to predict and is origin to much research and development at the seal manufactures. For most reciprocating applications it is therefore common to use seals specifically designed for the purpose (Flitney & Brown 2007).

The lubricant film is affected by the sliding speed, with increasing speed the hydrodynamic pressure (from the lubricant) increase, at moderate to high speeds the hydrodynamic pressure is large enough to deform the elastomer in the seal. This leads to an increased lubricant film thickness leading to

[1] (*Seals for extreme enviorments* 2011), (Trelleborg 2011a), (Polymod 2011)

reduced friction(Flitney & Brown 2007). Once the seal is operating in the fully developed hydrodynamic region, the friction will increase with further increase in speed, Figure 4.

Viscosity can has a significant effect on the lubricant film, as follows from Figure 4 the viscosity directly affects the thickness of the lubricant film. With decreasing viscosity the curve in Figure 4 moves left (Stachowiak & Batchelor 2005). Most seals are designed to work with a certain range of viscosities, therefore care must be taken when selecting the lubricant / working media(Flitney & Brown 2007).

At a certain pressure depending of the harness of the material, the elastomer will deform on the surface so that all surface asperities are flattened and full surface contact is attained. Increasing the pressure further from this point will not increase the area of contact. When this state is reached the friction-pressure curve flattens (Flitney & Brown 2007).

Surface texture has a direct effect on seal performance. Research has shown that although surface height parameters such as Ra has a dominant influence on friction and wear, they are only a starting point when considering the surface(Costa & Hutchings 2007). Ra is the arithmetic average value of the profile departure from the mean line, within a sampling length(Oberg & McCauley 2004). This means that entirely different surfaces can have the same Ra. Figure 9 shows three different surface profiles with the same Ra.

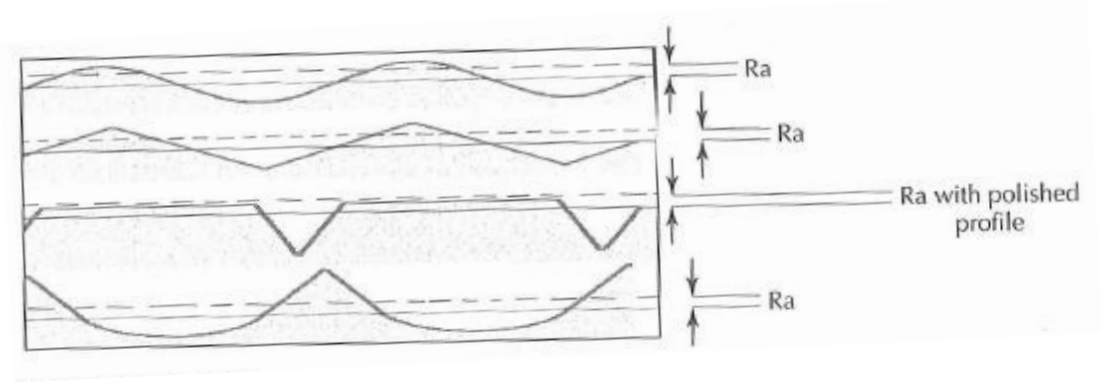

Figure 9, 3 different surface textures with the same surface roughness parameter Ra, (Flitney & Brown 2007)

A grinding operation will, no matter how fine it is, create a surface with sharp peaks. These peaks will penetrate the lubrication film and lead to increased wear Figure 10. The surface texture become extra important when the lubrication film is thin and we move into the elastohydrodynamic regime(Stachowiak & Batchelor 2005).

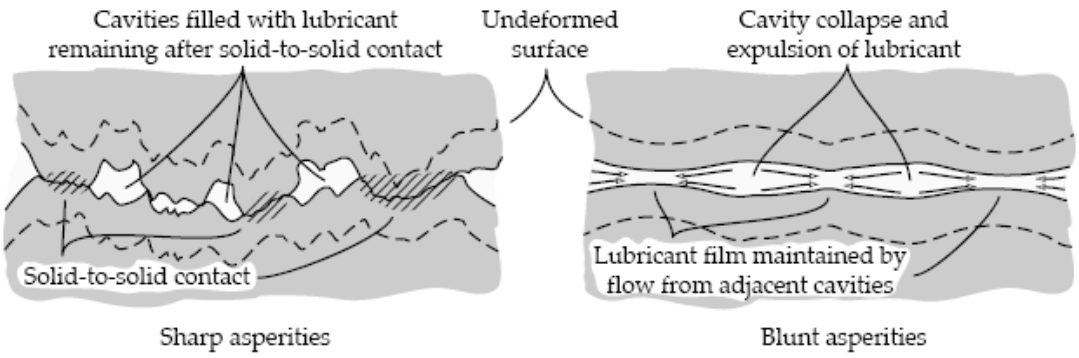

Figure 10, Effect of surface asperities sharpness, (Stachowiak & Batchelor 2005)

According to (Flitney & Brown 2007) seals based on plastic materials such as PTFE should not be used on surfaces with a roughness above Ra 0.25. In addition it is necessary to specify a finishing operation that provides an adequate bearing area and a surface with lubricant reservoirs; this will ensure a good basis for seal operation.

Surface treatment of the gas spring cylinder, piston and piston rod can help improve the performance of the gas springs. There are a large number of surface treatments on the market each designed to meet special needs. The treatments can help improve tribological and wear characteristics and/or protect against corrosion. Many of the surface treatments are also much harder and more scratch resistant which makes it easier to maintain a desired surface texture. Since the surface treatment surface properties may be substantially different from that of the ground material, care must be taken when selecting a seal to work with a surface treatment (Flitney & Brown 2007).

3.8.2 Pressure velocity coefficient (PV)

The product of pressure and velocity (PV) is sometimes used to compare different dynamic seal designs. Having a lower PV value is favorable giving less heat generation and less wear. The PV value can be useful in estimating seal reliability based on manufacturer data (Brown & Piff 2010). The maximum PV value a seal can withstand is usually dependent on temperature, and a higher temperature leads to a lower maintainable PV value for the seal(*Seals for extreme enviorments* 2011).

3.8.3 Static seals

The gas spring relies on a static seal between the gas spring cylinder and the gas spring flange (Figure 5), to seal the gas in the gas spring chamber when working in a double acting configuration.

Research done on static seals, shows that there are several feasible solutions for the 2B prototype (*Seals for extreme enviorments* 2011). The simplest solution is probably an o-ring (Torgersen 2011). The static seals are not a primary focus in this thesis.

4. Method

To obtain the desired understanding of the gas springs and the electromechanical system it is desired to have one or more models simulating the performance of the gas springs / system, and then be able to compare actual test data with the results from the theoretical model(s). The practical testing can also reveal design problems, these problems can then be investigated with theoretical analysis.

Since the 2B prototype was already designed and manufactured in august 2011, it was natural to start assembling the prototype and preparing it to test while at the same time studying gas springs theoretically. Before any testing could be done it was also necessary to develop test procedures and safety manuals. These are presented in appendix A - E.

The rough test plan is presented in Figure 11. The natural place to start is with a static fluid pressure test; this can be done safely at high pressures due to the low compressibility of fluids. This test will confirm the mechanical integrity and reveal potential leakage problems.

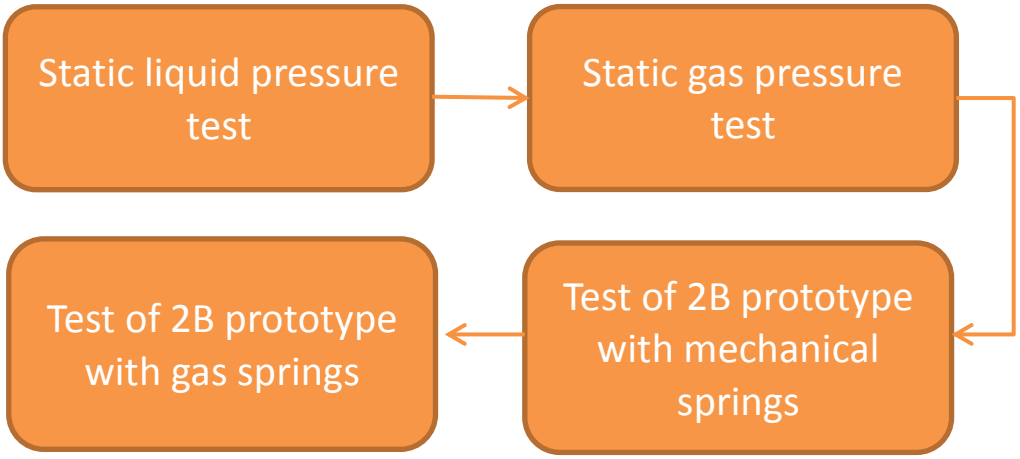

Figure 11, Test plan

The next step is a static gas pressure test; this test should be performed at a higher static pressure than the maximum dynamic pressure in the gas spring, but still lower than the static fluid test pressure. The static gas pressure tests will reveal potential gas leakage problems.

While the gas springs are pressure tested, the electromechanical part of the machine can be function tested using mechanical springs. Since the gas springs have unknown performance at the frequencies the machines is designed to operate (Kaller AB 2011), it is best to first separately test the electromechanical part of the machine to be sure that it is working as intended. This testing will be done by Resonator.

Before testing the gas springs on the machine, the machine should be analyzed to predict the behavior of the machine with gas springs. This analysis should identify structural and thermal limitations. The analysis should also identify what parameters related to the gas springs that are important for the prototype 2B's performance.

During the initial study of gas springs, frictional heating in the gas springs was identified as a potential problem, therefore Per Kristian Pedersen and John Sidders at NTNU was contacted. They agreed to conduct an independent thermal analysis of the gas springs.

After the static tests and the pre-analysis are performed and potential problems are solved, the gas springs can be mounted on the machine and be tested. The tests can indicate if the theoretical analysis is right and could reveal potential machine design problems. If the test data cohere with the theoretical analysis one may be able to use the experience and confidence gained from the tests to improve the design.

Table 5 summarizes the planed tests and analysis.

Table 5, Overview of tests and analysis to be done on the 2B prototype

What	How	Who	Purpose
Electromechanical test. Test of the machine with mechanical springs instead of gas springs	In safe container at the Resonator test center in Ås	Resonator AS	This is a test to test everything with the machine except the gas springs.
Tests of Resonators Gas spring design	- Static fluid pressure test - Static gas pressure test - Dynamic function test Tests are performed according to test procedures listed in the appendix.	Eirik Lind Hånes	Check if the design is working as predicted. How does temperature, friction and wear develop compared to what was predicted.
Electromechanical model, Developed by Resonator	Simscape (matlab)	Resonator AS / Eirik Lind Hånes	This model predicts resonance frequency, piston amplitude, internal pressure and electrical data
Thermal model	Matlab	Per Kristian Pedersen and John Sidders NTNU	Predict operating temperature
Thermal model	ANSYS	Eirik Lind Hånes	Predict operating temperature, compare with NTNU's theoretical model. Investigate potential thermal problems.
Simplified structural thermal models	MS Excel/ ANSYS /CosmosWorks	Eirik Lind Hånes	Predict internal pressure, Spring force and gas working temperature. Easy to use.

5. Analysis

5.1. Frequency analysis

To be able to analytically derive an expression for the mass-spring system it is convenient to use idealized linear springs where the force is proportional to the displacement. Figure 12 shows such a system with a damper included. The friction in the gas springs are also not included in this system, it is more difficult to model since it is pressure dependent.

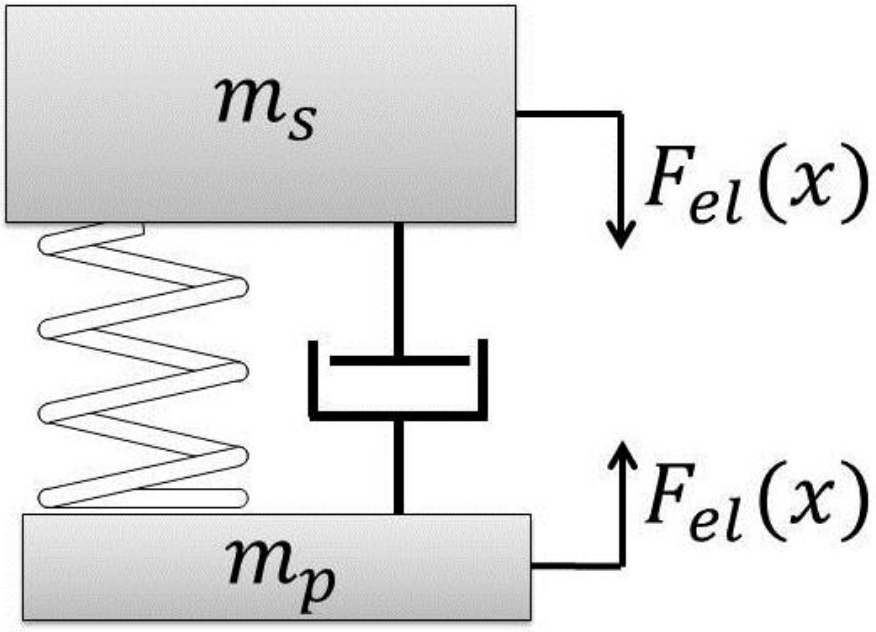

Figure 12, Simple free one spring two masses system.

To derive the differential equations of the system the bond graph method was used(Karnopp et al. 2006). Figure 13 shows Figure 12 represented by a bond graph. From this we can easily derive the differential equations for the system.

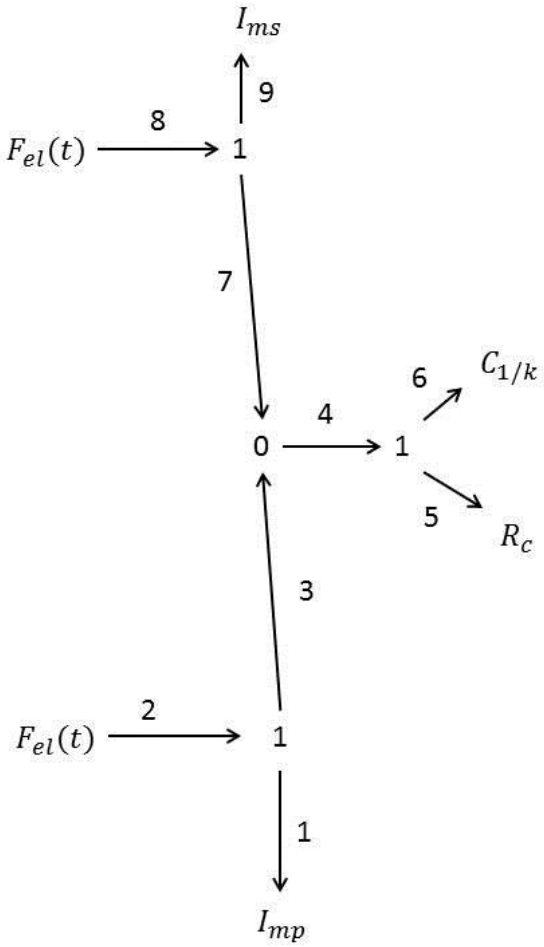

Figure 13, Shows Figure 12 represented by a bondgraph

Figure 13 gave the following 3 state-space equations:

(36)

$$\dot{p}_1 = F_2(x) - \frac{q_6}{C_6} - R_5\left(\frac{P_9}{I_9} + \frac{P_1}{I_1}\right)$$

(37)

$$\dot{q}_6 = -\frac{p_9}{I_9} - \frac{p_1}{I_1}$$

(38)

$$\dot{p}_9 = F_8(x) - \frac{q_6}{C_6} - R_5\left(\frac{P_9}{I_9} + \frac{P_1}{I_1}\right)$$

Where p is momentum, q is displacement, C is compliance, R is resistance, I is inertia, F(t) is the force as a function of time and the subsequent subscripts are the bond numbers. To solve this third order system we substitute C with 1/k, R with c, where k is the spring constant, c is the viscous damping coefficient. We substitute I_1 with m_p and I_9 with m_s, then we put equation (36) - (38) in to a matrix, and find the eigenvalues of the matrix, this yields the following natural frequency for the two mass system.

Undamped natural frequency:

(39)

$$\omega = \left(\frac{k}{m_s} + \frac{k}{m_p}\right)^{0.5}$$

Damped natural frequency:

(40)

$$\omega_d = \frac{-cm_s - cm_p + \sqrt{c^2 m_s + c^2 m_p + 4\,k\,m_s m_p}}{2\,m_s m_p}$$

To check the solution we can make one of the masses in equation (39)infinite, as if one of the masses were connected to earth with a spring this yields the well known $\omega = \sqrt{k/m}$.

The ratio between the velocities of the two masses can be derived the following way (Bostad 2011):

(41)

$$\vec{F}_{gs} = m_p \vec{a}_p(t) = -m_s \vec{a}_s(t) \quad \rightarrow \quad -\frac{\vec{a_s}(t)}{\vec{a_p}(t)} = \frac{m_p}{m_s}$$

Acceleration velocity and displacement are easily associated since the two objects resonate at the same constant frequency (ωt is the same for both masses).

(42)

$$\frac{m_p}{m_s} = -\frac{\vec{a_s}(t)}{\vec{a_p}(t)} = -\frac{\vec{v_s}(t)}{\vec{v_p}(t)} = \frac{v_s(t)}{v_p(t)}$$

This is an important relationship since this affects how much of the total kinetic energy that is stored in each of the two masses.

5.1.1 Gas spring stiffness equivalent

Solving the differential equations for the machine with gas springs is not trivial. Therefore resonator has made a model of the system solving the differential equations numerically. (The model is still under development). When testing the machine it is convenient to have an expression predicting the frequency of the machine. To optimize the gas spring chamber it is also convenient to have an expression for the gas spring stiffness.

To find the gas spring, equivalent to a linear spring, we know that the work during the stroke the two springs does must be the same, thus:

(43)

$$\int_{x_1}^{x_2} W_{linear} = \int_{x_1}^{x_2} W_{gas}$$

For the system in the resonator machine with two single acting gas springs, this can be written as:

(44)

$$\int_0^{x_{rel_m}} kx\,dx = \int_0^{x_{rel_m}} \left(F_{GS_1} - F_{GS_2}\right)dx$$

Substituting F_{GS_1} and F_{GS_2} with equation (6) and (7) yields

(45)

$$\int_0^{x_{rel_m}} kx\,dx = \int_0^{x_{rel_m}} \mathrm{A_{gs}p_0}\left(\left[\frac{\mathrm{x_{gsc}}}{\mathrm{x_{gsc}-x}}\right]^{\gamma} - \left[\frac{\mathrm{x_{gsc}}}{\mathrm{x_{gsc}+x}}\right]^{\gamma}\right)dx$$

Computing the integrals on both sides and solving for the gas spring stiffness equivalent (k) gives

(46)

$$k_{GS_{net}} = \frac{2A_{gs}\,P_0\left(-\left(\frac{x_{gsc}}{x_{gsc}+x_{rel_m}}\right)^{\gamma}\left(-\frac{x_{gsc}}{\gamma-1}+\frac{x_{rel_m}}{1-\gamma}\right)+\left(\frac{x_{gsc}}{x_{gsc}-x_{rel_m}}\right)^{\gamma}\left(\frac{x_{gsc}}{\gamma-1}+\frac{x_{rel_m}}{1-\gamma}\right)+\frac{2\,x_{gsc}}{\gamma-1}\right)}{x_{rel_m}^2}$$

Where A_{gs} is the gas spring area, P_0 is the initial pressure, x_{gsc} is the initial gas spring length, γ is the gas polytrophic coefficient and x_{rel_m} is the maximum relative amplitude between the gas spring piston and gas spring chamber.

When we have computed the Gas spring stiffness equivalent, we can use this to estimate the systems natural frequency $f_n = \omega_n/2\pi$. For two free masses ($m_1 and\ m_2$) connected with a spring we have the following natural frequency (eq. (39)):

(47)

$$f_n = \frac{1}{2\pi}\sqrt{\frac{k_{GS}}{m_1}+\frac{k_{GS}}{m_2}}$$

When applying this theory to the 2B prototype, it significantly changes the estimated initial and maximum pressure at 100 Hz and 16 mm amplitude. Table 6, Shows new and old nominal values. The pressure difference over the rod seal is almost 0 bar for the single acting configuration since there is no initial pressure (only atmospheric pressure in the inner chambers Figure 5).

Table 6, Shows new and old nominal values

Description	Unit	Initial values given (old)	New values calculated
Maximum piston velocity	m/s	10	10
Piston frequency	Hz	100	100
Piston amplitude	m	0.016	0.016
Initial pressure	Bar	60*	42
Maximum working pressure	Bar	330*	200
Maximum pressure difference piston seal	Bar	300*	200
Maximum pressure difference rod seal	Bar	330*	0
Life time	Cycles	$2 * 10^6$	$2 * 10^6$
*Old values were with double acting springs, new are with single acting (this means that the difference is even greater)			

Figure 14 shows a plot of frequency vs relative amplitude between piston and stator using the gas spring constant. Calculations are in appendix R.

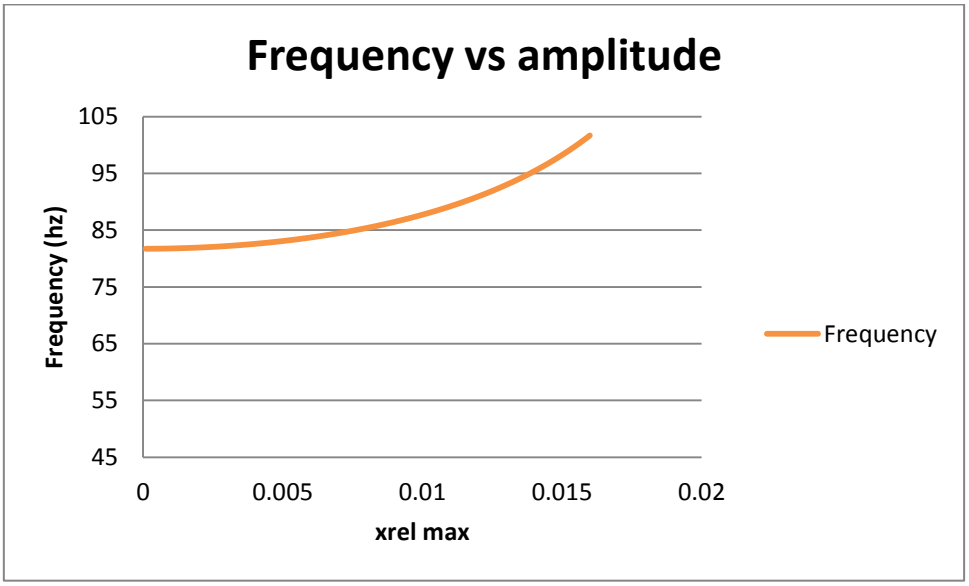

Figure 14, Frequency vs amplitude

5.1.2 Gas spring chamber optimization

It is desired to have an as low as possible maximum pressure in the gas spring chambers. At given relative amplitude, gas spring area and working gas, the gas spring stiffness equivalent depends on the initial pressure and gas spring chamber length. It is therefore interesting to optimize the gas

spring length, so that the maximum pressure is as low as possible at a given frequency. Using eq. (11) (46) and (47) we can perform such an analysis for the 2B prototype, by changing the gas spring length and initial pressure holding the natural frequency constant.(i.e. $k_{GS_{net}}$). This analysis was used by multiple goal seek in excel, the excel spreadsheet and the VBA code is in appendix S. Using the 2B nominal values as a starting point gave Figure 15.

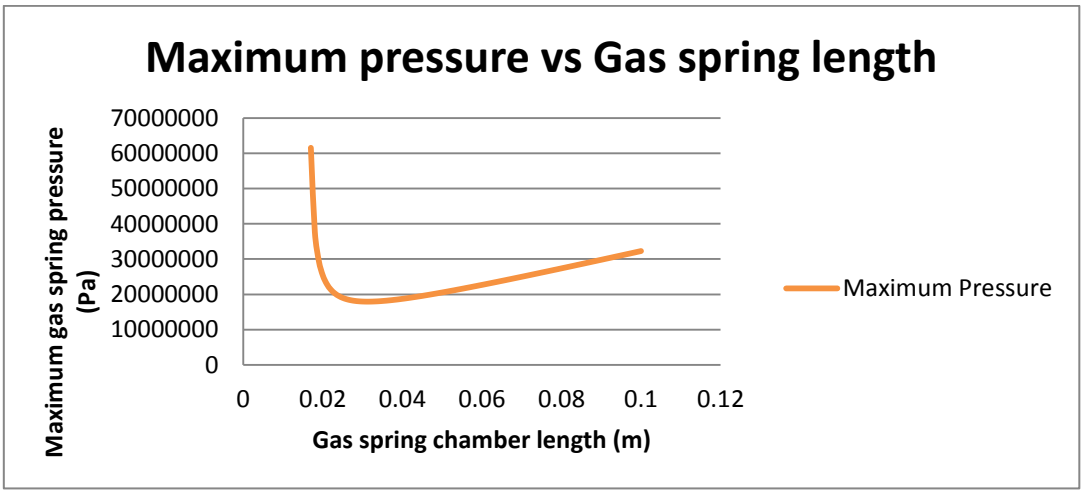

Figure 15, Maximum working pressure vs Gas spring chamber length for the 2B prototype at 100 Hz and 16 mm. stroke

If we assume that the machine is limited by the performance of the seals in the gas springs , which are generally limited by the product of velocity and pressure (*Seals for extreme enviorments* 2011), we see designing the gas springs to the right length, can substantially increase the performance of a machine as the 2B prototype. Additionally the force working on the structure is reduced, making the structural design easier.

5.1.3 Parameter study of the 2B prototype in test mode

To see how changing one parameter changes the performance of the machine a small parameter study was performed. It was performed under the following conditions; in a free piston resonating machine there will be a maximum allowable relative velocity. For the 2B prototype the maximum relative velocity is limited to 10 m/s (Resonator AS 2011), therefore this was set to constant. The nominal values for the 2B prototype were used as a starting point for the analysis. This parameter study does not consider whether the machine is able to deliver enough electrical power or withstand the increased forces induced by the changes. The nominal values for the 2B prototype are presented in Table 7.

Table 7, 2B nominal values

Parameter	Value	Unit
Total mass of machine	26.2	kg
Mass of stator	17.6	Kg
Mass of piston	8.6	Kg
Operating frequency	100	Hz
Maximum relative velocity	10	m/s
Linear spring stiffness equivalent	2180	N/mm
Electrical power	3.5	kW

The tree parameters that are investigated are; Total mass of machine, ratio between mass of stator and mass of piston and the total spring stiffness. Figure 16 shows how change in these three parameters affects the maximum available hammering power of the machine. The maximum available hammering power P_{hm} is a product of hammering frequency f and the energy per blow E_i. The maximum energy per blow is the kinetic energy of the stator housing. As we see from equation (1) the ROP for a drilling machine is greatly affected by this parameter.

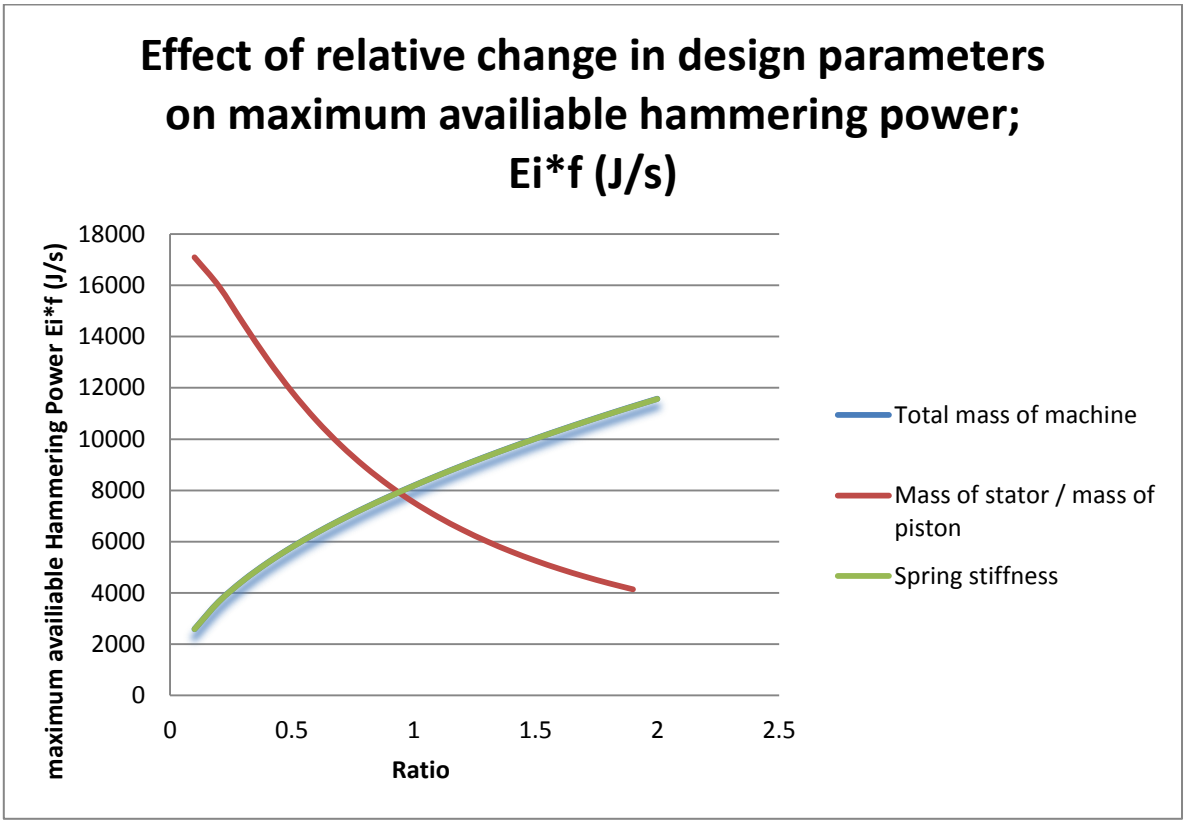

Figure 16, Parameter study

From Figure 16 we see that changing the total mass of the machine and changing the total spring stiffness have the same effect on the maximum available hammering power P_{hm}. We also see that changing the ratio between the stator mass and piston mass greatly affects P_{hm}. From Figure 16 it seems that the ratio should be as small as possible. There will however probably be a minimum value for this ratio. If the stator mass get very small compared to the piston mass, all the systems kinetic energy will be in the stator mass (follows from eq.(18) and (42)) , when the stator mass then hit the rock it loses all its kinetic energy. If there is no kinetic energy left in the machine it will go out of resonance, and have to restart, this will lead to a poor ROP. The calculations done in the parameter study can be found in appendix V.

It must be noted that the behavior of the machine in test mode (without top spring), is different from the behavior of a similar machine in drill mode. It is however still interesting to see how changing the parameters affects the behavior of the machine.

5.1.4 Frequency in drill mode

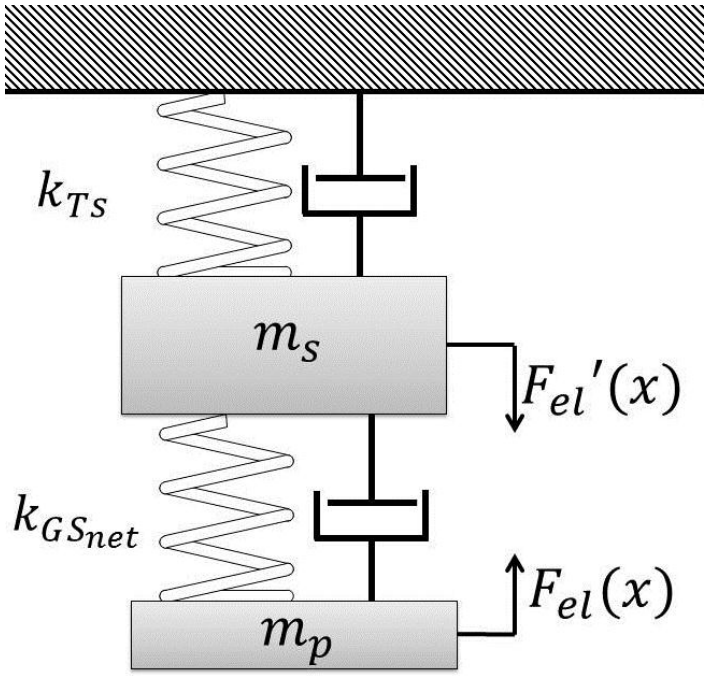

Figure 17, Principal drawing of the machine in drill mode

In the future Resonators plan is to use their machine for drilling. Then the machine will be connected to the drill string by an external spring. This affects the frequency and the amplitude relationship of the two masses in the system. These relationships are very important when analyzing if the use of gas springs is feasible in resonators application.

In this system we now have two degrees of freedom (giving 4 linear differential equations). If we neglect the effect of damping, friction and external forces, the differential equations for such a system is (free response)

(48)

$$m_s\ddot{x}_s = -k_{TS}x_s + k_{GS_{net}}(x_p - x_s)$$

(49)

$$m_p\ddot{x}_p = -k_{GS_{net}}(x_p - x_s)$$

If we solve this system we get the following relationship for the angular frequency (Terjesen 2011)

(50)

$$\omega_{1,2}^2 = \frac{A+B}{2} \pm \sqrt{\left(\frac{A-B}{2}\right)^2 + B\,C}$$

Where $= (k_{ts} + k_{GS_{net}})/2$, $B = \frac{k_{GS_{net}}}{m_p}$ and $C = \frac{k_{GS_{net}}}{m_s}$. Where k_{ts} is the top spring stiffness (external spring).

The system has the following solution (real)

(51)

$$x_s = A_s \sin(\omega t)$$

(52)

$$x_p = A_p \sin(\omega t)$$

Where A_s is the amplitude of the stator mass and A_p is the amplitude of the magnet piston. If we substitute the solution into eq. (48) and (49) we can find the relationship between the amplitudes of the two masses

(53)

$$\frac{A_s}{A_p} = \frac{K_{GS_{net}} - m_p\omega^2}{k_{GS_{net}}} \text{ and } \frac{A_s}{A_p} = \frac{k_{GS_{net}}}{k_{Ts} + k_{GS_{net}} - \omega^2 m_s}$$

For the first mode; when the masses are moving in phase, the relative amplitude is

(54)

$$x_{rel_m} = |A_p - A_s|$$

When the masses are moving in antiphase the relative amplitude is

(55)

$$x_{rel_m} = A_p + A_s$$

Eq. (50) has two solutions, however since the electrical force acting on the magnet piston also has an equal and opposite force acting on the stator, the machine must run in antiphase to function. Therefore only ω_2 is a viable solution for resonators application. Eq. (53) and (55) are important relationships when designing a resonating drill machine with gas springs, because with all gas spring solutions we will have a limited maximum relative velocity. The maximum relative velocity is directly related to the relative amplitude at a given frequency (eq. (42)).

It is important that the amplitude ratio has the right value, so that as much as possible of the kinetic energy in the machine is available for hammering (kinetic energy in stator). The ratio of kinetic energy in the stator to the total kinetic energy in the machine must however not be too big, because this means that the machine will lose too much of its energy at impact so that it will not be able to recharge to the next blow.

Since the amplitude relationship is of such importance, it is interesting to see if it is possible to change the amplitude relationship at a given frequency with given masses. Using Eq. (50) and (53) holding the frequency constant while changing the top spring and gas spring equivalent gave Figure 18 and Figure 19. The nominal values for prototype 2B were used as a starting point.

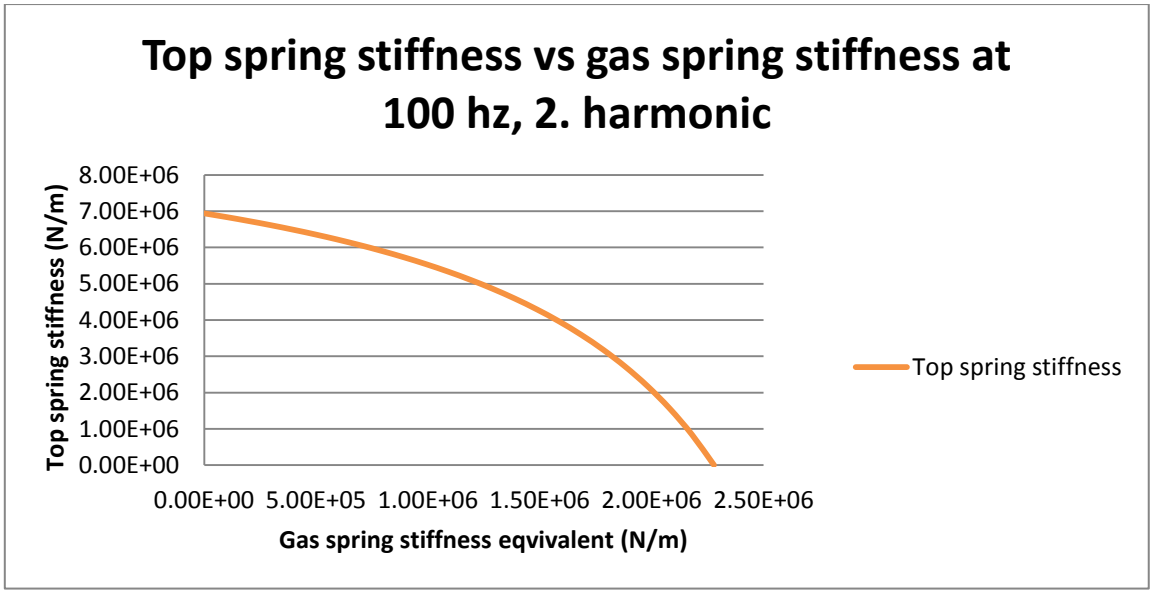

Figure 18, Top spring stiffness vs gas spring stiffness

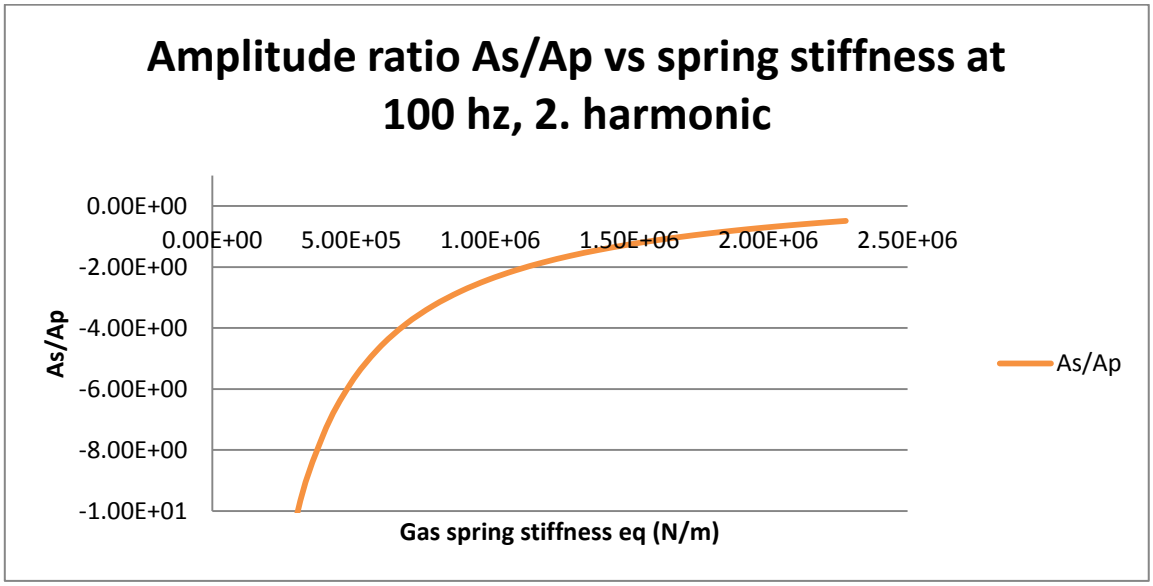

Figure 19, Amplitude ratio

As we see from Figure 19 the amplitude ratio can be changed considerably by changing the spring stiffness. From Figure 18 we see that at desired amplitude ratios the top spring is relatively soft and the gas spring stiffness equivalent is about the same as in test mode (equal stiffness gives equal frequency). This means that running the tests without top spring should give a good approximation to how the gas springs will function in an actual drilling application.

5.2. Structural Analysis

Although resonator had done some structural analysis when designing the prototype 2B, it was somewhat unclear what the structural limitations of the machine where. Before starting any dynamic tests of the 2B prototype, a structural analysis of some of the main components was therefore carried out. Accurate fatigue data for all the material used was not found, therefore data for similar

materials where used. The structural analysis in this section is not complete and only meant as a first approximate check on the strength.

Initially Resonator wanted to use double acting gas springs in each end of the machine. Figure 20 shows the forces acting on the piston in a machine with double acting springs. When the magnet piston moves right the gas in the right chamber on the left spring and the right chamber in the right spring is compressed. The net forces acting on the magnet piston in this scenario are shown in Figure 21. The forces acting on the stator housing are equal and opposite.

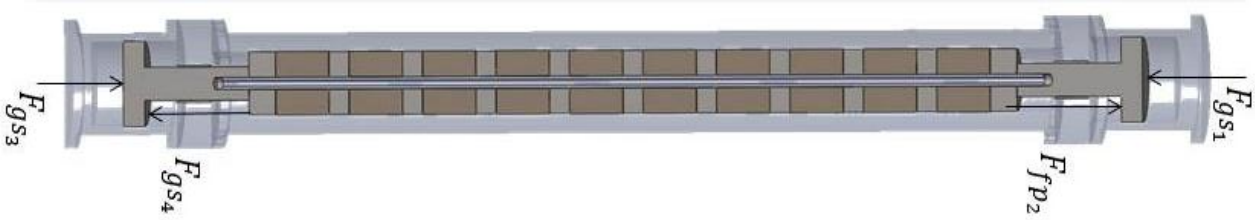

Figure 20, Forces on piston with double acting springs

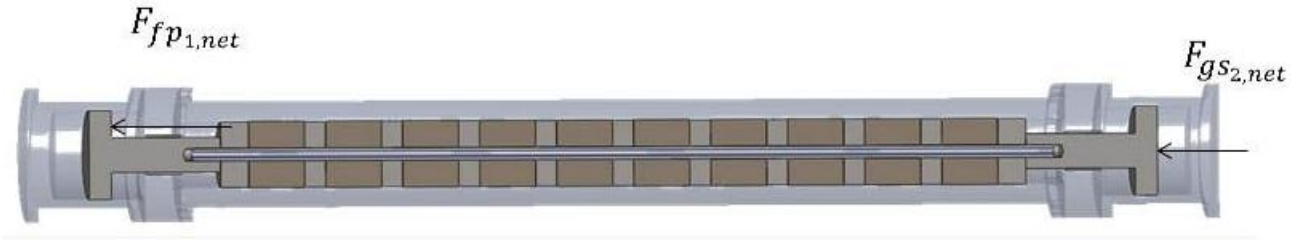

Figure 21, Net forces acting on the piston when it is right of the center position

The machine was initially designed to have the force from the two chambers in each spring to be equal (by having a higher initial pressure on the rod-side). This means that the tension force in the rod will be big during a part of the cycle. Figure 22 shows the rod force during one cycle, calculations are in appendix Q.

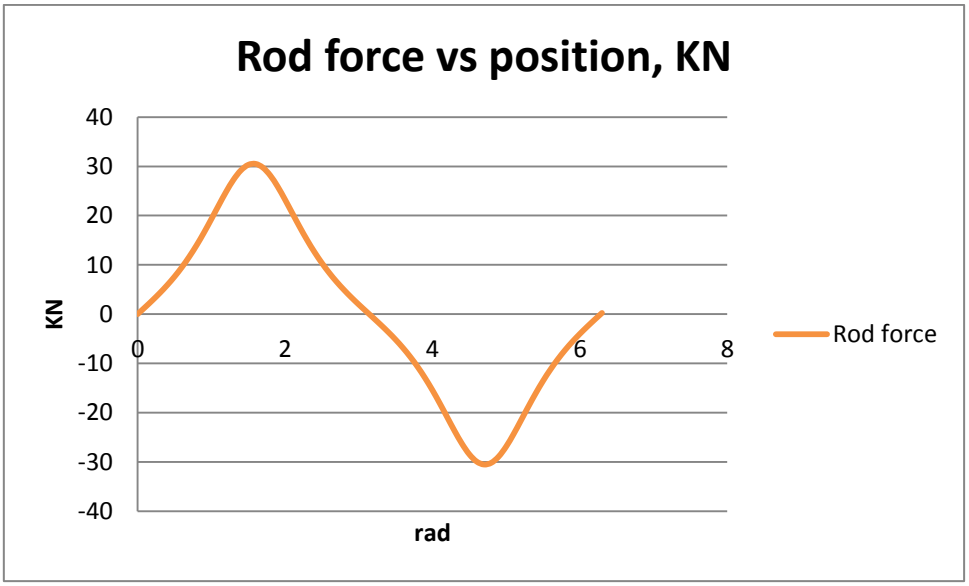

Figure 22, Rod force vs position for one of the double acting springs, at nominal values.

When investigating the detailed drawing of the gas spring and resonator machine Figure 21 and, we see that the magnet piston is attached to the gas spring by a small bolt (M10 X1 hollow (6 mm) bolt). This means that there is a very small tensile stress area.

The connection between the gas spring and the magnet piston cannot be pre-tightened the way prototype 2b is made. This means that the entire force tension force (30 kN) goes in to stress amplitude in the bolt. This gives the following maximum mean tensile stress in the connection

$$\bar{\sigma}_{Bolt} = \frac{F}{A_{tensile\ stress}} = \frac{30\,000N}{61.2mm\text{^}2 - 3.14 * 0{,}25 * 36mm\text{^}2} = 1010\ MPa$$

According to DNV-RP-203[2] the maximum allowable tensile stress in cut threads (present in this connection) are 21.05 MPa. This gives a safety factor of 0.02. It is easy to see that this is not a viable design. Based on this calculation it was decided not to use the inner chambers before a different design is made. Therefore all the other analysis done in this thesis is assuming single acting gas springs.

To increase the strength in tension connections we can incorporate pre-stressing, by extending the bolt through the pistons and adding a nut in both ends we will be able to pre-tighten the bolt.

In a pre-tightened bolt the force amplitude F_T is (Waløen 1971):

(56)

$$F_T = \frac{F_L}{1 + \frac{\sum_T \sigma_T}{\sum_A \sigma_A}}$$

Where σ_T is the deformation due to pre-tightening in the elements that experience an increasing force when the load $F_L$is applied, and σ_A is the elements that experience a decreasing load when the load F_L is applied. For the a-elements the load is distributed on an area equal to

$0.25 * \pi(2 * D_{tension\ element})^2$, as long as the outer diameter of the a-elements are bigger or equal to $2 * D_{tension\ element,}$ (Waløen 1971)

By dividing F_T by the tensile stress area (A_{TS}) we get the stress amplitude that the bolt is experiencing. Using the spread sheet in appendix T, we see that there is little to gain by increasing the bolt diameter past 16 mm. This is because this will increase the deformation in the A-elements since the outer diameter of the piston rod is only 25 mm.

We see that by pre-stressing the bolt the connection is able to withstand about 17 kN if we use a M16 bolt with rolled threads. A bolt with rolled threads can withstand a higher stress amplitude (36.84 MPa) (Det Norske 2010) than one with cut threads. Even with this upgrade there is a long way to the desired 30 kN load carrying capacity. To increase the strength we can generally do tree changes; increase the stiffness in the a-elements, decrease the stiffness in the t-elements or use a bolt that can withstand higher stress amplitude. This follows from equation (56) . To be able to increase the stiffness of the a-elements, we have to increase the gas spring rod diameter. This is one possibility, but it affects other parts in the assembly which would have to be changed. It also reduces the gas-spring volume and increase the difference in area between the two sides of the piston, which is undesired. To be able to decrease the stiffness and increase the strength of the bolt/t-elements we

[2] (Det Norske 2010)

have to look towards unconventional fasteners, maybe titanium which has a lower modulus of elasticity than steel.

Since only the outer chambers can be used, the pressure in these chambers has to be increased to reach the nominal values. This gives about 195 bar maximum pressure in the chambers. And a maximum rod force of 60 kN, Figure 23.

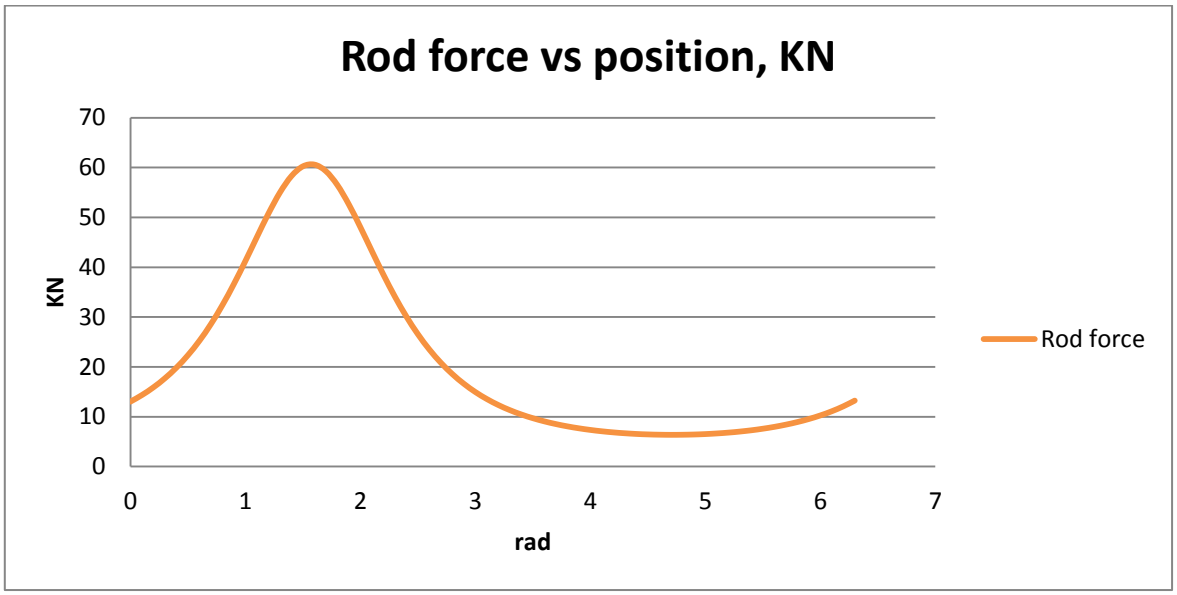

Figure 23, Rod force vs position single acting gas springs

5.2.1 Flange connection

By pre tightening the bolts to the right tensile stress, we increase the bolts strength substantially. But it requires good flange design to fully benefit the effects of pre-tightening. As discussed in the previous section we want stiff a-elements and elastic t-elements to increase the bolts strength.

If we study Figure 5, we see that there is a small (1 mm) gap between the gas spring chamber and the mating flange. This is not good for the stiffness of the a-elements. Originally there also where a flat gasket between the gas spring chamber and the flange which will drastically decrease the stiffness of the a-elements (if there is no metal to metal contact between the two parts). By machining of the 1 mm edge on the gas spring chamber and replacing the flat gasket by an o-ring seal (with a groove on the mating flange), we ensure metal to metal contact and much stiffer a-elements.

After doing these modifications the improved strength of the bolt connection can be calculated. Appendix U shows that after these modifications each bolt can withstand about 3.7kN force amplitude, which means that the flange connection can hold 12 * 3.7kN = 44.4 kN. This is less than the desired 55 kN (Figure 23) required to reach 100 Hz frequency and 16 mm amplitude. This will therefore limit the maximum frequency and or amplitude.

5.2.1 Pressure chamber and stator housing

When studying the pressure chamber and the stator housing, we observe that in most of the corners the filet radius is very small, approximately .25 mm. This means that we risk severe stress concentrations in these corners. The gas spring chamber was checked with a higher load than at nominal values (200 bar at 24 mm of the swept area) and found ok; Figure 25. The analysis was performed with 3 different meshes yielding about the same results. The very small radius does

generate some singularity problems so the analysis is not entirely unequivocal. And when a new design is made, increasing the fillet radiuses is strongly recommended.

The same goes for the gas spring attachment to the stator housing Figure 24 shows a simplified analysis of the stator housing underlining this point. In Figure 24 we see that the sharp radius create severe stress concentration. The filet radius is .25 mm, the load is 44.4 kN. Using hand calculations and the approximate theoretical stress concentration factor yields a maximum stress amplitude of around 190 Mpa (Budynas et al. 2008). We see that already at this load we are around the maximum allowable stress amplitude for infinite fatigue life for super duplex steel (250-350 MPa) (Guocai 2006), which are used in the stator housing.

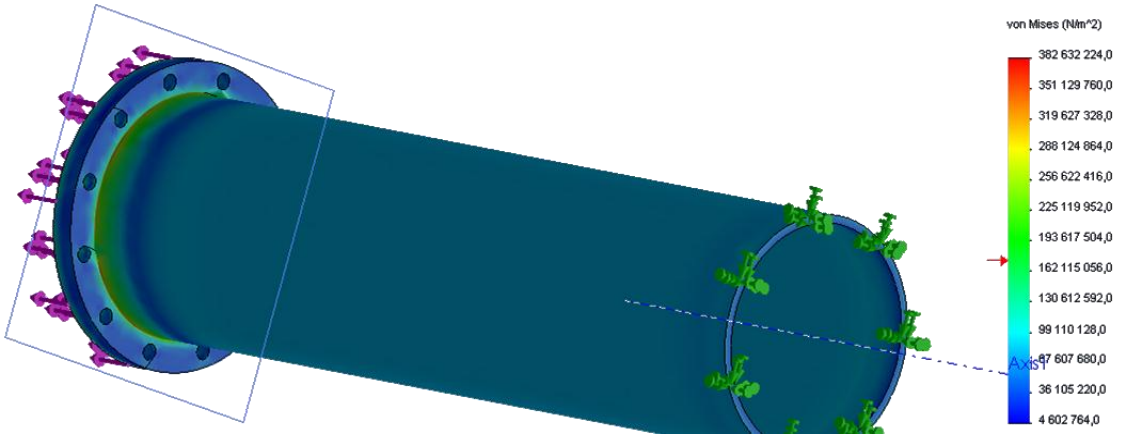

Figure 24, simplified analysis of attachment of gas spring to stator housing

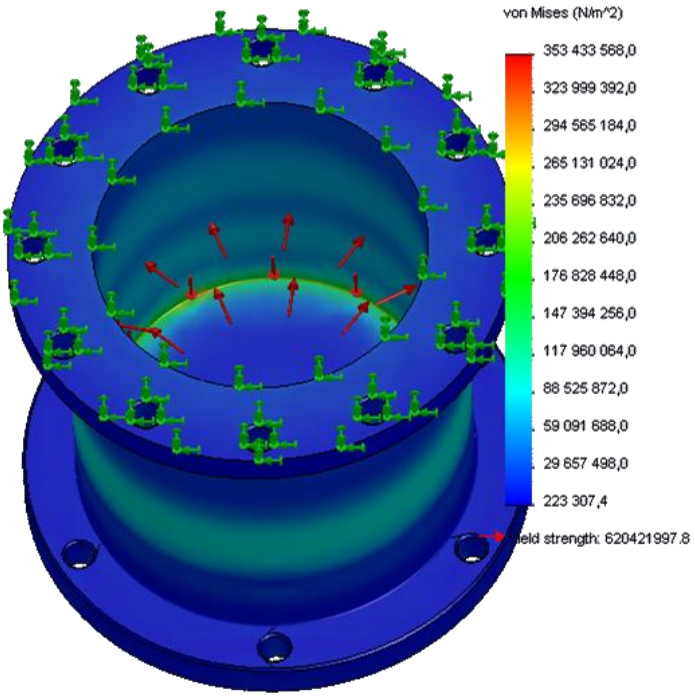

Figure 25, simplified analysis gas spring chamber.

5.3. Thermal analysis

Based on eq. (45) - (47) the necessary initial pressure needed to reach the nominal values was calculated. This initial pressure was used with equation (13) to estimate the friction force vs position, which gave the following graph, Figure 26. The calculations are in Appendix Q.

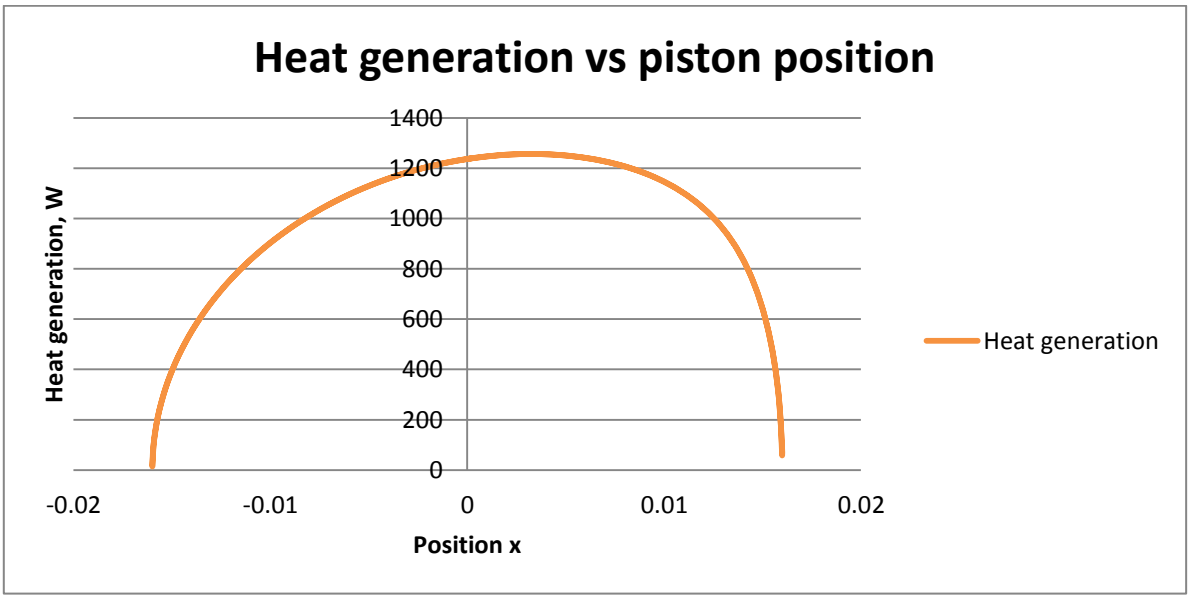

Figure 26, Heat generation vs position, nominal values.

This again resulted in an average heat generation of about 860 W over the swept area of the piston. No manufacturer data for the rod seal was found, these seals later have been replaced by a low friction (GGB 2011) non energized rod support. As long as the normal force at the rod is small the friction force in these bearings should be small. The normal force at the rod supports is small as long as there are no major misalignment problems in the machine. The frictional heat generation at the rod supports is therefore neglected.

Table 8, Analysis settings

Analysis settings	
Step end time	1500 s
Initial time step	15 s
Minimum time step	1,5 s
Maximum time step	150 s
Time integration	On
Mesh	Refinement in corners, and high heat flow areas.
Mesh	Refinement from coarser mesh showed little change in maximum temperature

As discussed in the background section, the variation in friction can be significant. It is therefore unnecessary to make a complicated thermal model. To get an estimate of the temperature development in the machine a finite element thermal model was made. Table 8 lists the analysis settings and table Table 9 lists the main assumptions and the explanation for them.

Assumptions

Table 9, Lists the most important assumptions and the explanation for them

Assumption	Explanation
All the frictional heat from the seal rubbing the cylinder goes into the cylinder wall	The seal thermal conductivity is much less than that of steel (4 orders of magnitude). There will be some heat transfer trough the lubricant film to the piston, but it is difficult to estimate how much. Conservative
The average heat generation is put on the swept area of the piston	Good assumption, the piston moves with very high frequency. The peak temperature in the middle of the gas spring cylinder would become somewhat higher with non-uniform heat generation. Non conservative.
The net heat flow from the gas to the machine is neglected	The net heat from the gas to the machine is small compared with the frictional heat generation. If we use the average gas temperature increase (appendix Q), an approximate convection coefficient and the inner gas spring area we can calculate the approximate heat transfer: A = 0.013 m2, h = 20w/m^2K (Pedersen 2011), delta T avg =25 -> 6.3 W-> neglect able, Non conservative.
The piston is not modeled	When the machine reaches steady state it is a fair assumption. Conservative
The thermal heat generation from the electrical and magnetic losses (400 W total) is applied directly on the inside of the stator shell. The copper windings etc. are not modeled.	Good assumption for the steady state solution.

The model was used for two different cases; the first case is with the machine in stagnant air, the second is with forced liquid convection. For the stagnant air case the built in table for convection coefficient in ANSYS was used, Figure 27. Convection and radiation was applied to all the outer surfaces.

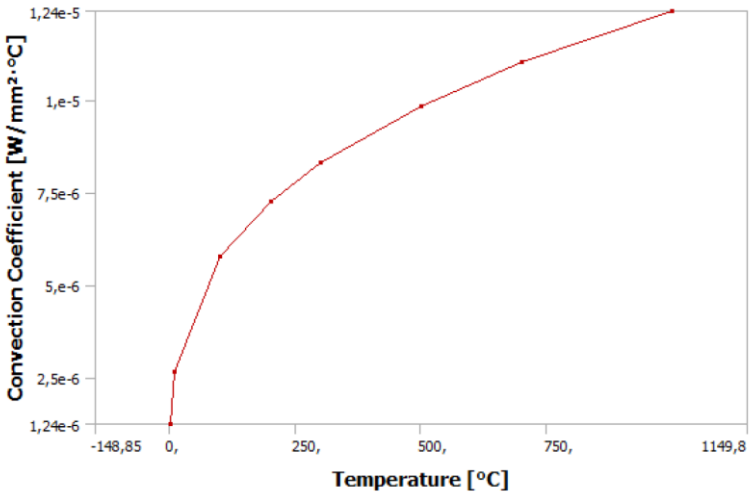

Figure 27, Convection coefficient stagnant air over cylinder

For the stagnant air case the analysis resulted in Figure 28, as we see running the 2B prototype with the assumed friction at the machines nominal values, results in overheating. It is clear that even with a substantial reduction in frictional heating, the machine needs cooling to reach the desired operating point.

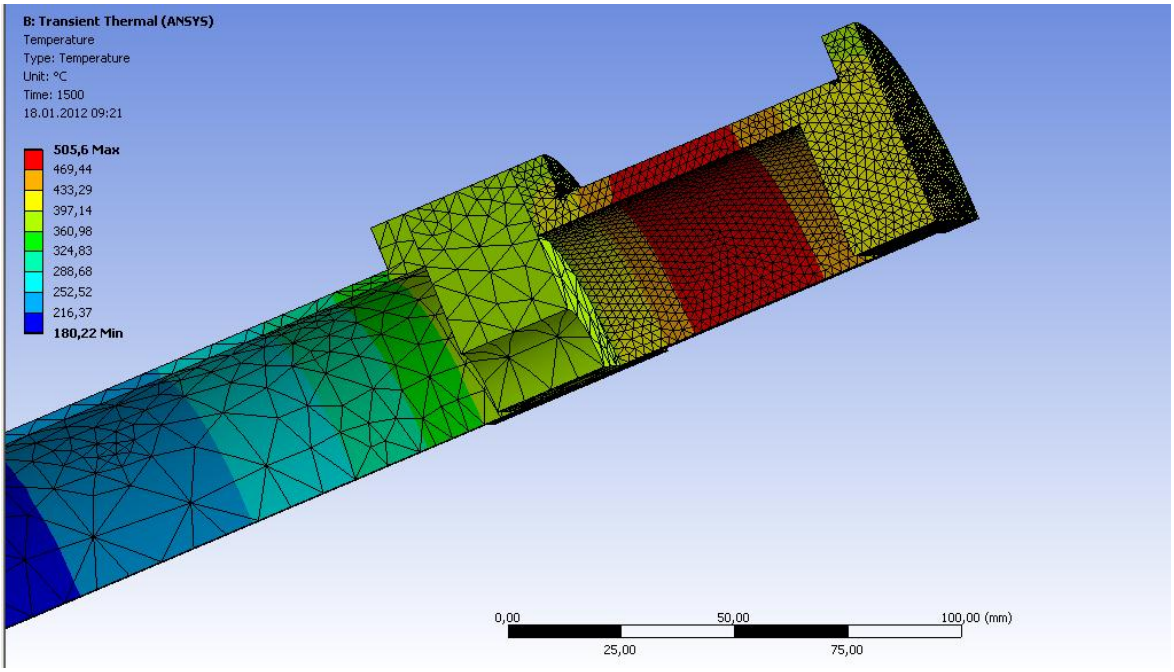

Figure 28, Thermal analysis of the machine with 860 W on piston swept area, convection to stagnant air and radiation to ambient.

To cool the machine we can apply forced liquid convection on the outside of the machine. If we assume a convection coefficient h=2000 W/m^{2}K (Pedersen 2011), it results in Figure 29.

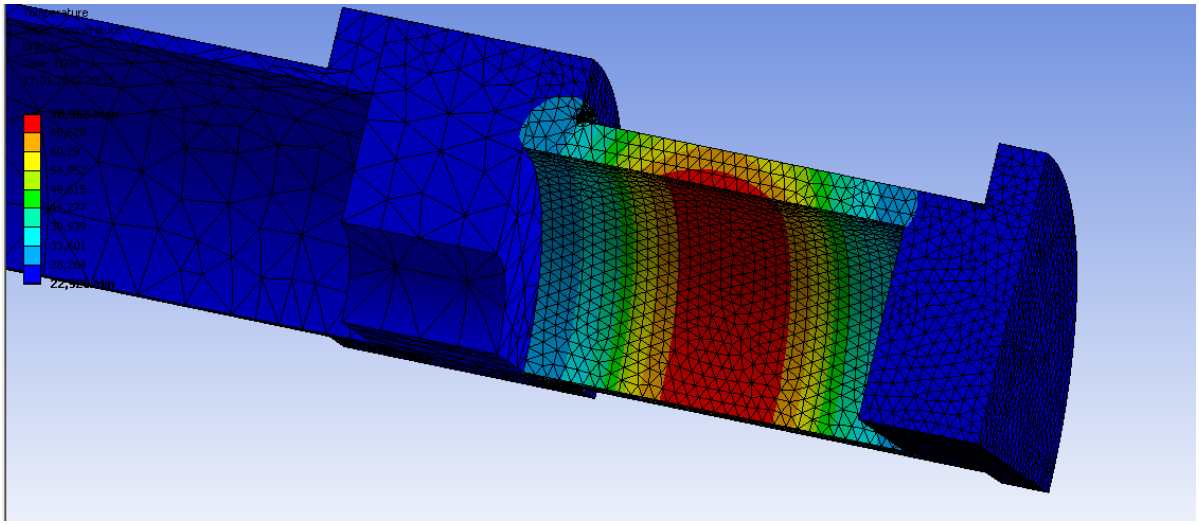

Figure 29, 860W, Water cooling of the machine h=2000w/(m^2 K)

The transient part of the analysis is not very interesting since not all the "thermal mass" is modeled, it is however interesting to see that the machine reach steady state much faster with liquid cooling.

5.4. Machine design

5.4.1 Lubrication

Initially the machine was grease lubricated resonators early tests (with mechanical springs) showed that most of the grease was scraped away from the piston working area. It was hard to determine if there was any fluid film left after running the machine.

(Zhang et al. 1997) concluded the following from his research:

"The friction and wear properties of the PTFE composites can be greatly improved with liquid paraffin lubrication. The wear of the PTFE composites can be decreased by 1 to 2 orders of magnitude compared with that under dry friction conditions, while the friction coefficients can be decreased by in order of magnitude."(Zhang et al. 1997)

It is clear that having proper lubrication is of great importance. Trelleborg's tests of the seal material (M12) were conducted in mineral oil, and the seal showed good performance at with this type of lubricant (Trelleborg 2011c). As discussed in the background section changing the lubricant viscosity can greatly affect the seal performance. Grease generally has substantially higher viscosity than mineral oil, therefore using mineral oil as a lubricant is suggested.

If we assume that the heavy vibration in the machine will splash the oil around in the gas spring chamber, a quasistatic analysis using Figure 2 shows that we will get a new fluid film layer at each stoke, replacing a potentially broken down layer from the previous stroke. An oil flow in the chamber will also help cool the areas with the highest temperature (where the seal swipes the cylinder wall). To get a full understanding of the lubricant flow in the gas spring chamber a CFD analysis must be carried out. When this is done one can analyze the squeeze flow under the seal and the film thickness. But this is outside the scope of this thesis.

5.4.2 Surface

Defining the right surface on the parts that are experiencing relative motion to other parts may greatly improve the performance of the machine. None of the surfaces in the 2B prototype have any surface treatment, and when handling the parts and assembling the machine it was experienced that making scratches and other damages to the surfaces was hard to avoid. Applying a surface treatment with a higher hardness than the ground material (super duplex) will increase the pats durability.

Based on a literature review a high velocity oxide fuel (HVOF) treatment may be suggested for some of the parts. One suggested coating may be SUME®2651 which is used in various reciprocating applications. It offers good corrosion resistance and excellent wear and tribological characteristics (Flitney & Brown 2007). The seal performance on HVOF coatings may be different from more traditional coatings like chrome. Reports show that although long life and low leakage is possible surface finish is more critical to obtain good seal performance (Flitney 2007). However with the right surface finish (super finished 0.15 μm)[3] and seal (energized PTFE) both leakage and wear can be smaller than when using traditional coatings (New material seals better on HVOF coatings 2007).

[3] The parameter (Ra, Rz etc.) was not specified

HVOF treatments cannot be used on bores under D = 150 mm, which means that another treatment must be considered for the gas spring cylinder.

Plasma spray is one alternative, it can provide a coating structure similar to that of a HVOF treatment and can be used on bores down to less than 40 mm (Flitney 2007). There are several coatings to choose from and both seal manufacturer(s) and surface treatment facilities should be contacted before making a decision.

Several adequate surface textures can be applied to the cylinder, piston and piston rod. Research indicate that having grooves parallel to the sliding direction may increase friction and wear considerably, specially under starved lubrication conditions (Costa & Hutchings 2007). Therefore having groves or at least grinding pattern perpendicular to the sliding direction is suggested as this may help maintain the lubricant film. Here the importance surface treatment returns, having a durable surface is essential to maintain the desired surface micro structure and avoid micro scratching of the surface. Having a durable surface is extra critical in the 2B application due to the extreme number of cycles required.

Based on the surface material and seal the counter surface parameters can be selected. Traditionally only the R_a or R_z, (average distance parameters) parameter has been specified from the seal manufactures as this has been adequate with traditional surface treatment process (chrome). With new manufacturing techniques limiting the surface specifications to these parameters has shown inadequate (Flitney 2009). It is therefore suggested to also specify the peak and valley parameters R_p and R_v (Figure 30), which has shown to be important parameters (Steep & Wüstenhagen 2006). The surface peak parameters indicate the surfaces initial abrasiveness. And some research has indicated that the R_{pkx} has great influence on the seal wear. Especially the first seal installed seem to be volatile to these peaks.

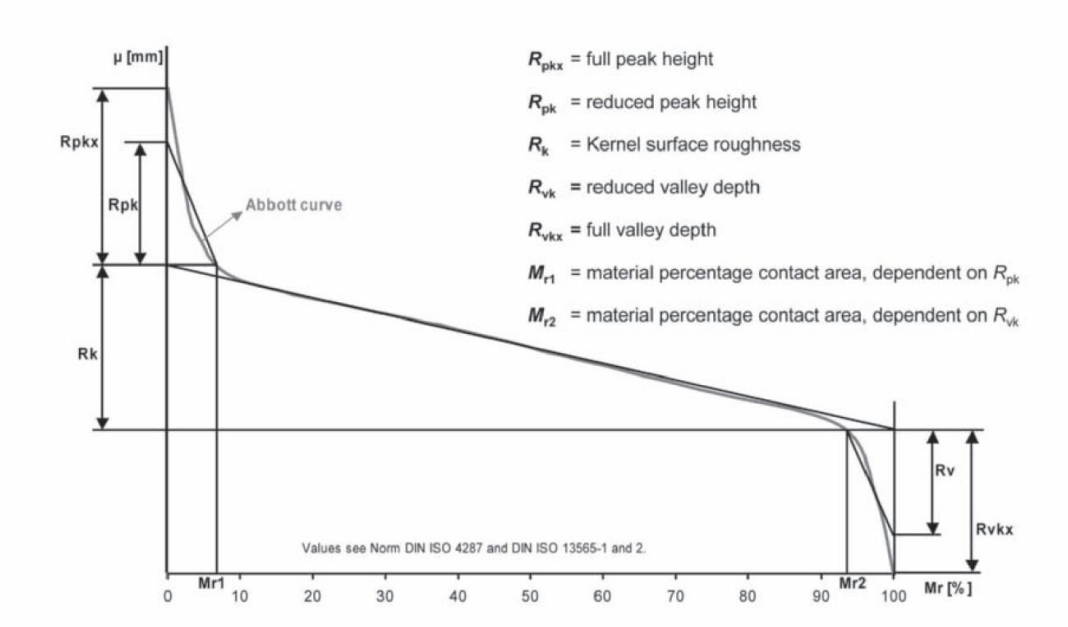

Figure 30, Abbott curve (Steep & Wüstenhagen 2006)

The valley parameters indicate the ability to build up a dynamic lubricant film, specially the R_{vk} has shown to be of interest. Table 10 shows the full range of surface parameters developed for heavy duty hydraulic operations (Steep & Wüstenhagen 2006) where the most important are discussed above.

Table 10, recommended surface parameters for dynamic stroke loaded steel counter surfaces, parameters described in Figure 30, Abbott curve (Steep & Wüstenhagen 2006)(Steep & Wüstenhagen 2006)

Parameter	Range (µm)	Parameter	Range (µm)
R_a	0.05 to 0.30	R_{pk}	0.00 to 0.50
R_{max}	0.00 to 2.50	R_{vk}	0.2 to 0.65
R_k	0.25 to 0.70	R_{vkx}	0.20 to 2.00
R_{pkx}	0.25 to 70		

These surface parameters has been implemented by several large engineering companies and the development of these surface parameters since 2006 has been small and wide spread (Steep 2012).

Additionally the material contact area R_{mr} should be specified, Figure 31 illustrates the importance of specifying this parameter (relative to only specifying R_a or R_z) (Trelleborg 2011a).

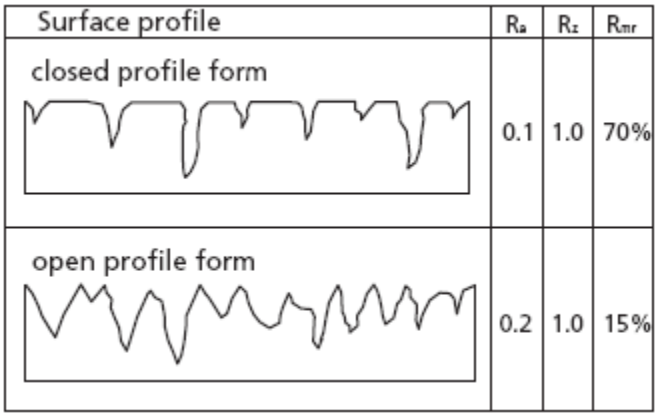

Figure 31, Illustration of the importance of specifying R_{mr}, the closed profile form is the desired profile giving a large contact area (Trelleborg 2011a)

Seal manufacturers have agreed to work towards better surface parameter specification(Flitney 2009), but this is yet to be fully implemented in the industry.

Some Norwegian surface treatment facilities where contacted and their handling time where around 3 months. This means that building a new gas spring with desired surfaces is outside the time frame of this project. The university workshop does not have the necessary equipment or competence to perform the surface treatments and surface finish described in this section. The necessary equipment to measure the surface profile is also unavailable in the university. Because of this and time limitations the surfaces of the parts are left as designed and manufactured with Ra =0.4 as the only specification.

Although the desired counter surface is not obtained, testing the gas spring may provide useful data. Especially the general machine design will be tested and potential problems can be revealed. Also

since no test data for frequencies over 15 Hz is available(Trelleborg 2011c); testing the seal beyond this point will provide interesting results.

5.4.3 External components affecting the gas springs

Any forces normal to the sliding direction will affect the friction and wear performance in the gas spring negatively. When visually inspecting the stator tube it is observed that the surface is very uneven which may cause uneven movement of the piston. When inspecting the magnet piston and the attachment to this the quality of the machining and assembly is also questioned. These observations were initially neglected (but commented on) since it's on the side of the scope of this thesis.

6. Testing, Results and analysis

Before the testing began a safety manual, pressure test manual and test procedures were made appendix A-E. The first stage was to check the mechanical integrity (static) and seal ability with static liquid pressure tests. During these tests, the tests together with analysis revealed several design and manufacturing problems. The problems had to be solved before the gas pressure test could be done.

After the liquid pressure test was done, and the problems discovered there were solved, the next stage was the static gas pressure tests. These tests revealed new problems, and showed that some of the improvements performed during the liquid static tests were unsatisfactory. Working with the parts also imposed some questions about the design. These questions was taken into the analysis of the machine and provided useful input. Table 4 lists an overview of the problems discovered during the initial pressure tests.

Table 11, List of problems discovered during the initial pressure tests.

Problem	Cause(s)	Action(s)	Comments
Leakage from M16 fitting connection on flange	Two different: 1, Undesired connection between the M16 bore and one of the flanges bolt bores. 2, One of the flange types had no sealing surface around the M16 bolt (round flange).	Sealing with Loctite 577; proved unsatisfactory. The M16 holes where therefore filled with epoxy.	M16 is a rarely used dimension for fittings and should be avoided. The port did also not have any special purpose.
Leakage from piston seal	Deformation of seal during assembly.	Assembly tools were made according to Technical bulletin. (Trelleborg 2011b)	Lead in chamfer should have been incorporated in the gas spring cylinder design (Trelleborg 2011a)
Leakage from ¼" NPT connection	NPT connections generally have a too large tolerance span which makes the ability to seal somewhat unpredictable (specially for gas) (Parker 2011)	1.5 turns of PTFE thread sealant tape	Tapered thread ports relies on metal to metal contact to seal, these are not recommended for multiple assemblies due to plastic deformation of the threads. Parallel threaded ports are recommended for prototype applications. If a tapered port is used another standard than NPT should be used for gas.(Parker 2011)
Leakage from flat gasket.	Flat gaskets often have some leakage of gas, they are generally not recommended over 200-250 bar.(Torgersen 2011). The gaskets installed leaked substantially under 80 bar, it is not certain why.	Gas spring end flange was modified and fitted with an o-ring groove based on manufacturer spec. (Torgersen 2011)	This problem could have been avoided by checking the flat gasket data sheet.

		Appendix H	
Next to impossible to install one of the rod seals	Probably groove tolerance, but this is difficult to measure.	One of the rod seals where not installed.	Further investigation of the seal grooves on the flange showed signs of poor machining and uneven tolerances Appendix P.
Alignment of end flange to gas spring cylinder	There were no alignment mechanism between the cylinder and flange	The piston/rod was used for alignment	Unsatisfactory solution
Heavy leakage due to use of He gas	Helium is much more difficult to seal, and none of the parts involved where approved for use of helium	Change the working gas to N_2	Resonator initially only had He available, a N_2 bottle therefore had to be obtained
Several dimensions where not as specified on the drawings	The work shop (external) had used the wrong drawings.	Some parts had to be modified, some had to be discarded.	Some of the parts also showed signs of poor machining. All the parts should have been thoroughly checked when arriving at Resonator. Many where inspected but not systematically.

During the static test period some analysis of the gas springs where done simultaneously, the analysis found some design problems that had to be dealt with before the dynamic testing could go on. Table 12 summarizes the limitations found during analysis, further explanation can be found in the analysis section.

Table 12, Summary of limitations found in analysis

Limitation	Explanation	Limit	Action
Flange connection, structural limitation (1)	An edge (1 mm) between the flange and the cylinder reduce the fatigue strength of the connection.	Unknown	Remove edge
Flange connection, structural limitation (2)	Bolts are not strong enough to hold maximum load in fatigue	Approximately 44 kN (infinite life), assuming that modification suggested in point 1 is performed	Limit initial pressure or maximum amplitude so that maximum force amplitude is well below the limit.
Gas spring magnet piston connection, structural limitation (3)	Connection between gas spring and magnet piston is very weak in tension	Approximately 1 kN (infinite life)	Only use outer chambers. If inner chambers are used initial pressure and amplitude must be greatly reduced.
Radius in transition between stator and flange on stator,	Very small radius in transition cause stress concentration	Approximately 45 kN (infinite life)	Ok if action in point 2 is followed.

structural limitation (4)			
Frictional heating, Thermal limitation (5)	The machine will according to the thermal analysis over heat in stagnant air	Depended on cooling	Use cooling, monitor temperature

After the limitations in Table 12 were taken into consideration, the next step was to prepare to dynamic tests. The procurement of the sensors and accompanying equipment was not finalized at this point, in spite of that it was decided to go on with a limited dynamic test. The primary purpose of this first test was to get the machine going and to see if there were any problems not yet discovered. The test was performed with limited initial pressure and amplitude. The test report is available in appendix K.

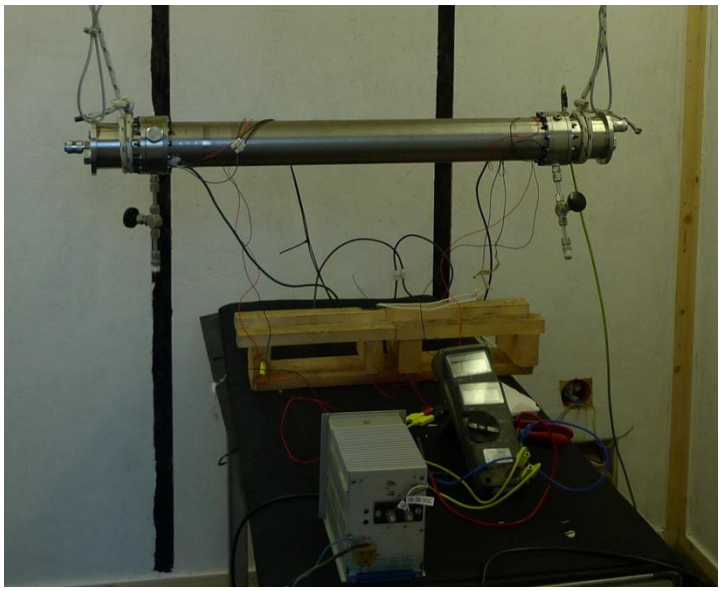

Figure 32, 2B prototype in first dynamic test

The first dynamic test revealed several problems, both the gas spring piston and rod sheared into the supporting surface causing heavy damage, Figure 33. The reason probably was a combination of several problems. Four plausible explanations are; misalignment between the parts generating forces normal to the sliding direction, seal arrangement used has poor load carrying capacity, poor lubrication and tolerances may be out of the desired range.

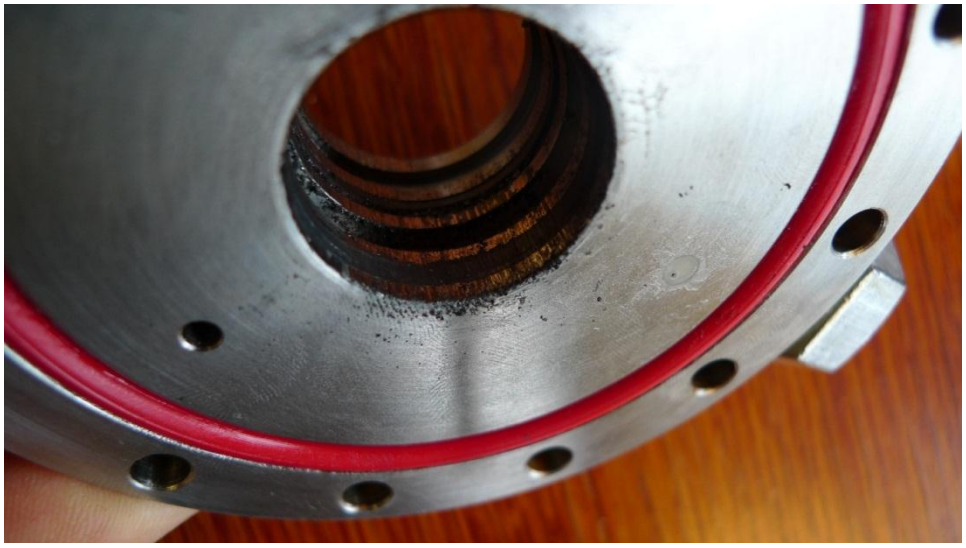

Figure 33, Damage on flange after first dynamic test

The experience from the first dynamic test was used to design a new end flange giving better support and solving some of the alignment problems. To solve the alignment problems circular edges fitting inside the gas spring cylinder and stator tube was added. The company Servi was contacted to supply high speed linear bushes for the end flange, they recommended DP4 a Teflon coated bushing. The fit for the bush in the flange was designed based on the manufacturer specification (GGB 2011). To increase the lubricant flow to the bush the edges was tapered towards the center; Figure 34. The complete engineering drawing is in appendix O.

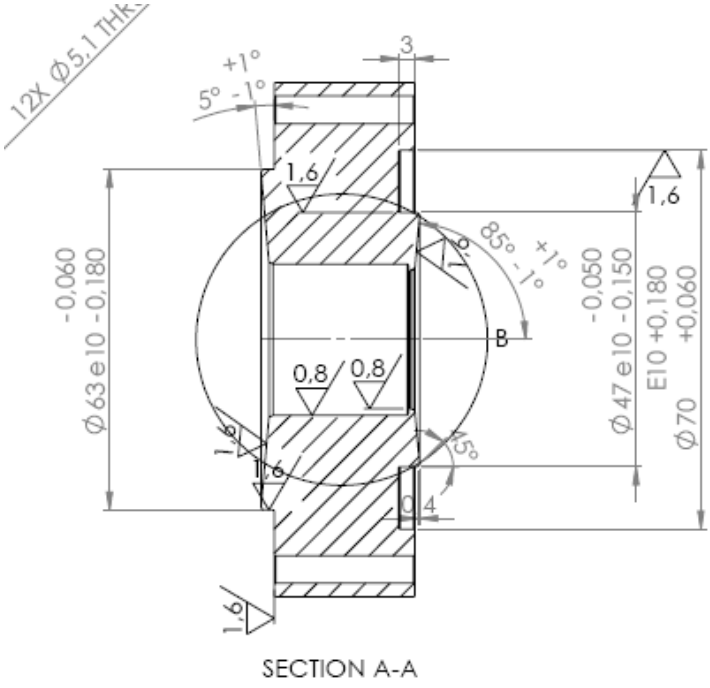

Figure 34, cross section of the new end flange

Based on the results from the first dynamic test and literature review, it was decided to use oil as lubricant instead of grease.

6.1. Test setup

When all the equipment necessary to log the machines performance had arrived it could be assembled and calibrated. Figure 35 shows the sensor setup.

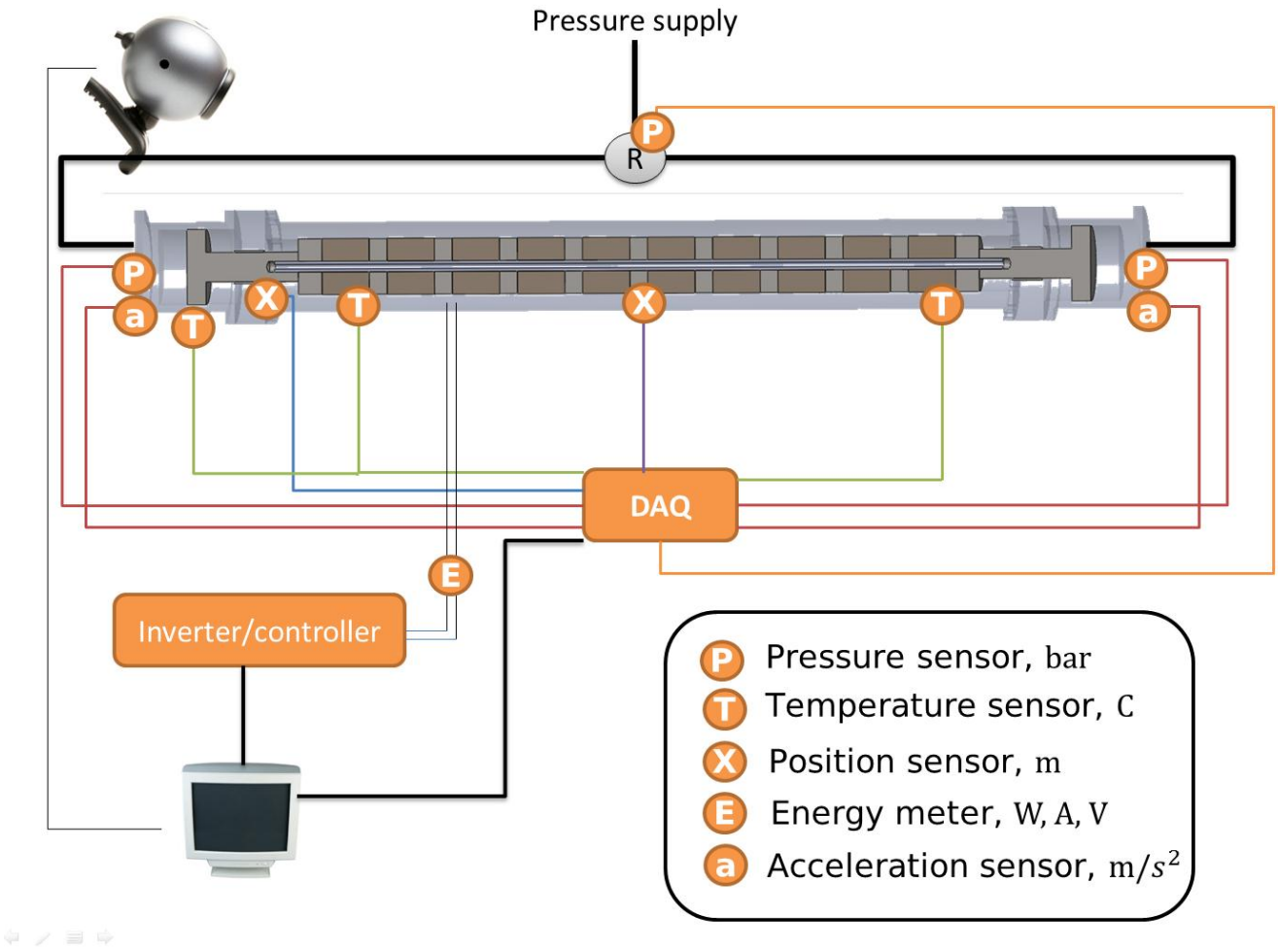

Figure 35, Overview of test setup

As we see from Figure 35 there is some redundancy in the sensor setup in case some of the sensors fail, however not all the measurements are available when the machine is running. Table 13 lists the different measuring equipment used and description of the different components.

Table 13, Measuring equipment used

Sensor	Position	Unit	Comment	Range/accuracy
Static pressure Keller Series 21R	Regulator	Bar	Static pressure sensor mounted on the regulator to monitor the filling pressure. Not active during machine operation.	0-700 bar, typical 0.5%, environment max 20 g
Delta pressure Kistler pressure sensor 6031	Both gas spring chambers	bar	Piezo electric sensors, can withstand extreme accelerations, only delta pressure measurement	250 bar
Position 1	Stator	m	By measuring the	32 mm, +-1 mm

			inductance in the stator one can estimate the position of the magnet piston. This cannot be done during operation	
Position 2 Hall effect calibrated by Resonator	Gas spring flange	m	Hall effect sensor, measures the position of the magnet piston by measuring the strength of the magnetic field	32 mm, +-1 mm
Acceleration Kistler accelerometer 8044	Gas spring ends	m/s^2	Piezo electric sensors, can withstand extreme accelerations. High frequency	30 000 g
Energy meter	Between inverter and machine	A, V, W	Monitors the electrical power, current and voltage.	
Stator temperature Reissmann temperature sensor PT100	Inside stator	C	Two internal temperature sensors are mounted inside the stator (one in each end) to monitor the temperature.	Accuracy +- 0.5 °C
Gas spring temperature Thermocouple	On the gas spring cylinder	C	Monitors the temperature of one of the gas springs	1°C <

Figure 36 Shows the Prototype 2B ready for test inside the safe container at Resonator.

Figure 36, Prototype 2B ready for test inside safe container

6.2. Dynamic tests

With the modified parts the machine seemed to perform better, in the two first tests one of the gas spring chambers did however heat up significantly more than the other. After assembly this was shown to be due to metal to metal grinding between the piston and cylinder, Figure 37.

Figure 37, Shows damaged piston after dynamic test

The accompanying rod to the damaged piston did not show signs of destructive wear, which indicates that the new rod supports outperform the previous rod supports. After some investigation, it appeared that the rubbing cold originate from forces normal to the sliding direction caused by an uneven magnet piston and/or different tolerances. Therefore the following actions were taken; a new magnet piston was made and the damaged piston and cylinder was replaced with a new set were the tolerances were matched to the well-functioning gas spring. Additionally the corners between the ribs on the piston were rounded of (on both springs) (Figure 5).

Table 14, Overview of measured tolerances in the gas springs, *0.01 mm

Item number	Piston rib (R)					Total Gap				
	Rod	R 1	R 2	R 3	Comment	Chambers	R 1	R 2	R 3	Comment
1	0	-1	0	-1		7.5	8.5	7.5	8.5	Failed in test at rib 1
2	-2	-3	-6	-6		4	10.5	13.5	13.5	Ok in test
3	-1	0	0	1		5	7.5	7.5	6.5	Sendt to modification
4	-3	-2	-2	-2	Failed in test					

* Where rib 3 is the one closest to the rod

After these modifications where made a new test was performed. It seemed that the modifications had significantly improved the performance of the machine. There were no significant heating of any of the chambers. The maximum relative amplitude indicated a doubling, with the same electrical input, compared to previous tests. The sensors did however show some inconsistency in the results,

which means that a new test has to be performed to confirm the results. The tests where done with limited amplitude and initial pressure.

When investigating the parts after the test, the parts showed no signs of damage or wear. This indicates that the tolerances in the cylinder, on the piston and rod have become satisfactory. The difference in diameter is around 0.12 mm , which is also in accordance to specifications on similar products from the seal manufacturer (Trelleborg 2011a). It also seems that the seal groove tolerances used (ISO 7425) is adequate, even though the seal is operating outside the known frequency region. It is unknown for how high pressures the design can withstand such high frequencies, the maximum pressure amplitude was 16.5 bar with an initial pressure of 19.1 bar at 61 Hz. This is well below the target values for the gas springs. It must also be noted that the test time was very limited and that more tests needs to be done to verify the results found.

The gas spring stiffness equivalent equation (46) was used together with equation (47) to estimate the resonant frequency in the tests. Results from the tests indicate that these expressions provide a good estimate for the resonant frequency.

The test reports for the three last tests are in appendix L-N.

7. Discussion

During the design phase Resonator calculated the initial and maximum pressure values necessary to reach 100 Hz at 16 mm. amplitude Table 1. The frequency analysis and testing in this thesis showed that these values were incorrect. Therefore new values were calculated (Table 7) based on the theory derived in this thesis; equation (46) and (47). The new values showed a lower initial and maximum pressure necessary to reach 100 Hz at 16 mm amplitude. The new values were further used in the analysis of the machine.

When only focusing on the gas springs, using a double acting design seem to be a good idea; it gives the same stiffness with a lower initial and maximum pressure. When investigating the product of velocity and pressure differential during the cycle we see that the double acting solution has a lower peak value than the single acting for the same stiffness; Figure 38 and Figure 39.

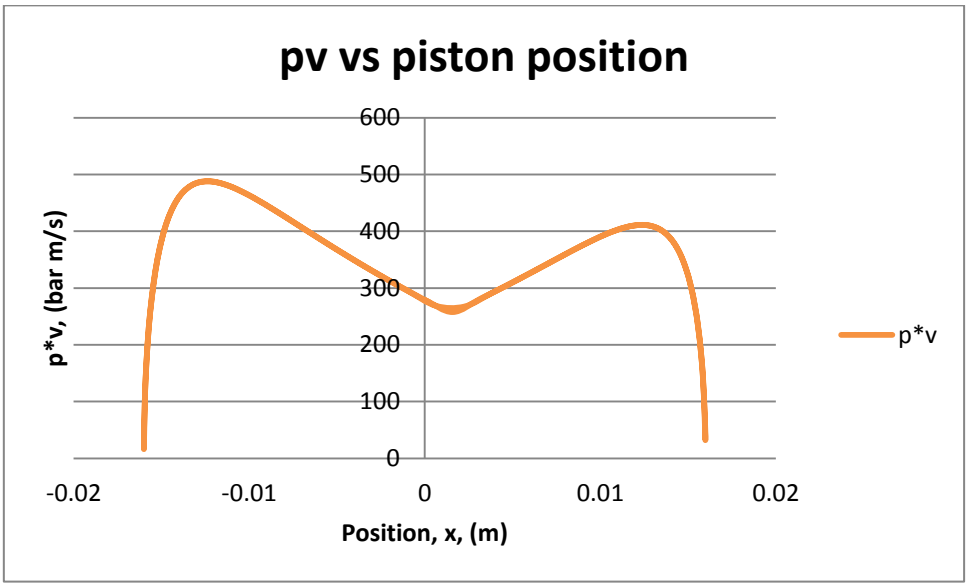

Figure 38, pressure velocity graph double acting spring

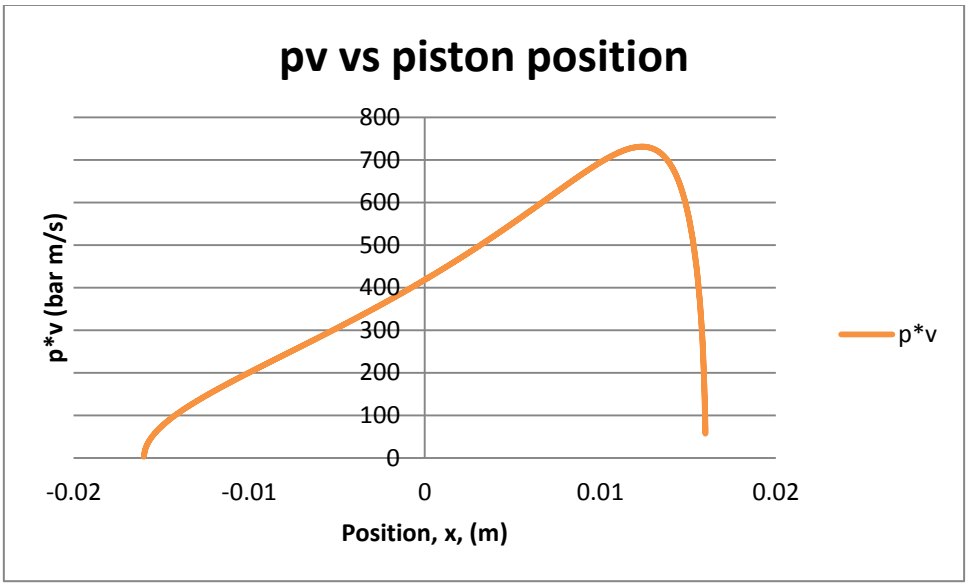

Figure 39, Pressure velocity graph single acting spring

Although the initial and maximum pressure is increased with about 60% when going from double acting springs to single the net heat generation is only increased by about 20W (2%) at the piston seal. The average PV value is also almost unchanged.

Introducing double acting springs also leads to the necessity of a rod seal; this will cause frictional heat generation. Frictional heat generation at the rod is more critical than in the cylinder since most of the heat goes in to the rod (the low thermal conductivity seal sits in the flange). The rod/magnet piston has no direct cooling and has to be indirectly cooled by the outer casing, which can lead to high temperatures.

Using double acting springs in a free piston linear machine will lead to a large fully reversed tension force in the gas spring rod. The gas spring rod somehow has to be connected to the magnet piston, and it is this connection that is challenging due to fatigue. One possibility discussed is using a larger diameter bolt going through the entire assembly Figure 40.

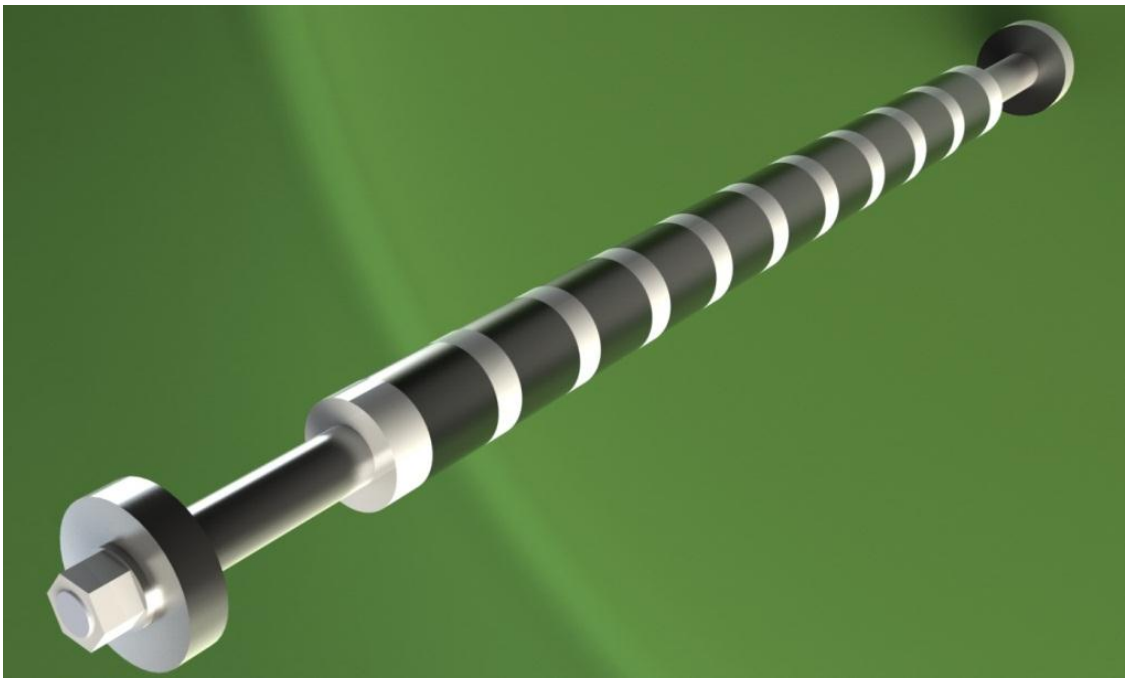

Figure 40, bolt through entire piston assembly

This enables the possibility of pre-tightening (the bolt) which increases the fatigue strength. This solution is however unsatisfactory with conventional rolled treads and the current design. It is possible to increase the fatigue strength of threaded connections by treating the threads and or using special nuts (Waløen 1971), but little manufacturer data for high cycle fatigue is found for these types of components.

Because of the structural limitations with the original parts most of the analysis has been done with focus on single acting springs. The structural limitations for the double acting configuration (in the 2B prototype) were so severe that no test results could be made for the machine with double acting springs.

The test results show that after some modifications the gas springs where able to withstand higher frequencies that commercially available gas springs offer. Commercially available gas springs are

limited to around 1 Hz, while the gas springs in the resonator 2B prototype was tested for a limited time up to approximately 70 Hz. Although more testing is needed it seems that it is possible to outperform commercially available gas springs with respect to frequency. Due to several design problems during the tests, the testing of a fully functioning machine was limited to one test. In this test the machine was not pushed to the rated frequency (100 hz) or amplitude (16 mm) due to several limitations found during analysis of the machine. It is however possible to push the machine further than what was done in this test, both with respect to amplitude and frequency. Before increasing the frequency and amplitude better cooling should be added to both the stator and gas springs. The thermal analysis showed that the machine will over heat at nominal values (both the gas springs and the stator) in stagnant air. This was partly confirmed by the tests as the machine sowed increase in temperature even at the limited reciprocating speeds obtained in the tests.

The thermal analysis performed at NTNU by Per Kristian Pedersen used the old initial values calculated by Resonator; their analysis therefore showed that the machine would experience an even larger temperature increase. Because of difference in initial values the thermal analysis performed in this thesis is not comparable to the analysis performed at NTNU.

Keeping the machine temperature at a moderate level is also beneficial when looking at the seal performance. Data found from seal manufacturers indicate that (PTFE) seals, although with good temperature resistance, can withstand a lower maximum PV value the higher the temperature is (*Seals for extreme enviorments* 2011). Temperature also limits what elastomer energizers that can be used (Trelleborg 2011a).

Based on the analysis in this thesis it is possible to substantially improve the performance of the gas springs. Regarding friction and wear there is much to gain by improving the surfaces that experience relative motion. The current design has the surface roughness parameter R_a = 0.4 as the only parameter on the piston, rod and cylinder. Literature indicates that the friction and wear performance can be substantially improved by reducing R_a to 0.15-0.2 on the seal counter face with the current material(Flitney & Brown 2007). Also specifying the surface contact area R_{mr} to between 0.5 and 0.7 will increase seal performance (Trelleborg 2011a). Additionally sharp asperities in the surface finish should be avoided. This can be done by specifying the right manufacturing technique; super finishing after grinding. It is also important to specify the direction for the different operations; they should be done so that the surface texture lines go perpendicular to the sliding direction.

Further some peak and valley parameters should be specified, specifying R_{pkx}= 0.00 to 0.50 µm and R_{vk}= 0.20 to 0.65 µm is recommended(Steep & Wüstenhagen 2006). Additionally more parameters from Table 10 could be specified to be on the safe side.

Performing these modifications to the surface should provide an improved counter surface, however with the current ground material (super duplex steel) the durability of the surface texture might be unsatisfactory. To improve the surface durability a surface treatment is suggested, but this has to be incorporated in a new design. If a surface treatment is performed, the surface parameters also have to be reconsidered based on what treatment is used.

Most of the counter surface research that has been done is on hydraulic applications, therefore using a lubricant with similar viscosity at the machines operating temperature to that of hydraulic oil (at typical hydraulic oil operating temperature) is recommended. If one deviate much from the typical

hydraulic operating conditions the parameters specified may not be satisfactory. The development of new surface parameters is not trivial.

On the original drawings only the tolerance class on the piston and cylinder was specified, with the tolerances used the two parts could end up with a (total) gap between 0.148 and 0.0 mm. This is unsatisfactory. The seal manufacturer used specifies, depending on the application, a gap between piston and cylinder with a variation around 0.01 mm. On the parts used for the final tests the tolerances were modified compared to the original drawings.

To further improve the gas spring performance in single acting mode the gas spring chamber length can be changed. Figure 15 shows an optimization for the gas spring chamber for the 2B prototype with 100 Hz and 16 mm amplitude.

By considering the assembly of the seal arrangement already in the design phase time and costs can be saved. For the prototype 2B special tools had to be made to be able to assemble some of the seals.

Super duplex was chosen as the ground material for both the gas springs and the stator housing because of its high strength. Super duplex is however costly and difficult (costly) to machine(International Molybdenum 1999). When investigating the structural design several small radiuses (0.25 mm), causing severe stress concentrations, are observed. These stress concentrations could have been significantly reduced by increasing the transition radiuses, giving higher strength. Since the machine is heavily fatigue loaded ($2 * 10^6$ cycles in 5.5 hours at nominal values) avoiding stress concentrations is extra important. With more focus on structural engineering in the design phase one could have obtained either; stronger parts giving better machine performance (the machine is limited by structural limitations) or cheaper parts with the same strength and a material that is cheaper and easier to machine which leads to faster production time.

During the project several problems with the prototype has been discovered. More focus on quality assurance in the design and procurement process could have avoided many of these problems, and saved time and costs. Generally more focus on the engineering and procurement phase, giving the right parts and equipment, at the right time to a planned cost, would improve progress in the project.

In the future Resonator wants to utilize the technology from the 2B prototype to build a full size drilling machine. Based on the analysis and test results from the 2B prototype we can approximate the size of a full size down the hole drilling machine, first we find the maximum power available for hammering P_{h_m}

$$P_{h_m} = P_{El_{in}} - \dot{E}_{g-fric} + \dot{E}_{g-EL}$$

The losses are

$$\dot{E}_{g-fric} + \dot{E}_{g-EL} = 2 * 860\,W + 400W = 2120\,W$$

Maximum electrical power in is $P_{El_{in}} = 3500\,W$

Then the maximum power available for hammering is then

$$P_{h_m} = 3500W - 2120W = 1380\ W$$

The necessary hammering power for a 95 mm hole eq. (2) is

$$E_i * f = (0.04 * A) * 100\ Hz = 28\ kW$$

If we assume that the electrical force (good approximation) and total losses (uncertain) is proportional with machine length we get that the machine has to be 28000W/1380W ~ 20 times longer than the prototype 2B. This leads to a huge machine almost 20 meters long, it is clear that this is not a feasible construction and that there is need for a great improvement in the machines efficiency. The estimated overall efficiency of the 2B prototype is 1380 W/3500 W = 39%, this is only including friction in the gas spring cylinders and the electrical losses, so the overall efficiency is probably even lower. The low efficiency also lead to substantial heat generation, for a full size machine the total heat generation would be a mere 44 kW which is challenging to cool.

The analysis performed here is very simplified, but it gives an idea of how much the machine has to be improved for it to be a product for the market. From this analysis we identify the overall efficiency and electrical power density as critical success parameters. The next step towards a full size machine is to work with these parameters and see if it is possible to improve them to a level such that one can get down to a more feasible size of the machine.

If Resonator wants to continue the development of gas springs, using the current prototype for a few more tests to get a wider data set is recommend. After that a full redesign with implementation of the improvements suggested in this thesis can be done. It is clear that an improved structural design is necessary to reach the targeted values set for the 2B prototype.

8. Conclusions and further work

Analysis and testing has shown that the gas springs performance has great influence on the overall performance of a free piston linear machine with gas springs. The main factors affecting the performance of a free piston linear machine is the spring stiffness, electrical power density and total losses.

The advantage of using gas springs in a free piston resonating machine is that high frequencies seem to be obtainable (more test results are needed). With the right design long life may also be obtainable, but there is no test results yet, showing any life predictions. The main disadvantage is the heat generation at the dynamic seals, which also significantly lowers the total machine efficiency.

There are many important factors to consider, when designing a gas spring solution. The most important are structural design, thermal analysis, surface specifications, seal configuration lubrication and tolerances. Additionally great emphasis should be taken to ensure the right alignment between the different parts.

When designing a gas spring solution to a free piston linear machine designing the right chamber length, based on the desired operating frequency and amplitude, is also crucial.

The gas springs tested was tested to a higher frequency than typical gas springs on the market are rated for, although with a lower pressure. It seems that it is possible to design gas springs that can withstand higher frequencies than what is on the market today, using the latest sealing technology. More tests should be done to confirm this.

To ease the analysis of gas spring systems a linear gas spring stiffness equivalent has been developed (equation (46)). This constant can be used like a linear spring constant to calculate the frequency for a system at given amplitude, using traditional theory (equation (47)). The expression for the gas spring constant can also be used to optimize the gas spring chamber length for a given frequency and amplitude. Using the gas spring constant seemed to predict the right operating frequency in the tests performed.

Based on the experience from this product development process it is noted that emphasis on engineering and procurement with a good quality assurance system is a crucial success factor.

During the testing and analysis of the prototype 2B, many improvements to the original design have been made. The testing and analysis performed in this thesis does however show that there is further room for substantial design improvements.

A simplified analysis indicates that substantial improvements must be done to the 2B prototype before the technology can be used to construct a competitive full size down-the-hole drilling machine.

8.1. Future work

There is much research and development to do before free piston linear machines with gas springs are ready for the market. For Resonator the first thing to do is to continue the testing of the 2B prototype to get more data.

Further it should be analyzed more accurately what performance from a down-the-hole drilling machine is necessary to outperform competing hammers. Resonator should also analyze how many percent of the total energy in the machine that can be taken out at each blow. Based on this, and results and analysis from the 2B prototype, a feasibility study of the use of gas springs in a free piston linear machine should be performed.

If this study shows that the gas spring concept (or a similar concept) used in the 2B prototype is feasible, the next step is to design a new machine. Before this is done a number of things should be analyzed.

Maintaining the lubricant film under the seal has been identified as an important factor to ensure as low wear and friction as possible. Therefore a lubricant flow analysis should be carried out, starting with an analysis (CFD) of the lubricant flow in the gas spring chamber.

Further an improved structural design should be made, included but not limited to, the connection between the gas spring and the stator, and if a double acting solution sis selected; the connection between the gas spring and the magnet piston.

Based on the analysis done in this thesis a surface treatment and surface finish can be specified and an improved spring can be manufactured.

8.2. List of improvements and suggested improvements

Table 11 and Table 15 lists the improvements done on the 2B prototype. Table 16 lists suggested improvements mainly applicable to a new design.

Table 15, List of improvements after dynamic tests

Improvement	Reason	Comment
New flange between gas spring and stator housing	The old design lacked a good way to align the spring-flange-stator assembly. Poor load carrying capacity on original design.	New design significantly improved machine performance.
New magnet piston	Old piston was not straight.	New piston significantly improved machine performance.
Round of edges on piston	Reduce risk of failure	Unknown influence
Use oil as lubricant	Oil is the standard lubricant used with this type of seal	
Modified tolerances	Match tolerance to well-functioning spring	

Table 16, suggested improvements

Improvement	Reason	Comment
Improve and specify the surface finish	Better surface can lead to lower wear and friction, reduced heat generation and increased efficiency	Suggested values can be found in Table 10
Apply surface treatment to gas spring cylinder, piston and rod.	Increased durability of surfaces	Can lead to lower wear of seal.
Specify the tolerable gap between the piston an cylinder	This tolerance is important for the gas spring performance	The value can be obtained from seal manufacturer based on the operating conditions.
Incorporate a system to control all tolerances on manufactured parts.	Detect problems at an early stage.	Quality control can save time and costs.
Incorporate seal assembly in the design	Easier to install seals, less chance for damage. Manufacturing of extra tools can be avoided	
Increase radiuses in corners / transitions	Lower stress concentrations, increased strength	The 2B prototypes performance is limited by structural limitations.
Increase strength of flange connection between gas spring and the rest of the machine.	The current solution is not strong enough to reach 100 Hz and 16 mm amplitude	
Incorporate water cooling	To reach the target values water cooling must be incorporated.	
Make a new stator tube	The stator tube used today has an unsatisfactory surface and is not straight.	Making a tube from fiber reinforced composites is suggested.
Use parallel threaded fittings with plastic/elastomeric seal.	Easier to seal, fast to assemble and disassemble	

Reference List

Kilder

Bostad, A. (2011). *Description and analysis of a resonating free-piston tubular permanent magnet linear machine, suitable for exploring the effects of increasing frequency in hammer drilling*. Master. Ås: Norwegian University of Life Sciences, DEPT. OF MATHEMATICAL SCIENCES AND TECHNOLOGY. 114 pp.

Brown, M. E. & Piff, H. M. (2010). *Handbook of reliability prediction prcedures for mechanical equipment*. West Bethesda: Naval surface warfare center carderock division.

Budynas, R. G., Shigley, J. E. & Nisbett, J. K. (2008). *Shigley's mechanical engineering design*. New York: McGraw-Hill. XXV, 1055 s. pp.

Costa, H. L. & Hutchings, I. M. (2007). Hydrodynamic lubrication of textured steel surfaces under reciprocating sliding conditions. *Tribology International*, 40 (8): 1227-1238.

Det Norske, v. (2010). *Fatigue design of offshore steel structures: April 2010*. Høvik: Det norske veritas. 142 s. pp.

Flitney, B. (2007). Alternatives to chrome for hydraulic actuators. *Sealing Technology*, 2007 (10): 8-12.

Flitney, B. (2009). Manufacturers agree to work towards improved texture specifications. *Sealing Technology*, 2009 (2): 11-12.

Flitney, R. K. & Brown, M. W. (2007). *Seals and sealing handbook*. Burlington, MA: Elsevier/Butterworth-Heinemann. 1 online resource (xii, 620 s.) pp.

GGB. (2011). *DP4 Designers Handbook*. GGB (ed.): EnPro Industries company.

Green, e. A. (2005). Single cutter impact tests investigate deep-well hammer-drilling performance. In *SPE Annual Technical Conference and Exhibition*. Dallas.

Guocai, C. (2006). Fatigue behaviour of duplex stainless steels in the very high cycle regime. *International Journal of Fatigue*, 28 (11): 1611-1617.

Hustruli.Wa & Fairhurs.C. (1972). Theoretical and Experimental Study of Percussive Drilling of Rock .4. Application of Model to Actual Percussion Drilling. *International Journal of Rock Mechanics and Mining Sciences*, 9 (3): 431-&.

Incropera, F. P., DeWitt, D. P., Bergman, T. L. & Lavine, A. S. (2010). *Fundamentals of heat and mass transfer*. New York: Wiley. s. pp.

International Molybdenum, A. (1999). MACHINING DUPLEX STAINLESS STEELS. 4.

Jewett, J. W. & Serway, R. A. (2010). *Physics for scientists and engineers with Modern physics*. [Belmont, Calif.]: Brooks/Cole. XXXII, 1440, [78] s. pp.

Kahraman, S., Bilgin, N. & Feridunoglu, C. (2003). Dominant rock properties affecting the penetration rate of percussive drills. *International Journal of Rock Mechanics and Mining Sciences*, 40 (5): 711-723.

Kaller AB. (2011). *Factory visit gas spring supplier Kaller AB* (Conversation Factory visit).

Kaller gas spring selection guide. (2009). 8 ed.: Strömsholmen AB.

Karnopp, D. C., Margolis, D. L. & Rosenberg, R. C. (2006). *System dynamics: modeling and simulation of mechatronic systems*. Hoboken, N.J.: Wiley. XII, 563 s. pp.

Moran, M. J. & Shapiro, H. N. (2010). *Fundamentals of engineering thermodynamics*. Hoboken, N.J.: Wiley. XI, 725 s. pp.

New material seals better on HVOF coatings. (2007). *Sealing Technology*, 2007 (4): 10-11.

Oberg, E. & McCauley, C. J. (2004). *Machinery's handbook: a reference book for the mechanical engineer, designer, manufacturing engineer, draftsman toolmaker and machinist*. New York: Industrial Press. ix, 2693 s. pp.

Parker. (2011). *Parker 4300 Catalog Assembly / Installation*: Parker. pp. T 3-9.

Pedersen, P. K. (2011). *Design of a hydraulic seal*. Project report. Trondheim: NTNU, Energy and process engineering.
Polymod. (2011). *Aerospace seals, rod and piston*. Fort Wayne: Polymod Technologies. Available at: http://www.polymod.com/ (accessed: 15.10.2011).
Resonator AS. (2011). *Metings, internal documents and email communication with Resonator AS*. Ås (Meetings, emails, internal documents fall 2011).
Seals for extreme enviorments. (2011). Connecticut: Advanced Products Company.
Somaloy SMC-Rings data sheet Resonator batch 1. (2011). Höganes, S. (ed.). Höganäs: Höganes AB.
Stachowiak, G. W. & Batchelor, A. W. (2005). *Engineering tribology*. Amsterdam: Elsevier Butterworth-Heinemann. xxiv, 801 s. pp.
Steep, F. & Wüstenhagen, G. (2006). Counter surfaces of hydraulic seals for heavy-duty applications. *Sealing Technology*, 2006 (12): 8-10.
Steep, F. (2012). *Re: Counter surfaces*. Ås (Email comunication 27.1.2012).
Szeri, A. Z. (2011). *Fluid film lubrication*. Cambridge: Cambridge University Press. XV, 547 s. pp.
Terjesen, G. (2011). *course TMP 301*: Norwegian university of life sciences (lecture hadout).
Tester, J. W. (2005). *Sustainable energy: choosing among options*. Cambridge, Mass.: MIT Press. XXIII, 846 s. pp.
Torgersen, J. H. (2011). *Phone and email communication*. Ås (September 2011).
Trelleborg. (2011a). *Hydraulic seals - linear*: Trelleborg AB.
Trelleborg. (2011b). *M12 seals Technical Buletin*: Trelleborg.
Trelleborg. (2011c). Turcon M12 unrivaled performance in hydraulic sealing: Trelleborg AB. 6 pp.
Waløen, Å. Ø. (1971). *Maskindeler 2*, vol. 2. Trondheim.
Wangen, R. (2011). *Phone Interview Reidar Vangen, Trelleborg*. Ås (Phone interview).
Wildi, T. (2006). *Electrical machines, drives, and power systems*. Upper Saddle River, N.J.: Pearson/Prentice Hall. XXIII, 934 s. pp.
Zhang, Z.-Z., Xue, Q.-J., Liu, W.-M. & Shen, W.-C. (1997). Friction and wear properties of metal powder filled PTFE composites under oil lubricated conditions. *Wear*, 210 (1–2): 151-156.

Appendix

Appendix A Resonator safety manual

Rev: 29.8.2011

Author: Eirik Lind Hånes

Resonator safety manual

General rules for testing

1. Everybody involved with testing must be familiar with the content in this safety manual.
2. There must at all times be at least two people present during tests.
3. All personnel should at all times wear safety glasses during tests.
4. During tests the warning light must be on, and all personnel at Resonator must be notified.
5. Ear protection must be used when the noise level exceed moderate levels*.
6. Protective gloves must be used when working with harmful liquids* such as hydraulic oil.
7. Appropriate respiratory protection must be used if there are harmful gases*, smoke or dust present during tests.
8. All activity at resonator should be according to S-002 N.
9. Each specific test type should have a specific manual.

*Refer to S-002 N for more detailed information.

Handling of Magnet

1. Remove all magnetic components (keys, credit card…) before get close to magnets
2. Always use plastic plate on top of the working bench
3. All unrelated components have to be removed from the working bench before start
4. Be aware of the squeeze danger between magnets and other magnetic compounds

Pressure test

1. Refer to the pressure test procedure

Appendix B Resonator Pressure Test Manual

Rev: 29.8.2011

Author: Eirik Lind Hånes

Resonator Pressure Test Manual

1. All parts that are going to be pressurized must first be pressure tested.
2. The parts must always be pressure tested with liquid to an equal or higher pressure than the gas test pressure.

Liquid pressure test*

Planning the test

1 All parts must be pressure tested to at least 125% of the maximum allowable operating pressure (MAOP). In general, the lowest pressure reading during the test period will be one factor in limiting the maximum allowable operating pressure in the system.

2 Pressure relief devices must also be identified and recorded. These devices should be removed or isolated as necessary.

3 It is recommended that the test be conducted in water. However, liquid hydrocarbons with a flashpoint greater than 60 degrees centigrade can also be used as the test medium. Fluid properties for these test mediums should be obtained prior to the test for pre-test and post-test calculations.

4 The facility operator shall provide an accurate description of the part being tested. It is recommended that the facility operator develop an isometric drawing showing accurate dimensions and location of valves and fittings. The test facility should also provide an accurate test procedure explaining the different steps.

5 To obtain accurate results it is important that the entire part is reasonably free of air or other entrapped gas. Eliminating air increases the accuracy of the test results and too much air may “mask” leaks during the pressure test

Pretest calculations

Theoretical DV/DP , prior to start-up of test activities, the facility operator should if possible perform a pre-test calculation to obtain a theoretical value of the DV/DP for the verified volume of the part under test and the appropriate test medium. This information can be used to determine whether entrained gas exists in the line under test. If the volume of the part is small, DV/DP can be difficult to obtain.

Test sensitivity

During a hydrotest several factors will affect the accuracy of test results. An overview of these factors follows:

1. Fluid temperature, if the fluid temperature change, this will affect the hydrotest pressure.
2. Entrained air may prevent stabilization of the testing fluid during a test or may mask the presence of an actual leak. The first indication of significant amount of entrained air will

usually occur during pressurization. Pressurization will not be immediate since water injected into the test section must displace a significant volume of highly compressible air. Also, expanding air may prevent the detection of an actual leak in the test segment. If a small leak is present, the expected pressure loss due to the leak may not be apparent since expanding air within the part will tend to keep the pressure constant.

3. The coefficient of thermal expansion of the test medium effects the calculated volume and pressure changes versus a change in temperature (DV/DT & DP/DT). Mediums with high thermal coefficients are very sensitive to changes in temperature. Therefore, for the same temperature recording accuracy, a product test would potentially show a higher volume or pressure change when compared with water as a test medium. This is the primary reason for using water as a test medium and for taking accurate temperature data.

Test Accuracy

The Pass/Fail criteria is dependent upon three variables that effect the calculated volume loss or gain during a hydrotest. These variables are the change in pressure during the test, the change in temperature experienced by the fluid during the test and the change in fluid volume.

1. Pressure recording devices should have an accuracy of +- 0.1 bar. A typical “clock” type chart recorder can be used for documentation purposes but should not be relied upon for providing actual pressure data that will be used in post-test calculations. Electronic pressure recorders with higher resolution may provide more frequent and accurate data sampling to enable pressure trending during the test.
2. Regardless of the test medium used, the temperature recording device should have a high accuracy. The output resolution for a water test should be 0.1°C and for a hydrocarbon test the recommended resolution is 0.01°C. A typical “clock” type chart recorder can be used for documentation purposes but should not be relied upon for providing the temperature data that will be used in post-test calculations.
3. Accurate determination of fluid volumes bled or injected should be accounted for during a test. Volumes should be measured using the most precise graduations available. If it is possible to visually inspect all possible leaks, this is a god way to detect changes in volume/leaks, but does not give data to a DV/DP calculations.

Safety Precautions

1. Follow the Resonator general safety manual
2. The part being tested should be placed behind a protective wall (Figure 1) during pressurization. The trajectory of any bolts, fittings valves etc. must be out of harm’s way.

Performing the Test

1. Record the accuracy of the instruments used and the ambient conditions (i.e. air and fluid temperature)
2. Follow the test procedure.

Gas Pressure Test

After a static pressure test is performed a gas pressure test can be performed. The purpose of a gas pressure test is to detect gas leaks.

Due to the high compressibility of gas, a risk analysis for the item being tested must be carried out. One must here look at the volume and pressure in the part and the volume in the test facility. If the volume and pressure (in the part) is large enough to cause damage to personnel, the test must be carried out inside a pressure safe container. If a pressure safe container is found unnecessary, the test must be carried out behind a protective wall Figure 1.

Planning the test

1 All parts must be pressure tested to at least 125% of the maximum allowable operating pressure (MAOP). In general, the lowest pressure reading during the test period will be one factor in limiting the maximum allowable operating pressure in the system.
2 Pressure relief devices must also be identified and recorded. These devices should be removed or isolated as necessary.
3 The facility operator shall provide an accurate description of the part being tested. It is recommended that the facility operator develop an isometric drawing showing accurate dimensions and location of valves and fittings. The test facility should also provide an accurate test procedure explaining the different steps.
4 The gas pressure test must be done with inert gases.

Test sensitivity

1. The gas pressure is highly affected by temperature and the temperature should therefore be monitored and recorded during tests. The gas pressure will not stabilize before the temperature does.

Test Accuracy

1. One can use water to submerge the part being tested. With the parts submerged, leaks can be detected visually (bubbles).
2. A typical “clock” type chart recorder can be used for documentation purposes. Electronic pressure recorders with higher resolution may provide more frequent and accurate data sampling to enable pressure trending during the test.

Safety Precautions

Follow the Resonator general safety manual and the guide lines stated in the beginning of this section (Gas pressure test).

Performing the Test

1. Record the accuracy of the instruments used and the ambient conditions (i.e. air temperature)

2. Follow the test procedure.

*The liquid pressure test was made based on: California State Lands Commission ; A Procedure for the Hydrostatic Pressure Testing of Marine Facility Piping.

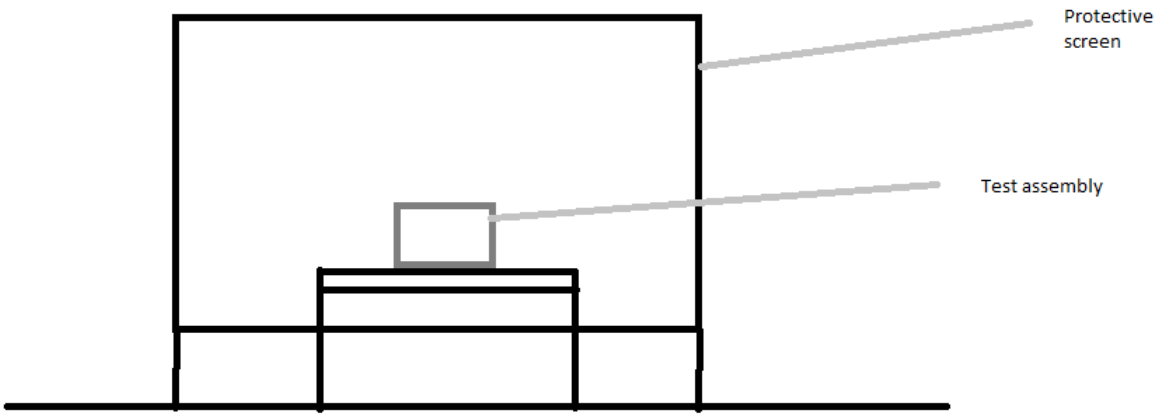

Figure 1

Appendix D Test procedure, Static liquid pressure test

Author: Eirik Lind Hånes, Ping Ju Li, August 2011

Test procedure, Static liquid pressure test

Preparation

1. Assembly the chamber
   1.1. Insert the piston into gas spring cylinder. The piston seal should be removed for this test. The pressure on both sides of the piston should be the same. Due to tight tolerances it is difficult to insert the piston. It is therefore recommended to use a lathe to align the piston and cylinder.
   1.2. Check the rod seal. Replace the seal if visible damage to the seal is found.
   1.3. Put a new gasket into the groove of flange (gas spring chamber ending plate)
   1.4. Put the flange with gasket onto the chamber; the piston rod goes through the central hole of the flange.
   1.5. Put on all fasten bolts / washer / nuts.
   1.6. Tighten all bolts evenly (do not tighten one bolt to the ending position, tighten bolts step by step, one by one). Tighten to specified torque: 8.3 Nm
2. Block 4 of the six ports (holes) on the chamber and flange. One of the other two is used as inlet of pressurized liquid, and is connected to a check / stop valve. The last one can be used to connect to pressure sensor / gauge. Use plugs and fittings supplied by Resonator.
3. Alternatively, block 5 of the six ports (holes) on the chamber and flange. The one left is used as inlet of pressurized liquid, and is connected to the pump / source; Use the pressure sensor / gauge at the pump outlet for pressure readings. Use plugs and fittings supplied by Resonator.
4. Visual inspection: see if there is visible damage, deformation to the chamber and fasteners
5. Dimensions: measure the outer diameter, inner diameter (before assembly), length of gas spring chamber; measure the length of bolts and its length over the nuts. Record all measured results.
6. Connect the chamber to pressurized liquid supply with pipe/hose.
7. There should be no knot along the hose.
8. There should be a valve between the pump and the cylinder.

Testing

9. Make sure the pressure in gas spring chamber is zero before starting the pump / turning on the pressurized liquid supply.
10. Undo one plug, start pumping fluid into the chamber and let it fill up with fluid before inserting the final plug. Then dry of the part, and start pressurizing observe if there is any visible leakage.
11. Pause for at least 3 minutes when the pressure is 50 bars. Close the valve, and observe the pressure drop per time, it should stabilize to less than 0.5 bar/minute.
12. Continue to increase the pressure to 100 bars.
13. Pause for at least 3. Close the valve and turn of the pump, observe and record the pressure drop per time, it should stabilize to less than 0.5 bar/minute.
14. Visual inspection: see if there is visible damage or deformation on the chamber and fasteners, or any leakage.
15. Continue to increase the pressure to 200 bars.

16. Repeat step 21-22.
17. Continue to increase the pressure to 300 bars.
18. Close the valve and turn of the pump, observe and record the pressure drop per time, it should stabilize to less than 0.5 bar/minute. Log pressure vs. time for 60 minutes. Visual inspection: see if there is visible damage or deformation on the chamber and fasteners, or any leakage.
19. Release the pressure to zero.
20. Disconnect the pressurized liquid supply pipe(s).

Post-test checking

21. Make sure the pressure in gas spring chamber is zero.
22. Visual inspection: see if there is visible damage, deformation to the chamber and fasteners
23. Dimensions: measure the outer diameter, inner diameter (after disassembly), and length of gas spring chamber; measure the length of bolts and its length over the nuts. Record all measured results.
24. Disassembly the testing set
    24.1. Remove the plugs which block the ports on the chamber and flange.
    24.2. Loosening all fasteners step by step and in turn.
25. Check the rod seal to see if there is any visible damage, deformation
26. Check the piston rod to see if there is any visible damage, deformation.

Appendix E Test procedure, static gas pressure test

Author: Eirik Lind Hånes, September 2011

Test procedure, static gas pressure test

Preparation

1. Assembly the chamber
   1.1. Assemble all the seals according to the procedure from Trelleborg technical bulletin, supplied by resonatoer. Usually the piston seal deforms plastically during installation. If this happens use the piston ring compressor supplied by Resonator, to compress the piston seal to the right diameter.
   1.2. Insert the piston into gas spring cylinder. Due to tight tolerances it is difficult to insert the piston. It is therefore recommended to use a special compression and assembly tool. This is supplied by Resonator.
   1.3. Check the rod seal. Replace the seal if visible damage to the seal is found.
   1.4. Put a new seal into the groove of flange (gas spring chamber ending plate)
   1.5. Put the flange with seal onto the chamber; the piston rod goes through the central hole of the flange.
   1.6. Put on all fasten bolts / washer / nuts.
   1.7. Tighten all bolts evenly (do not tighten one bolt to the ending position, tighten bolts step by step, one by one). Tighten to specified torque 8.3 Nm, use the bolts supplied.
2. Block 4 of the six ports (holes) on the chamber and flange, two on each. One of the other two is used as inlet of pressurized gas, and is connected to a check / stop valve. The last one can be used to connect to pressure sensor / gauge, or be left open. Use plugs and fittings supplied by Resonator.
3. Visual inspection: see if there is visible damage, deformation to the chamber and fasteners
4. Connect the chamber to the pressurized gas supply.
5. There should be no knot along the hose.
6. There should be a valve between the gas supply and the cylinder.
7. Place the chamber in a transparent container; fill it with water, so that the entire chamber is submerged.

Testing

8. Make sure the pressure in gas spring chamber is zero before opening the valve to the pressurized gas supply.
9. Start pressurizing from one side, start testing the rod seal side. Observe if there are any leaks.
10. Pressurize slowly up to 50 bar, pause for at least 3 minutes when the pressure is 50 bars. Close the valve, and observe the pressure drop per time, it should stabilize to less than 0.5 bar/minute relatively fast.
11. Continue to increase the pressure to 100 bars.
12. Pause for at least 3 minutes. Close the valve and turn of the pump, observe and record the pressure drop per time, it should stabilize to less than 0.5 bar/minute.

13. Visual inspection: see if there is visible damage or deformation on the chamber and fasteners, or any leakage.
14. Continue to increase the pressure to 250 bars.
15. Close the valve and turn of the pump, observe and record the pressure drop per time, it should stabilize to less than 0.5 bar/minute. Log pressure vs. time for 20 minutes. Visual inspection: see if there is visible damage or deformation on the chamber and fasteners, or any leakage.
16. Release the pressure to zero carefully.
17. Disconnect the pressurized gas supply pipe(s).

Post-test checking

18. Make sure the pressure in gas spring chamber is zero.
19. Visual inspection: see if there is visible damage, deformation to the chamber and fasteners
20. Disassembly the testing set
    20.1. Remove the plugs which block the ports on the chamber and flange.
    20.2. Loosening all fasteners step by step and in turn.
21. Check the rod seal to see if there is any visible damage, deformation
22. Check the piston rod to see if there is any visible damage, deformation.

Filling

To fill the gas spring figure 1 shows a suggested method.

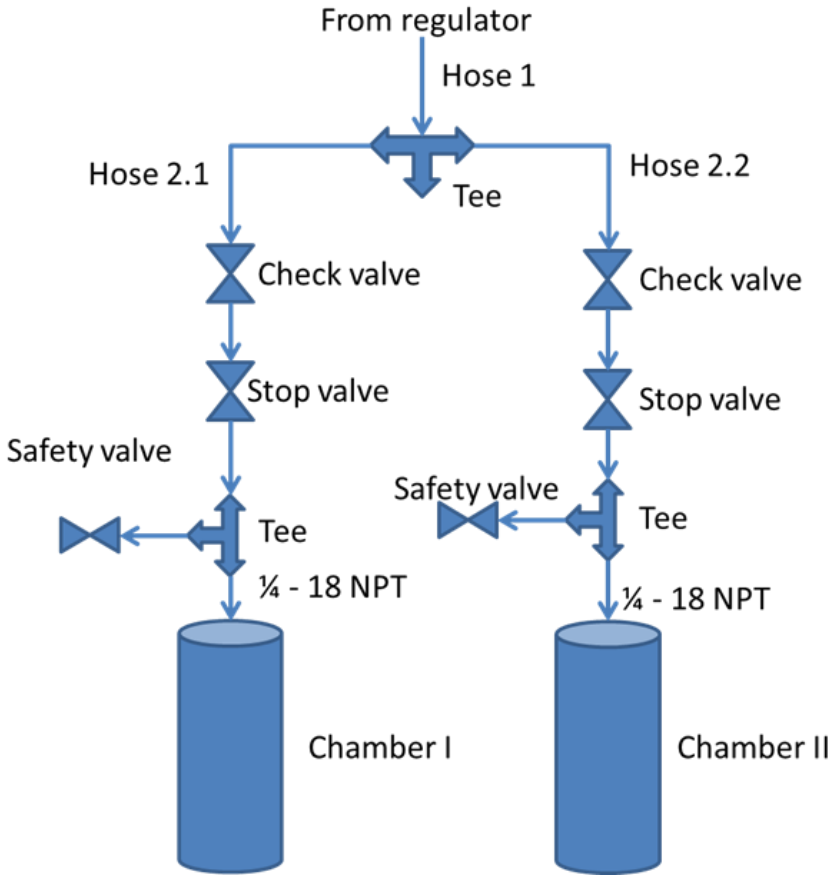

Figure 2, Suggested filling method, (Resonator 2011)

It is important to be sure that the piston is in the right position after filling; this can be checked using a dial gauge measuring the length of the piston rod.

Appendix F Test report hydraulic pressure test 12.8.2011

Date: 12.08.2011, Author: Eirik Lind Hånes Location: Servi test centre, Ski.

Test report

Hydraulic pressure test of gas spring pressure chamber, for the prototype 2B gas spring.

Purpose

- Check mechanical Integrity
- Check for leaks and verify the seal design.

Procedure

Followed the test procedure from appendix 1.

Results:

Gas spring 1:

Due to untraditional connections to the gas spring chamber we used some time to get all the holes sealed. At 100 bar we had a leakage at the M16x2, this plug was replaced with a better solution. We also saw some leakage (air) at one of the M6 bolt, the one adjacent to the M16 (this was due to a manufacturing error only present on spring 1 and 2). But once the air had leaked out it seemed to seal fine.

The test at 200 bar gave the following results

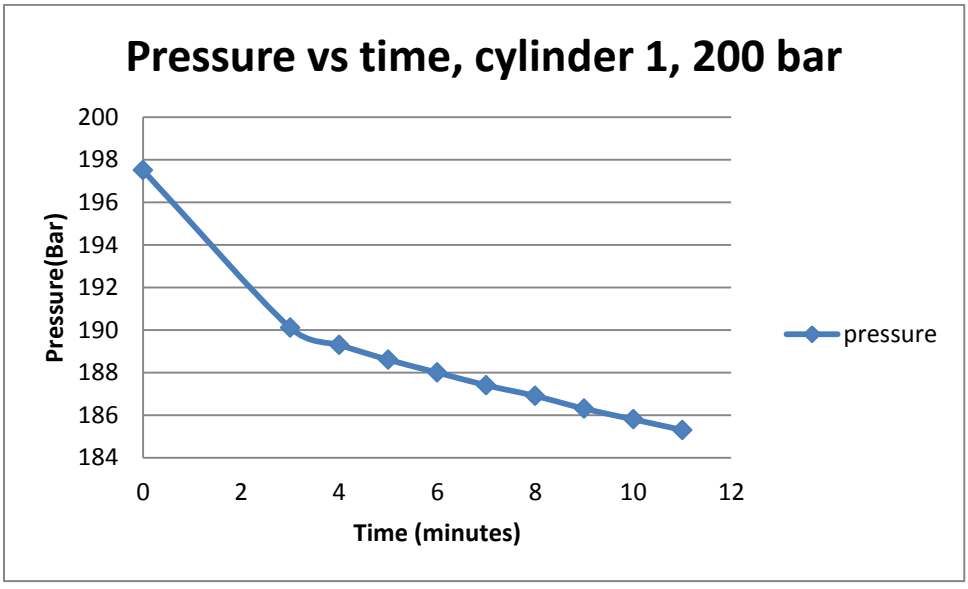

We see that the pressure drop stabilize to about 0.5 bar/minute. This drop can be due to the untraditional fittings, thermal contraction or leakage at the mentioned M6 bolt. There were no visual leaks.

At 300 bar we had a leakage at the M16X2 bolt again. This was fixed. A needle valve was also mounted to be sure that the cylinder was sealed off from the pump.

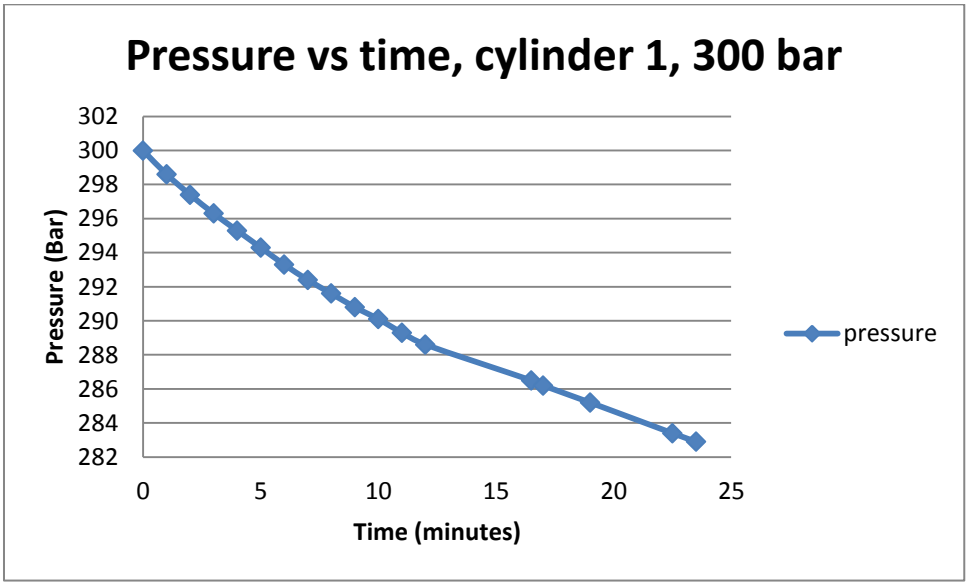

Again we see that it stabilize at about 0.5 bar/minute.

Cylinder 2

After ramping the pressure up to 120 bar and then ramping it down to 100 bar the pressure drop stabilized to just over 0.5 bar/minute at 100 bar (after 5 minutes). At 200 bar a similar pattern was observed.

At 300 bar the following was observed.

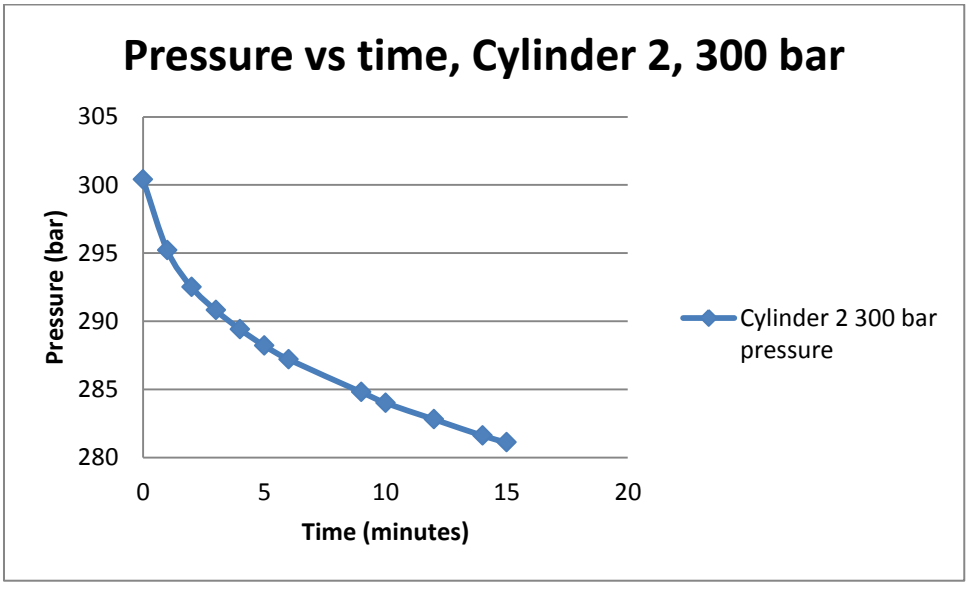

Conclusion

New plugs and fittings should be ordered, to rule out the problems related to the plugs and connections to the cylinder. The leaks around the M6 bolt should be investigated. If there no viable solution for sealing around the M6 bolt, spring 1 and 2 must be discarded. The cylinders mechanical integrity was confirmed.

I suggest trying to fix the problems around the M6 bolt as good as possible, and go on with the gas pressure test.

After this test one can't without further investigation conclude that the cylinders are 100% sealed.

Appendix G Gas pressure test of gas spring 18.08.2011

Date: 18.08.2011 Author: Eirik Lind Hånes Location: Servi test center, Ski.

Test report

Gas pressure test of gas spring pressure chamber, for the prototype 2B gas spring.

Purpose

- Check for leaks and verify the seal design.

Procedure

Followed the test procedure from appendix E. From the last test new fittings where mounted. The problematic M6 threaded hole was sealed with two opposing set screws with Loctite 577. Loctite 577 was recommended for this purpose (gas sealing) by the Norwegian distributor.

Results:

The chamber was pressurized to between 50 and 100 bar, and leaked heavily from the M6 threaded hole.

Conclusion

This end flange must be discarded, and replaced with an end flange without the problematic connection between the M16 and the M6 hole on the end flange.

Appendix H Progress report 7.9.2011

Progress report

Date: 7.9.2011, Author: Eirik Lind Hånes

After the gas pressure test 18.8.2011 at Servi we decided that new end flanges had to be made due to a manufacturing mistake on the first end flanges. We also decided to purchase a accumulator filling kit to be able to do the gas pressure tests in-house.

On the first end flanges – cylinder set a quick solution for sealing had been made. The original end flange had been modified, a grove for a flat gasket had been cut into the end flange. I questioned the gasket solution between the end flange and the cylinder Figure 3. Before ordering any new modifications on the end flanges, I wanted to clarify what sealing solution was the best for our application. So I contacted Otto Ohlsen AS. They recommended an O-ring solution for our high pressure high frequency application. They questioned Resonators initial Teflon flat gasket solution, due to the present of small leaks in this kind of gaskets at the elevated pressures in our application. If we wanted to use a flat gasket solution they recommended a metal reinforced graphite gasket, which can withstand higher pressures and temperatures than Teflon. But they still recommended us to use a polyurethane (PUR) O-ring solution.

Therefore an O-ring grove was designed based on specifications from Otto Ohlsen, and PUR O-rings where ordered, (Figure 4) Design proposal O-ring groove on end flange.

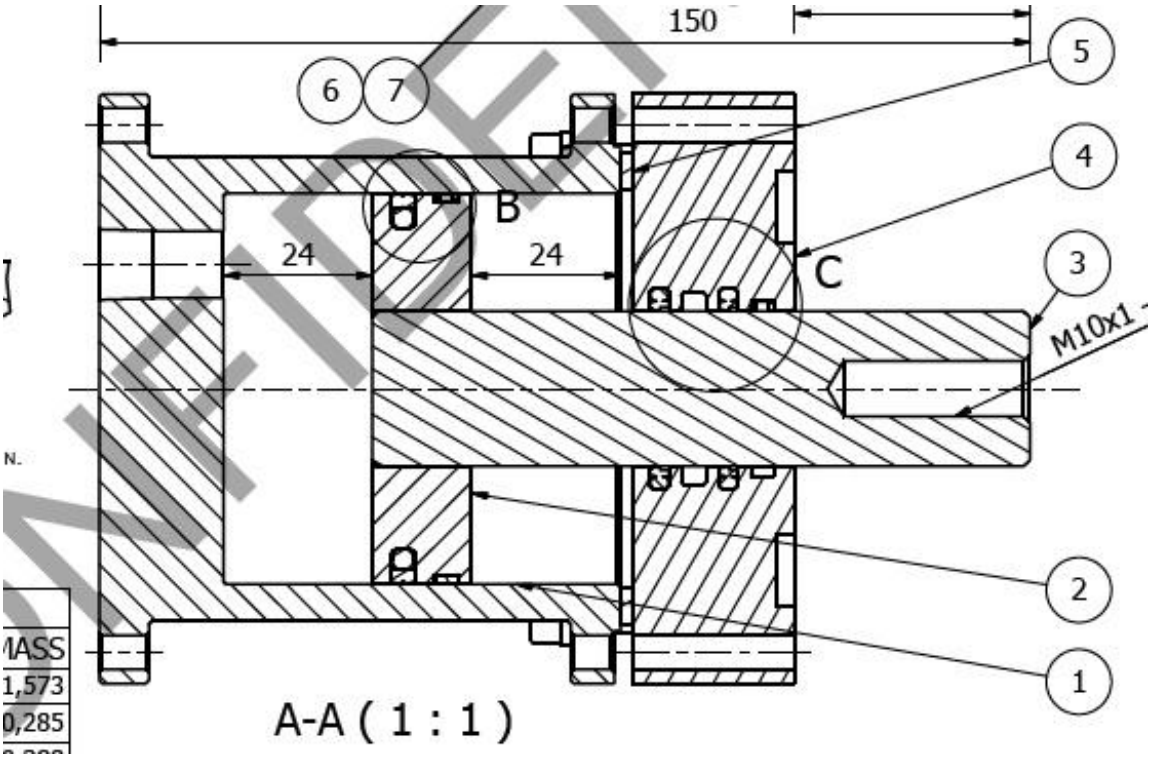

Figure 3, 5 flat gasket.

After we received the new end flanges I right away noticed several problems. There was still a connection between the M16 hole and the bolt hole on the flange (now a 5.3 mm through hole). Looking closer on the M16 hole, I also noticed that this was in fact not a M16x2 threaded hole as specified in the drawing. Finally I noticed that these end flanges had a different design than the first

end flanges. They had no flat surface around the M10x1 and M16X2 connections, making it impossible to make proper sealing around these connections.

While discussing the problems with the parts, and how to handle the mistakes made by the workshop, I decided to give the original end flanges another try.

I contacted my contact at Lindberg og Lund a polymer distributor. And we together discussed a solution using a special high temperature epoxy adequate to our application. I used this epoxy to fill the M16 hole on the end flange and cured the part in a heating cabinet. The epoxy seemed to cure fine, and the gas spring was reassembled, and prepped for a new pressure test.

At resonator the only available gas supply is Helium. When trying to fill helium into the gas spring it leaked heavily from the regulator. It seemed that the regulator was not approved for helium. The difference in molecular size between He and N2 apparently affects the ability to seal the gas. This was something that I was not aware of, and another problem that has to be solved.

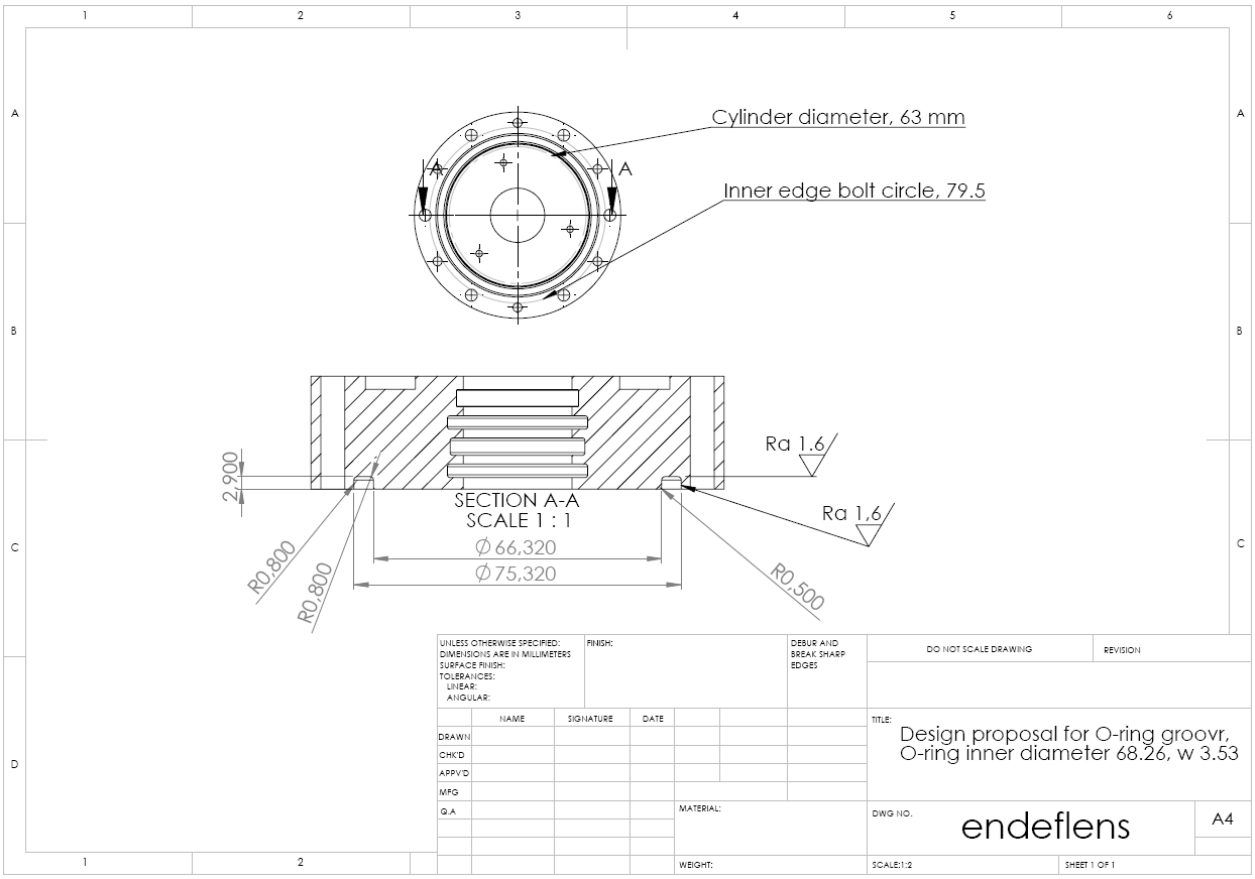

Figure 4, Design proposal

Appendix I Gas pressure test of gas spring 13.9.2011

Date: 13.09.2011 Location: Resonator test center, Ås.
Test medium: Nitrogen Author: Eirik Lind Hånes

Test report

Gas pressure test of gas spring pressure chamber, for the prototype 2B gas spring.

Purpose

- Check for leaks and verify check the seal design.

Procedure

Followed test procedure from appendix E. The problematic M6 threaded hole was sealed with two opposing set screws with Loctite 577 last time. Loctite 577 was recommended for this purpose (gas sealing) by the Norwegian distributor, but this did prove insufficient. So as mentioned in the progress report (written 7.9.2011), the M16 hole was blocked using a special epoxy resin.

Results and discussion:

The chambers where pressurized to around 100 bar. When the pressure was increased to over 100 bar, heavy leakage from the flat gasket appeared, and the pressure dropped fast (in a few minutes) down to around 100bar. As the pressure dropped further the leakage from the flat gasket decreased to around one bubble/second at 80 bar. Both chambers also had a slight leakage at the ¼" NPT connections, but this can probably be fixed by using Loctite 577 or tightening the fitting harder. The epoxy fix seemed to work fine for both chambers. Also the M10x1 and M16x2 plugs showed no leakage.

For chamber 2, both the piston seal and the rod seal showed no leakage, even at burst pressures at around 150 bar, which is promising.

For chamber 1 there is a different story, the piston seal did not function as intended. It leaked even at 20 bar. This must be investigated further. To check the chamber for other leaks, the holes in the end of the cylinder was blocked.

After opening cylinder 1, it was clear that the piston seal had been damaged, probably during assembly. It seems that new assembly procedures have to be made.

Figure 5 shows the test results from this pressure test.

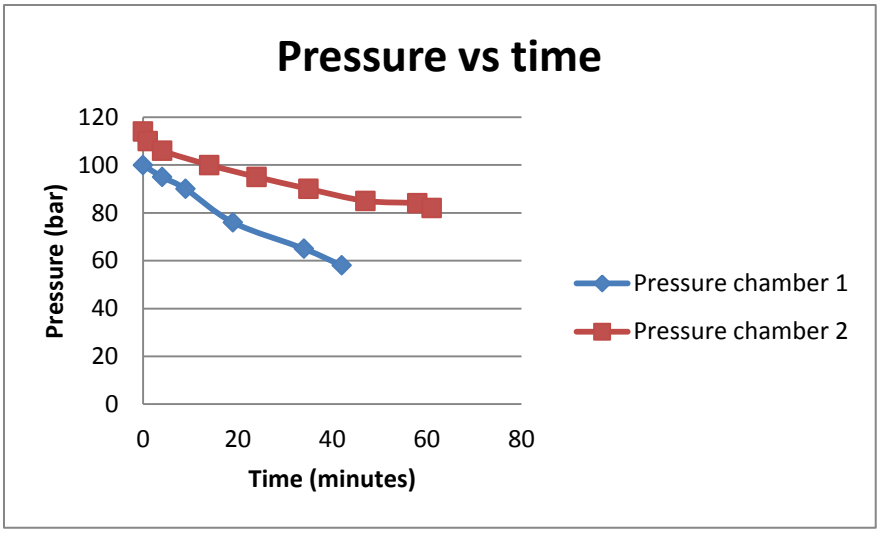

Figure 5, Showing gas pressure in chamber 1 and 2

Conclusion

Another solution for the seal between the cylinder and the end flange must be used. Either an O-ring solution or a different flat gasket must be used. A new piston ring seal must be fitted, and the assembly procedures reviewed.

Appendix J Gas pressure test of gas spring 19.9.2011

Date: 19.09.2011 Location: Resonator test center, Ås.
Test medium: Nitrogen Author: Eirik Lind Hånes

Test report

Gas pressure test of gas spring pressure chamber, for the prototype 2B gas spring.

Purpose

Check for leaks and verify the new seal design.

Procedure

Followed the test procedure from appendix E.

Results, discussion and conclusion:

The test results from the test of chamber 1 is shown in the table below

					Flange		Chamber bottom		
Time	P (bar)	Rod	Piston	NPT	M10x1	M16x2	NPT	M10x1	M16x2
13:53	160	X	X						
14:05	158	X	X						
14:16	158	x	x						
14:20	158	X	X						
14:40	158	X	X						
15:02	158	x	x						
15:30	156	X	X		bubbles 1/s	bubbles 2/s			
15:48	156	x	X		bubbles 1/s	bubbles 2/s			
16:02	156	x	X		bubbles 1/s	bubbles 2/s			
17:03	147	x	x	steady stream	bubbles 1/s	bubbles 2/s			
Rod seal	Only one								
Piston seal	One								

As we see from the table the gas springs ability to seal gas has increased substantially and is now at an adequate level. The design should however be improved when a new spring is made. The test pressure was limited to the gas tank pressure; 160 bar. This should be considered in future tests.

Appendix K 2B-1.1 Test report 3.10.2011

Author: Andre Dahl Jacobsen Date: 3.10.2011
Reviewed by: Eirik Lind Hånes Date: 5.10.2011

2B-1.1 Test report

Test-running the machine with gas springs

Description

This test was performed to investigate the performance of the gas springs when running the machine on no-load. No mechanical springs was used.

Parts involved

- 2x DH2B-P-013-B01 - Gas spring piston B (combined)
- 2x DH2B-P-012-B01 - Gas spring cylinder ending plate B
- 2x DH2B-P-001-C01 - Gas spring chamber C
- DH2B-Stator-01 - Stator

Test description

- Piston
  - O-ring, seal and scraper were installed.
- Flange
  - Rod seals were installed but left flange only had one rod seal.
  - Scrapers were mounted only on left flange.
- M16x2 & M10x1 ports both on the flange and bottom of the chamber were blocked with Epoxy.
- All contact surfaces were greased.

Test setup

Tested two different conditions:

1. 8 bar pressure in outer gas spring chambers, 6 bar pressure in inner chambers
   a. Gas type: Air
   b. Filling was done with compressor in the workshop
2. 25 bar pressure in outer gas springs, atmospheric pressure in the inner chambers
   a. Gas type: N2
   b. Filling was done with gas bottle

This test was carried out from Oct. 6 to Oct. 7, 2011 at UMB workshop, ÅS

Results

Appendix

The amount of raw results can become substantial, so these should be stored elsewhere, and only the most essential results should be presented here

Observations

During operation

- Common results:
    - For both tests a reciprocating motion was achieved, i.e. the gas springs worked as mechanical spring equivalents. Visible movement of the outer casing.
    - Some erratic behavior was noticed, non-periodic noise, jerky movement.
    - For the time the machine ran smoothly a significant drop in current was seen when the machine was ran close to the pre-calculated resonant frequency.
    - Heat generation in the left flange, noticeable hotter than the stator
    - Machine stopped working after a restart, got "stuck".
    - Pressure unknown in the all four gas springs chambers after operation

- 8 bar pressure in outer gas spring chambers, 6 bar pressure in inner chambers
    - Heat generation in the left flange, noticeable hotter than the stator
    - Pressure unknown in the all four gas springs chambers after operation,
    - Suspected leakage, assumed to be due to the compressed air-fittings.

- 25 bar pressure in outer gas springs, atmospheric pressure in the inner chambers
    - Heat generation in the left flange, noticeable hotter than the stator
    - Pressure unknown in the outer gas springs chambers after operation

After disassembling

- 8 bar pressure in outer gas spring chambers, 6 bar pressure in inner chambers
    - Piston had moved away from central position, assumed to be due to leakage, massive friction or both
- Left side gas spring (1)
    - Visible metal cuttings, mostly located at the piston rod around the flange area
    - Heavy piston rod damage. The piston rod seals were badly damaged
    - The damage appears to be gravity sensitive, i.e. the damage is located on a 180° arc on the flange and rod.
    - Piston and cylinder unharmed.

- Right side gas spring (2)
    - Some minor damages to the flange and rod. Not serious.
    - Piston and cylinder unharmed.

Test results

Test code:	2B – 1.1				
Test procedure code	**Description / procedure**	**Ref.**	**Resp.**	**Test performed**	**Comments and notes**
2B – 1.0.T.1			AB		
2B – 1.0.T.2			PL		
2B – 1.0.T.2			AB		
2B – 1.0.T.3			ADJ		

Analysis

Results are analyzed and presented so as to be understood by new employees.

Theories on why the piston rod and flange were damaged:

1. **Misalignment of the gas spring chambers to the stator casing**
    a. Earlier the mounting holes on the gas spring chambers had to be enlarged to assemble machine. This enlargement was done by hand at Skaug Mek. The result is that the bolt holes are larger, though varyingly, than the bolts.
    b. Measurements
        i. Flange hole : 5,4 mm
        ii. Bolt diameter : 4,8 mm

    It's clear then that the mounting procedure is essential to avoid misalignment. This can be counteracted by cross-tightening the bolts.

2. **Tolerances of the flange versus the rod during design and machining**
    a. If the rod seal groove is too big then the rod seal may be compressed too much due to gravity and metal to metal action may occur.
    b. This may be corrected by machining off some of the flange material, i.e. making the inner flange diameter larger.
    c. Another fix may be to install a stronger O-ring to increase the expanding force on the rod seal
    d. Measurements
        i. Flange 1 gas side diameter : 25,06 mm
        ii. Flange 1 stator side diameter : 25,06 mm
        iii. Piston 1 rod diameter : 24,97 mm
        iv. Flange 2 gas side diameter : 25,01 mm
        v. Flange 2 stator side diameter : 25,21 mm
        vi. Piston 2 rod diameter : 24,99

    The measurements yield a somewhat contradictive result with regards to tolerance. The undamaged flange (flange 2) has a larger difference in tolerance over the axial width than the damage one. This then implies that there's misalignment or that the

grooves in the flanges are not identical. Finally the rod seals may have been incorrectly installed due to the tolerances of the grooves or rod seal handling.

Conclusion

Conclusions are drawn and compared to the expectations and goals listed in the test plan.

Main hypothesis:

The conclusion may be that there are many different problems acting simultaneously but the main problem seems to be the tolerances of the flange grooves and flange inner diameter. Gravity forces on the piston assembly compressed the seal too much. Metal against metal friction without or with minimal lubrication caused a large local heat generation. The resulting metal filings and cuttings destroyed what little bearing the seals produced and a negative sequence of events followed.

Further work

Based on the conclusion, this chapter is the base of the subsequent test plan. All tests and analyses imply a next step based on the performance of the machine during testing.

After increasing the flange inner diameter and taking the edges of the groove separators a new test should be performed. For this test the gas pressures should be monitored and recorded. Hopefully some form of position sensoring will also be installed.

Appendix L Test report 2B gas 2, 12.12.2011

Test number: 2B gas 2	Date: 12.12.2011	Author: Eirik Lind Hånes
Person(s) responsible:	Andre Dahl Jacobsen, Eirik Lind Hånes	
Purpose of the test: Function test of machine with slightly modified gas springs. Test the new flange design. Detailed test log refer to vacon log file 12.12		

Test personnel are familiar with; Resonator safety manual, Gas filling procedure and the current test procedure.				X
Lubrication type:	Lubrication amount	**Parts used:** Piston 1,2, short modified gas chambers, flange with DP4 bush.		
0W-30	Outer 7ml, inner 5ml			
Pre-tightening:	Flange bolts: 8.3 Nm	Pressure sensor adapter to housing. 6.5Nm		Pressure s. to adapter 5 Nm
Sensors used:	Kissler pressure sensor top and bottom chamber.	Hall effect position (relative amplitude)	Acceleration sensor, stator	Thermocouple lower gas chamber
Machine configuration: Hanging, with single acting gas springs and oil lubrication, DP4 rod supports.				
Key Test data:				
Initial pressure	Aprox. 20 bar	Indication of resonance band 60-70 hz		
	Top chamber 60 C +	Bottom chamber 42 C	Stator top 48 C	Stator bot 42
	Current avg 14 A	Voltage 21-22 V		
	Pressure amplitude	6.5 bar max		
	Electrical Power in	150-300W	(increasing)	

Observations: Check small difference between pressure sensors, calibration. Too much noise on the hall effect sensor to get proper amplitude measurement. The machine ran smoothly on and off for approximately 1 hr, running at frequencies between 50 and 75 hz. The longest continues run lasted 22 minutes. The temperature increased gradually to the measured maximum temperature. The top of the machine reached a higher temperature than the bottom. The current where relatively stable with increasing voltage. No leakage where detected during the test.
Did the test go according to plan? Comments: The machine behaved approximately as expected. However the temperature got higher in the top chamber. This has happened before, but there is no obvious explanation for why this is happening.
Did the test raise any new questions (if it did, what are they)? Why does the machine heat up more in the top than in the bottom.

Other comments: Most of the oil on the flange side probably leaked out before test start. An O-ring groove should be made on these flanges (on both sides) to prevent oil from leaking out of the machine. When centering the machine prior to gas filling, check the measured hall effect voltage, then after filling check the hall effect voltage again to confirm that the piston has not moved. To run the machine harder, better cooling must be constructed. A softer back O-ring on the piston seal can be considered to decrease the friction. The flange bolts should be mounted in the opposite direction (with the unbraco head facing the stator), to ease the tightening of the bolts. A more accurate pressure measurement should be available when filling the gas springs.

Appendix M Test report 2B gas 3, 14.12.2011

Test number: 2B gas 3	Date: 14.12.2011	Author: E.L Hånes
Person(s) responsible:	Andre Dahl Jacobsen, Eirik Lind Hånes	
Purpose of the test: Check if turning the machine "upside down" changes the temperature development in the machine. Check if adding an analog filter on the hall effect sensor improves the signal. Check if the theoretically calculated natural frequency corresponds with the observed natural frequency. Detailed test log refer to vacon log file 13.12		

Test personnel are familiar with; Resonator safety manual, Gas filling procedure and the current test procedure.				**X**
Lubrication type:	Lubrication amount	**Parts used:** Piston 1,2, short modified gas chambers, flange with DP4 bush.		
0W-30	Outer 7ml, inner 5ml			
Pre-tightening:	Flange bolts: 8.3 Nm	Pressure sensor adapter to housing. 6.5Nm		Pressure s. to adapter 5 Nm
Sensors used:	Kissler pressure sensor top and bottom chamber.	Hall effect position (relative amplitude)	Acceleration sensor, stator,	Thermocouple lower gas chamber
di regulator for pressure filling.				
Machine configuration: Hanging, with single acting gas springs and oil lubrication, DP4 rod supports.				
Key Test data:				
Initial pressure	Aprox. 20 bar	Initial hall effect center voltage 1.873v Inductance 1441,5 micro henry @100hz Inductance 580,9 micro henry @ 10 khz Resistance 0.4436 ohm @ 100 Hz		
	bottom chamber 60 C +	top chamber 42 C	Stator top 36 C	Stator bot 41
	Current avg 12-13 A	Voltage 21-22 V		
	Pressure amplitude upperchamber	16 bar max	Pressure amplitude lower	5-6 bar
	Electrical Power in	150-300W	(increasing)	

Observations: The bottom chamber got hotter, so it seems that there is some difference between the two chambers. The piston moved upwards, it seems that there might have been some leakage from the upper chamber. The machine ran for approximately 20 minutes. After disassembly cylinder 1 and piston 1(bottom chamber) showed signs of metal to metal grinding. This explains the increased temperature in this spring.
Did the test go according to plan? Comments: The machine behaved approximately as expected. However the temperature got higher in the bottom chamber.

Did the test raise any new questions (if it did, what are they)? Why does one chamber get metal to metal grinding? Tolerances? Misalignment? Straightness of magnet piston.
Other comments: Most of the oil on the flange side probably leaked out before test start. An O-ring groove should be made on these flanges (on both sides) to prevent oil from leaking out of the machine. After disassembly it seemed that there was enough oil in the chambers. To run the machine harder, better cooling must be constructed. A softer back O-ring on the piston seal can be considered to decrease the friction. The flange bolts should be mounted in the opposite direction (with the unbraco head facing the stator), to ease the tightening of the bolts. The test of theoretical frequency is inconclusive due to different pressure readings in the two chambers. Tolerances of the new parts should be matched to the gas spring that did not fail.

Appendix N Test report 2B gas 4, 15.12.2011

Test number: 2B gas 4	Date: 15.12.2011	Author: E.L Hånes
Person(s) responsible:	Andre Dahl Jacobsen, Eirik Lind Hånes	
Purpose of the test: Check how the machine performs with the new parts. A new magnet piston was manufactured since the last test. The piston and cylinder that was damaged in the last test was replaced with new modified parts. The modified parts where matched to the gas spring that did not fail. Both the gas spring pistons got the corners rounded to r=.5 mm. If the machine works as expected try to increase the input power Detailed test log refer to vacon log file 15.12 and Labview log file (15 des).		

Test personnel are familiar with; Resonator safety manual, Gas filling procedure and the current test procedure.	**X**			
Lubrication type:	Lubrication amount	**Parts used:** Piston 1,2, short modified gas chambers, flange with DP4 bush.		
0W-30	Outer 5ml, inner 4ml			
Pre-tightening:	Flange bolts: 8.3 Nm	Pressure sensor adapter to housing. 6.5Nm		Pressure s. to adapter 5 Nm
Sensors used:	Kissler pressure sensor top and bottom chamber.	Hall effect position (relative amplitude)	Acceleration sensor, stator,	Thermocouple upper gas chamber
Keller digital pressure sensor on regulator for gas filling.				
Machine configuration: Hanging, with single acting gas springs and oil lubrication, DP4 rod supports.				
Key Test data:				
Initial pressure	19.1 bar	Initial hall effect center voltage 1.856v Inductance 1441,5 micro henry @100hz Inductance 580,9 micro henry @ 10 khz Resistance 0.4436 ohm @ 100 Hz		
	bottom chamber 30 C +	top chamber 30C	Stator top 30 C	Stator bot 41
	Current avg 12-14 A	Voltage 21-22 V		
	Pressure amplitude Upper chamber	33 bar max	Pressure amplitude lower	Inconclusive, significantly less than upper.
	Electrical Power in	150-400W	(increasing)	
	resonance	61 hz	indication	
	Inductance after	1443,7 @ 100hz – 1mm 591,8 @ 10 khz – out of range	Coil resistance 0.4555 ohm	(almost cooled down)
	Hall effect after	1.868 v		

Observations: The machine ran smoothly with the new parts. The amplitude was bigger than before with the same electrical input power. The middle of the stator was the part that got the highest temperature; this is

probably due to electrical losses. Fan cooling was added to the springs, they remained cool during the test. (they did not heat up significantly before cooling was added).

There was a significant difference in the pressure measured in the two chambers, it is not clear why. The measurements are conflicting, the hall effect and the 100hz inductance measurement say that the magnet piston has not shifted significantly, while the pressure sensor and the 10 khz inductance measurement say that the piston has shifted significantly.

If the piston are in the middle, the observed frequency seem to cohere with the calculated frequency.

Based on the pressure readings in the upper chamber the maximum relative amplitude at 30 bar (61 hz, 13 A) is approximately 6 mm. The maximum relative amplitude in the test is estimated to 8 mm (38 bar).

Did the test go according to plan? Comments:
The machine behaved approximately as expected.

Did the test raise any new questions (if it did, what are they)?
Has the piston shifted significantly? Which measurements are right?

Other comments:
An O-ring groove should be made on the flanges (on both sides) to prevent oil from leaking out of the machine.

To run the machine harder, better cooling must be constructed. Another thermocouple should be fitted on the bottom chamber. Resistive pressure sensors should be added in addition to the piezoelectric pressure sensors, so that one can observe the static pressure in the gas springs when the machine is not running.

A softer back O-ring on the piston seal can be considered to decrease the friction.

The observed frequency seem to match the calculated, but more test should be done to confirm the results. The sensors have to be checked before the next test. A new inductance and hall effect calibration should be done.

The machine performed significantly better with the new parts, a bigger amplitude was observed with the same input power.

Appendix O End flange for DP4 rod support

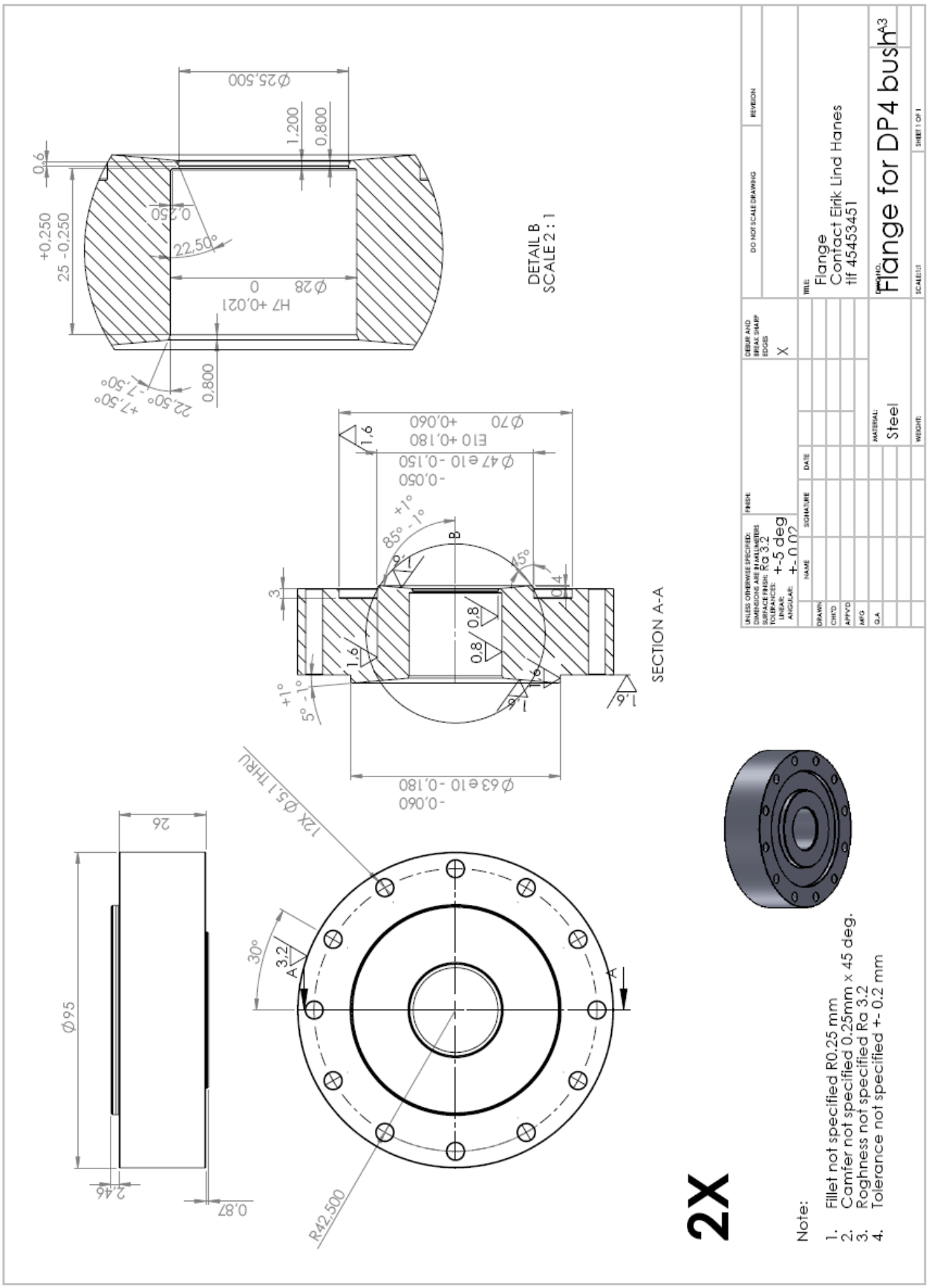

Appendix P Original end flange tolerances

Tolerance controll 2B Prototype			
Flanges			
Flange number	Tolerance Pressure side	Tolerance non pressure side	Comment
1	6.5	6.5	
2	7	7	
3	22	6	scrape marks from test
4	7	7	Failed in test

Files on attached CD

Appendix Q Misc. gas spring calculations

Appendix R Frequency vs amplitude

Appendix S Gas spring chamber optimization

Appendix T Pre-tightening of M16 bolt

Appendix U Pre-tightening of M5 flange bolts

Appendix V Parameter study